Zurich University of Applied Sciences (ZHAW)

School of Life Sciences and Facility Management (LSFM) Institute of Natural Resource Sciences (IUNR)



University of Natural Resources and Applied Sciences (BOKU)

Department of Water, Atmosphere and Environment (WAU) Institute of Hydrobiology and Aquatic Ecosystem Management (IHG)



Aquatic macroinvertebrates as indicators for hydropeaking — Development and validation of specific multimetric indices



Wädenswil, 12.09.2025

Commissioned by the Federal Office for the Environment (FOEN)

Imprint

Commissioned by

Federal Office for the Environment (FOEN), Water Division, CH-3003 Berne The FOEN is an agency of the Federal Department of the Environment, Transport, Energy and Communications (DETEC).

Contractor

Zurich University of Applied Sciences (ZHAW) Institute of Natural Resource Sciences (IUNR) Grüentalstrasse 14, Postfach CH-8820 Wädenswil

Sub-contractors

BOKU University of Natural Resources and Life Sciences Institute of Hydrobiology and Aquatic Ecosystem Management (IHG) Gregor-Mendel-Strasse 33 AT-1180 Vienna

Aquabug – Pascal Stucki Chemin de la Ramée 6B CH-2074 Marin

Authors

TONOLLA Diego, AUHSER Alexander, ANTONETTI Manuel, KASTENHOFER Olivier, WIRTH Sarah, STUCKI Pascal, LEITNER Patrick

Collaborators and contributors

GRAF Wolfram (BOKU), GREIMEL Franz (BOKU), GUFLER Christa (ZHAW), HAUER Christoph (BOKU), LOOSER Denise (ZHAW), SCHAER Bettina (EAWAG), SCHEIB Mirjam (ZHAW)

FOEN support

GORLA Lorenzo

Hydropower plants support

Landquart: Repower; Moesa: OIM & AXPO; Plessur: Arosa Energie; Saane: Groupe-e; Sitter: SAK; Ticino: OFIBLE & AET; Vorderrhein: AXPO

Note

This study/report was prepared under contract to the Federal Office for the Environment (FOEN). The contractor bears sole responsibility for the content.

Content

1		
2		
	2.1 River typification	
	2.1.1 Hydropeaked rivers	
	2.1.2 Reference rivers	
	2.2 Determination of study sites	
3	Sampling and identification of macroinvertebrates (WP 2)	16
	3.1 Macroinvertebrate sampling design	16
	3.2 Sample treatment and identification of taxa	
	3.2.1 Field-screening	
	3.2.2 Laboratory	20
	3.2.3 Data structure for further analyses	22
	3.3 Environmental data	
	3.3.1 Reconstruction of flow data	26
	3.3.2 Data structure for further analyses	28
4	Hydropeaking-sensitive assessment index (WP 3)	29
	4.1 Introduction	
	4.2 Material and methods	30
	4.2.1 Candidate metrics	30
	4.2.2 Metric selection	31
	4.2.3 Calculation and validation of multimetric indices	33
	4.3 Results	34
	4.3.1 Metric selection – Comparison of field-screening and laboratory identification	
	4.3.2 Metric selection – Indication quality	34
	4.3.3 Metric selection – Influence of environmental covariates	
	4.3.4 Metrics selection – Metrics suitable for multimetric indices.	38
	4.3.5 Validation of the multimetric indices	40
	4.4 Discussion	44
5		
	5.1 Introduction	
	5.2 Material and methods	47
	5.2.1 Selected study sites and field survey	47
	5.2.2 Pre-processing – Hydrodynamic modeling	
	5.2.3 Univariate habitat modeling	
	5.3 Results	
	5.4 Discussion	55
6	General discussion and conclusions	57
	6.1 Methodological approach for assessing the response of macroinvertebrates to hydropeaking -	drift,
	stranding, changing habitat conditions	57
	6.2 Evaluation and effects of hydropeaking variables on macroinvertebrates	58
	6.3 Conclusions and recommendations	
7	References	62
8	Annex	70
	8.1 Macroinvertebrate data ZHAW and Aquabug	70
	8.2 Environmental variables	70
	8.3 Macroinvertebrate data BOKU	70
	8.4 Potential influence of silicate bedrock	
	8.5 Reference values for metric calculation	
	8.6 Validation of the multimetric indices	
	8.6.1 Scatterplots	
	8.6.2 Correlation between single biological and single hydrological metrics	
	8.6.3 Hydrological variables across biogeographical regions and rivers	
	8.6.4 Influence of flow-data reliability	
	8.7 Spatial distribution of flow velocity classes	
	8.8 Data delivery	

1 General Introduction and objectives

In numerous Alpine regions, hydropower stands out as one of the primary sources of renewable energy. In Switzerland, it presently accounts for 57.6% of the nation's total electricity generation (SFOE, 2024). The Energy Strategy 2050 aims to increase hydroelectric power production by around 1.34 TWh, representing a 3.8% increase, by the year 2050 (SFOE, 2024). Concurrently, the energy storage capacity of Swiss hydropower reservoirs is projected to rise by 1.2 TWh over the same period, constituting approximately 20% of the current storage capacity (Boes et al., 2021). This expansion of hydropower, coupled with its integration with variable renewable energy sources like wind and solar, is anticipated to intensify hydropeaking operation and impose greater pressures on sustainable environmental flows. It is also expected to exacerbate hydromorphological and ecological impacts on downstream riverine habitats, organisms, and ecosystem functioning (Bruder et al., 2016; Young et al., 2011; Hayes et al., 2022; Alp et al., 2023; Bipa et al., 2024; and references therein). Consequently, there is an urgent imperative to implement appropriate and effective ecological measures to mitigate the impacts of hydropeaking in rivers (Hayes et al., 2023).

Aquatic macroinvertebrates play a crucial role in assessing anthropogenic alterations (Hering et al., 2003; Lear et al., 2009; FOEN, 2019a). However, research and practice regarding hydropeaking-related impacts and mitigation measures have predominantly focused on fish and, to a lesser extent, benthic invertebrate fauna. Moreover, the habitat requirements of aquatic macroinvertebrates are less known compared to fish, owing to their vast diversity in taxa and traits, as well as their specialized habitat utilization. Nevertheless, macroinvertebrates represent a taxonomically reach and functionally diverse biological group, essential for maintaining a healthy river ecosystem. They influence nutrient cycling, primary production, and decomposition, while also serving as a crucial food source for various aquatic (e.g., fish) and riparian (e.g., arthropods, spiders) predators (Wallace & Webster, 1996; Rader 1997; Krell et al., 2015; Naman et al. 2016; and references therein).

The effects of hydropeaking on macroinvertebrates are manifold and complex, with different taxa exhibiting varying vulnerability and responses to flow alteration. Numerous studies have comprehensively described the potential short- and long-term consequences of hydropeaking on aquatic macroinvertebrates, considering various hydropeaking intensity parameters and their respective effects. Increases in flow amplitude and discharge-associated hydraulic stress, expressed, for example, as increases in flow velocity, combined with an increase in the up-ramping rate, promote (i) passive drift of benthic organisms (Gibbins et al., 2016; Schülting et al., 2023; Tonolla et al., 2023; Friese et al., submitted). Furthermore, fluctuations in the wetted area between base and peak flow (dependent on the flow ratio), in combination with an increase in the down-ramping rate, can lead to increased (ii) stranding (Kroger, 1973; Perry & Perry, 1986; Tanno et al., 2016; Tonolla et al., 2023). Additionally, (iii) alterations in hydromorphological habitat conditions (mainly hydraulic conditions and substrate) and (iv) the reduction of persistent suitable habitats (Bätz et al., 2023) are known to affect colonization patterns of benthic populations in hydropeaked rivers (Cushman, 1985; Bretschko & Moog, 1990; Leitner et al., 2017; Kjaerstad et al., 2018). The strong interactions between drift, stranding and changing habitat conditions often result in reduced macroinvertebrate biomass and abundance of certain taxa (Cushman, 1985; Bretschko & Moog, 1990; Leitner et al., 2017; Abernethy et al., 2021; Tonolla et al., 2023), occasionally altering richness and population composition as well (Auhser et al., in prep.). For example, this could favor rheobiontic and rheophilic taxa (Bretschko & Moog, 1990; Cushman, 1985; Ruhi et al., 2018) over taxa associated with lentic (e.g., limnophilic and limno-rheophilic) and flowexposed substrate-surface areas (Graf et al., 2013; Schülting et al., 2023).

Despite ongoing research efforts, it remains largely unknown which of the hydropeaking effects (i – iv) constitutes the most limiting factor for the long-term distribution and colonization of riverbeds by

aquatic macroinvertebrates in hydropeaked rivers (Bipa et al., 2024). However, river-specific hydropeaking intensity, particularly the extent of the dewatering area and the maximum hydraulic impact (e.g., expressed by high flow velocity or bed shear stress), along with the frequency of hydropeaking events (Kjærstad et al., 2018; Hayes et al., 2024) and the river-specific morphological and sedimentary characteristics (e.g., unsuitable substrate like sand), might play pivotal roles (e.g., Tonolla et al., 2023). Areas not subjected to excessively high hydraulic conditions during peak flow theoretically offer opportunities for colonization during base flow periods (Schmutz et al., 2013). Other significant factors, such as thermopeaking (Bruno et al., 2013; Schülting et al., 2016), substantial glacial- or snowmelt with associated high suspended sediment concentrations (turbidity) and clogging, as well as the absence of organic material and/or plant cover (especially algae and moss), can also act as limiting factors on macroinvertebrate distribution and colonization. Additionally, there is limited understanding regarding which macroinvertebrate community should be targeted when implementing mitigation measures, as data on macroinvertebrates from comparable near-natural rivers (in terms of discharge, region, size) are often lacking. This gap in knowledge is particularly pronounced in countries like Switzerland, where most rivers experience highly modified flow and sediment regimes and are often channelized or otherwise morphologically altered due to multiple pressures from land use, hydropower generation and flood control.

To achieve sustainable management of hydropeaking and the conservation of river ecosystems, there is a critical need to enhance our understanding of how hydropeaking, both independently and in conjunction with other potential limiting factors such as the morphological and sedimentological context, impacts macroinvertebrate communities over the long term. Furthermore, it is essential to investigate which mitigation measures may offer the most effective ecological, economic, and energetic outcomes. Based on current knowledge, utilizing existing macroinvertebrate communities for ecological assessments of hydropeaked rivers appears reasonable, as these communities represent the cumulative effects of all hydropeaking impacts and provide insights into the long-term consequences. For example, drift and stranding are short-term phenomena that are often challenging to detect and generalize. Despite numerous studies and promising approaches, there remains a deficiency in adequate methods based on macroinvertebrate communities to assess hydropeaking-specific stressor gradients. Particularly in Alpine rivers with highly modified flow regimes due to hydropeaking, it is imperative to develop and refine methods capable of linking hydromorphology with ecological responses (Arthington et al., 2018; Poff, 2018; Horne et al., 2019). Such methods are essential for promoting sustainable water resource management.

The primary aim of this study was to develop a hydropeaking-sensitive assessment index based on the response of the established aquatic macroinvertebrate community in both Swiss hydropeaked rivers and those that have a (near-) natural flow regime. This index is intended to facilitate assessments both before and after the implementation of mitigation or restoration measures, enabling analyses of stressor-specific deficiencies and causes, as well as monitoring the effectiveness of measures. Additionally, the new index was compared with a state-of-the-art habitat modeling technique. Our hypotheses are as follows:

- a. Unlike traditional semi-quantitative multi-habitat sampling methods, such as the Swiss IBCH (FOEN, 2019a), a stressor-specific hydropeaking index can be developed based on field-screening methods, offering a time- and cost-efficient alternative.
- b. The effects of hydropeaking on macroinvertebrate communities are best captured using metrics specifically sensitive to hydrological alteration. Recently developed metrics, such as the proportion of surface-to-interstitial taxa, provide a more effective assessment than traditional abundance-based metrics and can ultimately be integrated into a multimetric index.

c. The univariate modeling approach based on the generalized macroinvertebrate flow-velocity preference curve developed by Schmidlin et al. (2023) (Chapter 5.2.3) can be validated against the data collected in this study and changes induced by hydropeaking in the availability of hydraulically suitable habitats can be captured. However, we expect that the habitat modeling outcomes don't align with the multimetric index developed in this study, due to the implicit differences underlying the two methods.

To test these hypotheses, we structured our work into four distinct work packages (WPs):

- 1. We typified Swiss hydropeaked river reaches, identified comparable river reaches with a (near-) natural flow regime as hydrological references, and defined representative study sites to conduct our research (WP 1; Chapter 2).
- 2. We defined sampling and identification methods for aquatic macroinvertebrates along with relevant environmental variables (WP 2; Chapter 3). These variables encompass descriptors of hydropeaking intensity and the broader environmental context relevant to the established macroinvertebrate community.
- 3. Based on WP 1 and WP 2 we developed a hydropeaking-sensitive assessment index (WP 3; Chapter 4).
- 4. We developed habitat models for selected study sites and applied univariate modeling approaches to assess hydropeaking-induced changes in the availability of hydraulically suitable habitats. The results were then compared with the index developed in WP 3 (WP 4; Chapter 5).

2 River typification and study sites selection (WP 1)

For a comprehensive study yielding generally applicable conclusions, it is imperative to typologically define hydropeaked river reaches and establish representative study sites. Evaluating the ecological status of a hydropeaked river involves analyzing deviations in the established aquatic macroinvertebrate community compared to equivalent reference rivers, i.e., rivers with similar characteristics. Hence, assessing macroinvertebrate data from (hydrologically) unaffected reference sites is crucial for a thorough evaluation.

2.1 River typification

2.1.1 Hydropeaked rivers

To typify and select Swiss river reaches affected by hydropeaking, we conducted the following four steps:

- 1. We selected 53 of the around 100 hydropower plants with obligation to mitigate hydropeaking ("sanierungspflichtig" according to the cantonal planning) and the corresponding hydropeaked rivers according to a WWF map (no more available).
- 2. We subdivided the hydropeaked rivers into reaches, considering factors such as the location of hydropower plant water release, presence of large tributaries, lakes, and additional hydropower plants. Only reaches with Strahler order ≥ 3 were considered for subsequent analysis, while small single sections (< 1 km) were excluded. This division and pre-selection yielded a total of 53 hydropeaked river reaches spanning 480 kilometers.</p>
- 3. We defined criteria deemed relevant for typifying hydropeaked rivers, which are also pertinent to the macroinvertebrate community (Table 1). While river morphology and tributaries were not considered at this stage, they were evaluated later during the selection of the study sites (Chapter 2.2) and especially during the selection of environmental data for further analyses (Chapter 3.3).
- 4. We processed and extracted the defined criteria in GIS, utilizing them in four models employing Hierarchical Clustering on Principle Components (HCPC) applied to multiple factor analyses (MFA). This approach enabled the identification of the most significant criteria and finally the categorization/typification of hydropeaked river reaches (Table 2, Figure 1). HCPC facilitates the integration of principal component methods with clustering methods. As our criteria comprised mixed data types (continuous and categorical variables), MFA was applied as the principal component method. Dendrograms were utilized to visualize the results generated by hierarchical clustering. Statistical analyses were performed using R version 4.2.2 (R Core Team, 2023), with HCPC and MFA executed using the R package "FactoMineR" (Le et al., 2008), and dendrograms visualized using the R package "factoextra" (Kasssambara & Mundt, 2020).

Table 1. Criteria defined for the typification of hydropeaked river-reaches. Classification indicates the classes considered for the analyses at the reach level (n=53) and whether the most frequent class or the mean of the classes was used if the reach comprised more than one class.

Criterion	Classification	Source & Comment
Biogeographical region	Northern Alps, Southern Alps, Jura, Central Plateau, Western Central Alps, Eastern Central Alps; most frequent class	Biogeographical regions (FOEN, 2020)
Strahler order	1 – 9; most frequent class	Strahler stream order (FOEN, 2014)
Mean annual natural discharge	Small (0.05 m 3 /s), medium (0.05 – 1 m 3 /s), large (> 1 m 3 /s); most frequent class	River typology (FOEN, 2013b)
8	Absolute values; mean	Mean runoff (FOEN, 2013a)
	Lowland (<600 masl), montane (600-1800 masl), alpine (> 1800 masl); most frequent class	River typology (FOEN, 2013b)
Elevation	200-600 masl, 601-1000 masl, 1001-1400 masl, 1401-1800 masl, > 1800 masl; absolute value at the hydropower plant water release	Elevation classes for macroinvertebrate sampling IBCH (FOEN, 2019a); extracted in GIS
Longitudinal slope	Plain (< 0,5 %), moderately steep (0.5-5 %), steep (> 5 %); most frequent class	River typology (FOEN, 2013b)
	Absolute values; mean	Extracted in GIS
Geological bedrock	Carbonate, silicate; most frequent class	River typology (FOEN, 2013b)
Hydropeaking intensity	Flow ratio: $Q_{ratio} = Q_{max} / Q_{min}$	Data of the cantonal planning; for four reaches data complemented by D. Tonolla; for 8 reaches data not available

Table 2. Hierarchical Clustering on Principle Components (HCPC) applied to multiple factor analyses (MFA).

Model Nr	Criteria considered	Significant criteria	Goodness of the model & nr. main groups
1	Biogeographical region, Strahler order, discharge (mean), elevation (IBCH), slope (most frequent class), bedrock	Continuous: Discharge, elevation and Strahler order (p < 0.001) Categorical: Slope and biogeographical region (p < 0.001), bedrock (p < 0.05)	40.4% = 25.6% + 14.8% 3 reach clusters
2	Like model 1 + Q _{ratio}	Like model 1 Q _{ratio} not significant	37.8% = 23.5% + 14.3%: 3 reach clusters
3	Biogeographical region, Strahler order, elevation (IBCH), slope (most frequent class)	Continuous: Elevation and Strahler order (p < 0.001) Categorical: Biogeographical region and slope (p < 0.001)	39.6% = 23.4% + 16.2%: 3 reach clusters
4	Like model 3 + Q _{ratio}	Like model 3 Q _{ratio} not significant	31.5% = 15.4% + 21.1%: 3 reach clusters

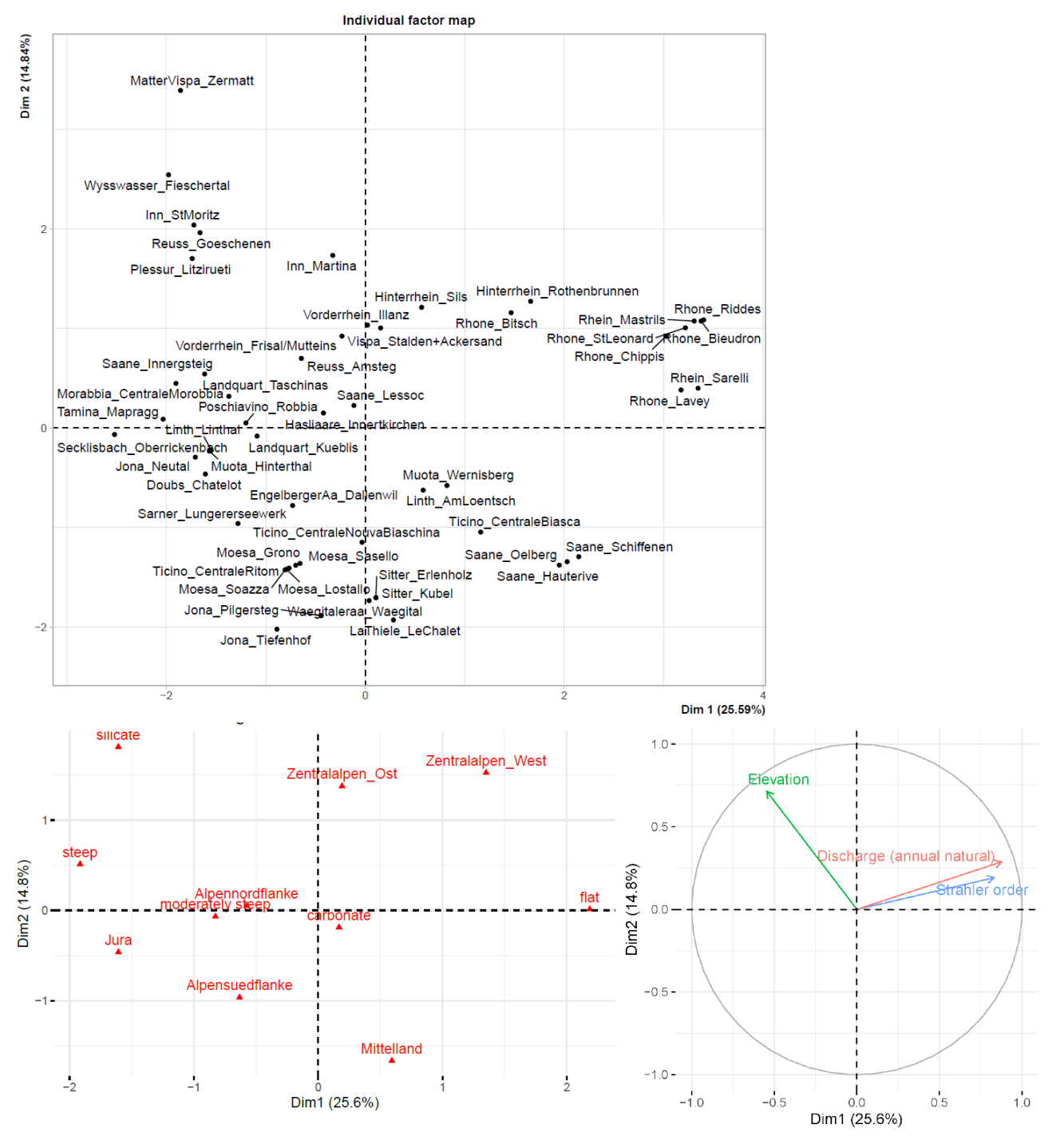


Figure 1. Typification of hydropeaked river-reaches and identification of the most significant criteria. As an example, the results for model 1 are displayed. Top panel: Factor map showing the results (position of hydropeaked reaches) of the Multiple Factor Analysis (MFA). Bottom panels: position of the categorical (left plot) and direction of the continuous (arrows; right plot) criteria defined in Table 2. Note the differences in scales.

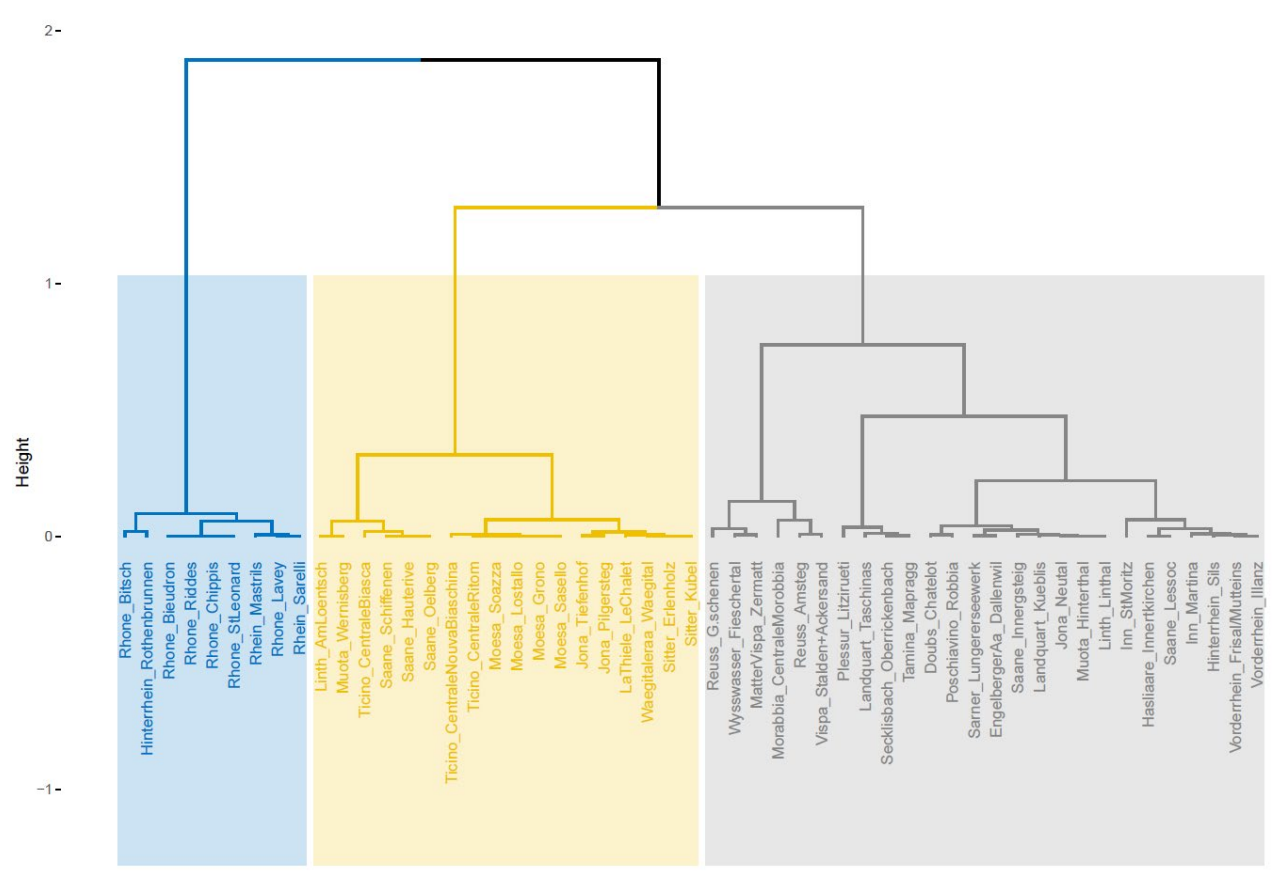


Figure 1. (continued). Typification of hydropeaked river-reaches and identification of the most significant criteria. As an example, the results for model 1 are displayed. Cluster dendogram showing the hydropeaked reach-groups according to Hierarchical Clustering on Principle Components (HCPC). Hydropeaked reaches labels consist of the river name followed by the hydropower plant name.

Model 1 exhibited the best performance, with results closely mirroring those of model 2 (which included the same criteria as model 1 plus Q_{ratio} as a proxy for hydropeaking intensity) (Table 2). 40.4% of the total variation in the distributions of hydropeaked river reaches could be explained by the selected criteria. Among these criteria, the mean annual natural discharge (p < 0.001), elevation (p < 0.001), longitudinal slope (p < 0.001), biogeographical region (p < 0.001), Strahler order (p < 0.001), and geological bedrock (p < 0.05) emerged as the main determinants for categorizing the hydropeaked riverreaches (Figure 1). The inclusion of Q_{ratio} in the models did not alter the results, and Q_{ratio} did not emerge as a significant criterion.

The cluster dendograms analysis grouped the hydropeaked river-reaches into three main clusters/typologies (Table 2, Figure 1). Subsequently, we refined this statistical clustering to define six distinct types of hydropeaked river reaches (Table 3). Type 1a and 1b encompass large plain river reaches primarily situated in the Western or Eastern Central Alps biogeographical regions. Nine reaches of three rivers (Rhône, Alpenrhein, Hinterrhein) belong to these two types. Type 1b reaches exhibit a larger mean annual natural discharge and are located at lower altitudes compared to type 1a reaches. Types 2a and 2b represent plain to moderately steep medium-sized river reaches predominantly located in the Central Plateau and Southern Alps, ranging from 200 to 600 meters above sea level. 18 reaches from nine rivers fall into these types, with multiple reaches from rivers such as the Moesa (n=4), Ticino (n=3), Saane (n=3), Sitter (n=2), and Jona (n=2). Type 2a reaches generally have a higher mean annual natural discharge and are plainer compared to type 2b reaches. Type 3 reaches exhibit substantial diversity, with a total of 26 reaches, most of which are situated in the Northern Alps biogeographical region at elevations ranging from 601 to 1000 meters above sea level. The rivers Reuss, Saane, Inn, and

Vorderrhein were represented by two reaches. Type 3a reaches typically have a lower mean annual natural discharge and are steeper compared to type 3b reaches (Table 3).

Table 3. Characteristics of the six hydropeaked river-reach types. The most represented category is indicated in green color.

Criterium	Type 1a	Type 1b	Type 2a Central	Type 2b	Type 3a	Type 3b
Biogeographical region	Central Alps	Central Alps Northern Alps	Plateau Northern Alps Southern Alps	Southern Alps Central Plateau	Northern Alps Central Alps Southern Alps	Northern Alps Central Alps
Strahler order	6-7	7-8	5,6,7	4,5,6	3,4,5,6	4,5,6,7
Mean annual natural discharge [m ³ /s]	40-60	> 100	10-20 20-40 40-60	< 10 10-20 20-40	< 10 10-20 20-40	< 10 10-20 20-40 40-60
Elevation [masl]	601-1000	200-600	200-600	200-600	601-1000 1001-1400 1401-1800	200-600 601-1000 1401-1800 > 1800
Longitudinal slope [%]	< 0.5	< 0.5	< 0.5	< 0.5 0.5-3	0.5-3 >3	0.5-3
Geological bedrock	Carbonate	Carbonate	Carbonate	Carbonate	Carbonate Silicate	Carbonate
River reach	Rhône-Bitsch, Hinterrhein- Rothenbrunnen	Rhône- Chippis, Rhône-St. Leonard, Rhône- Bieudron, Rhône- Riddes, Rhône-Lavey Alpenrhein- Sarelli, Alpenrhein- Mastrils	Saane- Schiffenen, Saane- Hauterive, Saane- Oelberg, Linth- AmLoentsch, Muota- Wernisberg, Ticino-Biasca	Ticino-Ritom, Ticino- NuovaBiaschina, Moesa-Soazza, Moesa-Lostallo, Moesa-Grono, Moesa-Sassello Jona-Tiefenhof, Jona-Pilgersteig, LaThiele- LeChalet, Wägitaleraa- Wägital, Sitter- Erlenholz, Sitter- Kubel	Reuss-Goeschenen, Reuss-Amsteg, Wyswasser-Fieschertal, MatterVispa-Zermatt Morobbia-Morobbia, Vispa-StaldenAckersand, Plessur-Litzirüti, Landquart-Taschinas, Secklisbach-Oberrick., Tamina-Mapragg	Doubs-Chatelot, Poschiavino- Robbia, Sarner- Lungererseewerk, Engelbergeraa- Dallenwil, Saane- Innergsteig, Landquart- Küblis, Jona- Neutal, Muota- Hinterthal, Linth- Linthal Inn-StMoritz, Hasliaare- Innertkir., Saane- Lessoc, Inn- Martina, Hinterrhein-Sils, Vorderrhein- FrisalMutteins, Vorderrhein- Ilanz

The selection of river reaches aimed to encompass the primary river types affected by hydropeaking. However, reaches classified as type 1a or 1b were excluded due to their substantial glacial influence, resulting in high turbidity (e.g., Rhône reaches), and because they would pose considerable challenges for sampling (high discharge; multiple hydropower plants releasing water into the same river, making it nearly impossible to find suitable base flow conditions). Additionally, reaches characterized by steep gradients (>7%), and/or elevations exceeding 1800 meters above sea level, and/or composed of silicate bedrock (e.g., Reuss-Goeschenen, Wyswasser-Fieschertal, MatterVispa-Zermatt, Tamina-Mapragg) were also excluded. Based on this typification of river reaches, we selected eight hydropeaked rivers for this study: Saane, Ticino, Moesa, Sitter, Thur, Plessur, Landquart, and Vorderrhein (Table 4).

2.1.2 Reference rivers

To effectively evaluate the impact of hydropeaking on the macroinvertebrate community, it is essential to use a comparative scale. Therefore, alongside river reaches affected by hydropeaking, it was necessary to determine river reaches with minimal or no hydrological alteration. Comparative rivers were initially selected based on the same typological criteria outlined in Table 4, consequently ensuring that similar macroinvertebrates communities could be expected under (near-) natural flow conditions. To refine this selection, we sought input from experts, including representatives from WWF, SFV, Aquaplus, and Cantons AG, BE, SG, and ZH. Their feedback and suggestions helped us compile a comprehensive list of 63 potential reference rivers. Successively, we eliminated rivers with an annual natural discharge of less than 2 m³/s and a Strahler order of less than 5, as smaller rivers are not comparable to typical medium-large hydropeaked rivers. Rivers with minor hydrological impacts, such as small water intakes in tributaries or run-off the river hydropower plants without storage capacity, were not discarded. Finally, after thorough consideration and comparison with the selected hydropeaked rivers based on the criteria outlined in Table 4, we ultimately selected four reference rivers: Sense, Verzasca, Thur, and Glenner. These rivers were deemed comparable to the hydropeaked rivers in terms of their characteristics and suitability as reference sites for this study.

Table 4. Characteristics of the selected hydropeaked and reference rivers (light-grey background). Characteristics refer to the river section between the study sites. HP: hydropower plants with obligation to mitigate hydropeaking; RF: residual flow, RO: run-off the river hydropower plant. For the location of the selected study sites see Figure 2. If the river is located in more than one biogeographical region, than the abbreviation of the study site is indicated in bracket. Classes for the hydrological pressure were estimated by D. Tonolla, based on data of the cantonal planning and other studies. Attention, the data in Table 4 can differ from the data collected and analyzed further in Chapter 3.3 because they were summarized in this preliminary step.

River	Hyropeaked	Biogeographical	Strahler	Mean annual	Elevation [masl]	Hydrological	Morphological,	
Nr study sites (Figure 2)	river type (Table 3)	region	stream order	natural discharge [m³/s]	Long- slope [%]	pressure	sedimentological condition	
Saane 8	2a	Central Plateau	7-8	37-57	460-570 < 0.5% (0.5-5%)	Large 3 HPs (Hauterive, Oelberg, Schiffenen)	Natural to heavily impaired morphology Carbonate sediment Glaciation 0%	
Sense	Reference for Saane	Central Plateau	6-7	8-10	485-580 0.5-5%	None (natural regime)	Natural to heavily impaired morphology Carbonate sediment Glaciation 0%	
Ticino 3	2a	Southern Alps	6	41-67	230-265 < 0.5%	Medium-Large 2 HPs (Biasca, Nuova Biaschina)	Less to heavily impaired morphology Carbonate sediment Glaciation < 0.5%	
Moesa 8	2b	Southern Alps	5	7-20	235-470 0.5-5%	Medium 4 HPs (Soazza, Lostallo, Grono, Sassello)	Natural to artificial morphology Carbonate sediment	

							Glaciation < 0.5%
Verzasca	Reference				575-740	None (mat. 1	Natural morphology
3	for Moesa (and Ticino)	Southern Alps	5	5-9	0.5-5%	None (natural regime)	Silicate sediment
							Glaciation 0% Natural to
Sitter	2b	Northern Alps (S1, SR)	6	7-12	475-600 (460 Thur)	Medium	heavily impaired morphology
7 (incl. 1 in the Thur)		Central Plateau (S2-S6)	(7 Thur)	(38 Thur)	< 0.5% 0.5-5%	1 HP (Kubel)	Carbonate sediment
							Glaciation 0%
Thur	D 0	Northern Alps			475-640		Natural to heavily impaired morphology
5	Reference for Sitter	(TH1-TH3) Central Plateau (TH4, TH5)	5-7	9-25	< 0.5% 0.5-5%	Near-natural (some ROs)	Carbonate sediment
							Glaciation 0%
Plessur		Eastern Central			1040- 1400	Small-Medium	Natural morphology
4	3a	Alps	5-6	2-5	0.5-5% (>5%)	1 HP (Litzirüti)	Carbonate sediment
							Glaciation 0% Natural
Obere Glenner					1145- 1375		morphology
(Lugnezer Ast)	Reference for Plessur	Eastern Central Alps	6	2-3	0.5-5%	None (natural regime)	Carbonate sediment
2					>5%		Glaciation < 0.5%
Landquart					575-835	Medium	Less to heavily impaired morphology
5	3b	Eastern Central Alps	5-6	11-23	0.5-5%	2 HPs (Küblis, Taschinas)	Carbonate sediment
							Glaciation < 1%
Vorderrhein					605-780	Large	Natural to heavily impaired morphology
6	3b	Eastern Central Alps	6-7	23-53	< 0.5% 0.5-5%	2 HPs (Frisal/Mutteins, Ilanz 1 & 2)	Carbonate sediment
	D.C.						Glaciation < 2% Natural to less impaired
Untere Glenner	Reference for Landquart	Eastern Central	6	11-13	710-825	Near-natural (one tributary	morphology Carbonate
4	and Vorderrhein	Alps	v	11-13	0.5-5%	RF)	sediment
	_						Glaciation < 1.5%

2.2 Determination of study sites

To comprehensively assess the ecological impacts of hydropeaking on the macroinvertebrate community, it is essential to account for both the hydropeaking intensity and the morphological/sedimentological condition of the river. Since hydropeaking intensity typically decreases with increasing distance from the hydropower plant water release due to retention effects and tributaries (Hauer et al., 2013; Greimel et al., 2025), it is imperative to distribute study sites along the longitudinal river profile based on a gradient of hydrological and morphological/sedimentological conditions.

The following criteria were established for the selection of study sites:

- 1. The study sites should be located within the designated rivers as outlined in Table 4.
- 2. For reaches in hydropeaked rivers, study sites should include areas representing both the highest and lowest hydropeaking intensities. The highest intensity areas are typically found in close proximity to the hydropower plant water release, while the lowest intensity areas are usually located in the lower quarter of the considered river reach or upstream of any other water release. Additionally, an area within the residual flow section, as close as possible to the hydropower plant water release, could be considered and used for comparative purposes.
- 3. Study sites should incorporate, where available, areas with different morphological/sedimentological conditions. Additionally, areas downstream of significant tributaries (Strahler order ≥ 3) should also be considered. These tributaries may alter the hydrological conditions in the main river, potentially enlarging the channel cross-section downstream of their confluence and influencing the morphological/sedimentological condition. Moreover, they may serve as potential refuge habitats and sources of recolonization for macroinvertebrate larvae (Bruno et al., 2016; Milner et al., 2019).
- 4. Whenever feasible, study sites should be selected to encompass comparable flow velocity gradients and minimize possible local morphological/sedimentological effects. To achieve this, study sites should incorporate gravel bars or be situated near morphologically unconsolidated riparian areas or (near)-natural morphological structures.

A total of 59 study sites were defined along the 11 rivers. Among these, 34 sites were located in hydropeaked river reaches, seven in reaches with residual flow conditions, and 18 in reaches with (near-) natural flow regimes (reference reaches) (Figure 2; Table 5).

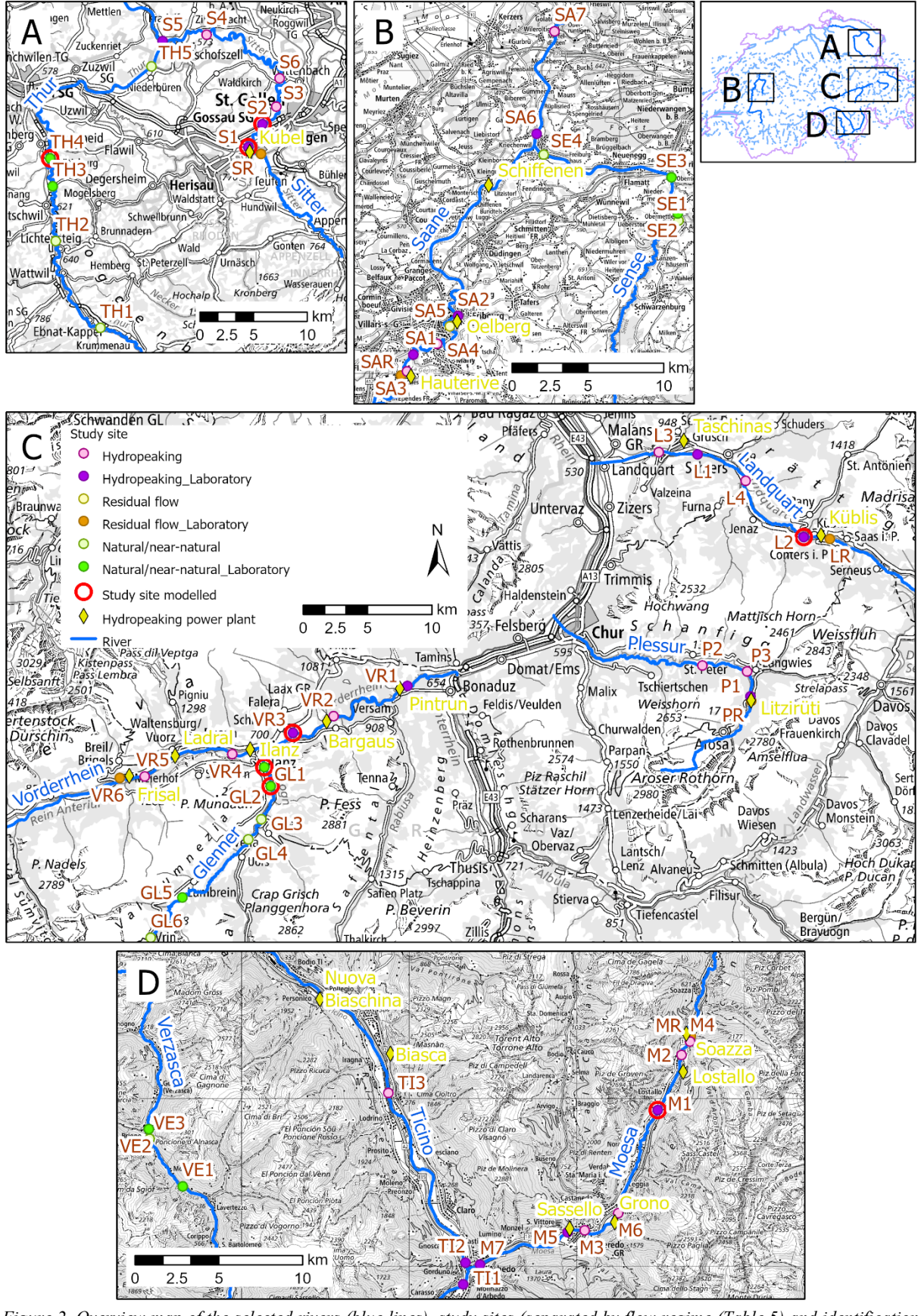


Figure 2. Overview map of the selected rivers (blue lines), study sites (separated by flow regime (Table 5) and identification method (Chapter 3.2)), and hydropeaking power plants (yellow). Background map: Swiss National Map (© Swisstopo).

3 Sampling and identification of macroinvertebrates (WP 2)

3.1 Macroinvertebrate sampling design

Macroinvertebrates were sampled at all 59 study sites during the priority sampling period outlined by FOEN (2019a), before the snow and glacier melt, from March to April in both 2022 and 2023. However, due to a flood event occurring a few days before the scheduled sampling date, two study sites each in the Sense (SE2, SE3) and the Thur (TH3, TH4) were sampled again approximately one month later (i.e., outside the optimal sampling period). Consequently, a total of 63 sites were sampled (Table 5). While it is possible that a few species of mayflies, stoneflies, and caddisflies were no longer present due to emergence, this is not expected to significantly impact the analyses and interpretation of the results (P. Stucki personal communication).

At each study site, 12 benthic macroinvertebrate samples were collected during daylight hours using a kick net with a sampling area of 25 x 25 cm and a mesh size of 500 μm. Four transects (T1 – T4) were established from downstream to upstream along a gravel bar, with three samples (1-3) taken per transect. These samples were collected from the bar margin to the in-stream area along a hydraulic gradient, aiming to capture taxa with different hydraulic preferences (Figure 3). Transect T1 was located at the lower end of the gravel bar, corresponding to the habitat type run/glide. Transect T2 was placed in the transition area between T1 and T3, immediately after the slope change. Transect T3 was located within the slope change, representing the habitat type riffle. Transect T4 was placed in the transition area at the gravel bank head prior the slope change, corresponding to the habitat type run/glide. The specific location of transects and habitat types may vary depending on prevailing conditions at each study site. For example, at sites with a homogeneous gravel bar with little mesohabitat variation or at steep sites where no gravel bar is present. Nonetheless, the transects delineated "representative" habitat types, and the samples varied in their distance to the waterline and hydraulic conditions. Sample 1 was positioned near the bar in the permanently wetted area, sample 3 was furthest from the bar and corresponded to the deepest still wadable or fastest flowing location, and sample 2 was placed between samples 1 and 3 (Figure 3). Sampling in hydropeaked reaches was conducted in the permanently wetted area during base flow. For this purpose, operators of the hydropeaking power plants were informed and collaborated to ensure safe fieldwork. The decision to sample only along gravel bars aimed to capture habitats that were as morphologically unaltered as possible, thereby better reflecting the hydrological/hydraulic stressor on the macroinvertebrate community.



Figure 3. Example for transects (T1 - T4) and samples distribution (1 - 3). Left: Sitter; Background map: \mathbb{Q} Swisstopo, Swissimage: Right: Moesa.

3.2 Sample treatment and identification of taxa

3.2.1 Field-screening

In total, 756 samples (63 sites x 12 samples) were collected, identified, and counted in the field using a field-screening method (Table 5). This method allows for the estimation of abundances of various macroinvertebrate taxa directly in the field. It offers the advantage of reducing time effort, costs, and the number of animals killed compared to traditional sampling methods and laboratory identification. In Switzerland, a field-screening method is utilized, for instance, to compare reference sites with sites affected by wastewater pollution (module G for water quality analysis according to Ilg et al., 2022). Similarly, in Austria, a field-screening method is employed as a rapid field assessment for an orienting estimation of the ecological status class ("screening method" according to Ofenböck et al., 2019).

After sampling, each individual sample was meticulously separated from coarse inorganic material such as stones and gravel, and then transferred to a laboratory tray filled with water including a marked subsample grid (4 x 4) (Figure 4). Large organic materials such as leaves and branches as well as from remaining smaller inorganic materials like gravel and sand were extracted from the samples. Macroinvertebrates were then identified in the field with the naked eye up to the lowest possible taxonomic level (Table 6) and the abundance of each taxonomic group was recorded. It's important to note that within a taxon, the lowest determinable taxonomic level could vary, especially as smaller individuals in early stages may not exhibit distinct identification features. For taxa with high abundance or small individuals (e.g., taxa of the family Chironomidae), estimates were made using the subsample grid to extrapolate their abundance. For example, if one grid of the laboratory tray was counted for taxon X, the count was multiplied by 16 to estimate the total abundance. Extrapolations were subject to a plausibility check, involving a rough count of a second cell or cell combination, to verify whether the magnitudes of the counts matched. Throughout the identification process, attention was paid to movements such as swimming behavior and gill movements, as well as visual characteristics like colors, to facilitate the distinction between taxa.





Figure 4. Left: Identification setting in the field with one person identifying and counting macroinvertebrates, and another person recording taxa names and numbers of individuals. Right: Subsample grid with identification protocol.

Table 5. Study sites used for field-screening and laboratory identification as well as for habitat modeling (Chapter 5). SE2, SE3, TH3 and TH4 were sampled twice because of a flood event (Chapter 3.1). Study sites in light grey were not used for further analyses. For study location see Figure 2.

River	Study site	Flow regime	Sampling date	Field- screening	Laboratory	Modelin
Moesa	M1	Hydropeaking	02.03.2022	X	X	X
Moesa	M2	Hydropeaking	03.03.2022	X		
Moesa	M3	Hydropeaking	03.03.2022	X		
Moesa	M4	Hydropeaking	04.03.2022	X		
Moesa	M5	Hydropeaking	04.03.2022	X	X	
Moesa	M6	Hydropeaking	05.03.2022	X		
Moesa	M7	Hydropeaking	05.03.2022	X	X	
Moesa	MR	Residual flow	04.03.2022	X	X	
Ticino	TI1	Hydropeaking	05.03.2022	X	X	
Ticino	TI2	Hydropeaking	06.03.2022	X	X	
Ticino	TI3	Hydropeaking	06.03.2022	X		
Sitter	S1	Hydropeaking	21.03.2022	X	X	X
Sitter	S2	Hydropeaking	21.03.2022	X	X	X
Sitter	S3	Hydropeaking	22.03.2022	X		
Sitter	S4	Hydropeaking	22.03.2022	X		
Thur	S5	Hydropeaking	23.03.2022	X	X	
Sitter	S6	Hydropeaking	23.03.2022	X		
Sitter	SR	Residual flow	22.03.2022	X	X	
Saane	SA1	Hydropeaking	24.03.2022	X	X	
Saane	SA2	Hydropeaking	25.03.2022	X	X	
Saane	SA3	Hydropeaking	26.03.2022	X	71	
Saane	SA4	Hydropeaking	26.03.2022	X		
Saane	SA6	Hydropeaking	27.03.2022	X	X	
Saane	SA7	Hydropeaking	27.03.2022	X	Α	
Saane	SAR	Residual flow	25.03.2022	X	X	
Saane	SAS	Residual flow		X	Λ	
	L1	Hydropeaking	26.03.2022	X	X	
Landquart	L1 L2		10.04.2022	X	X	X
Landquart		Hydropeaking	11.04.2022		Λ	Λ
Landquart	L3	Hydropeaking	12.04.2022	X		
Landquart	L4	Hydropeaking	13.04.2022	X	37	
Landquart	LR	Residual flow	11.04.2022	X	X	
Plessur	P1	Hydropeaking	29.04.2022	X	X	
Plessur	P2	Hydropeaking	29.04.2022	X		
Plessur	P3	Hydropeaking	30.04.2022	X		
Plessur	PR	Residual flow	29.04.2022	X	X	
Verzasca	VE1	Natural/near-natural	03.04.2023	X	X	
Verzasca	VE2	Natural/near-natural	03.04.2023	X		
Verzasca	VE3	Natural/near-natural	02.04.2023	X	X	
Vorderrhein	VR1	Hydropeaking	09.04.2023	X	X	
Vorderrhein	VR2	Hydropeaking	08.04.2023	X		
Vorderrhein	VR3	Hydropeaking	07.04.2023	X	X	X
Vorderrhein	VR4	Hydropeaking	07.04.2023	X		
Vorderrhein	VR5	Hydropeaking	08.04.2023	X		
Vorderrhein	VR6	Residual flow	08.04.2023	X	X	
Untere Glenner	GL1	Natural/near-natural	09.04.2023	X	X	X
Untere Glenner	GL2	Natural/near-natural	09.04.2023	X	X	X
Untere Glenner	GL3	Natural/near-natural	10.04.2023	X		11
Untere Glenner	GL3 GL4	Natural/near-natural	10.04.2023	X		
Obere Glenner	GL4 GL5	Natural/near-natural	19.04.2023	X	X	
	GL5 GL6	Natural/near-natural	19.04.2023	X	21	
Obere Glenner						
Obere Glenner Sense	SE1 (flood)	Natural/near-natural	16.03.2023	X		

Sense	SE3 (flood)	Natural/near-natural	17.03.2023	X		
Sense	SE4 (flood)	Natural/near-natural	17.03.2023	X		
Sense	SE2	Natural/near-natural	22.04.2023	X	X	
Sense	SE3	Natural/near-natural	22.04.2023	X	X	
Thur	TH1 (flood)	Natural/near-natural	19.03.2023	X		
Thur	TH2 (flood)	Natural/near-natural	19.03.2023	X		
Thur	TH3 (flood)	Natural/near-natural	18.03.2023	X		
Thur	TH4 (flood)	Natural/near-natural	18.03.2023	X		
Thur	TH5 (flood)	Natural/near-natural	19.03.2023	X		
Thur	TH3	Natural/near-natural	27.04.2023	X	X	
Thur	TH4	Natural/near-natural	27.04.2023	X	X	X

Pupae and larvae were counted together, as we believe that the presence of pupae indicates the entire life cycle of a species and should therefore be assessed. Except for Chironomidae (1877 pupae) and Simuliidae (311 pupae), pupae were rarely (Rhyacophilidae 9 pupae, Diamesinae and Trichoptera each 8 pupae) or not found for all other taxa. Terrestrial invertebrates were excluded from further analyses. Adult Elmidae were counted together with Elmidae larvae due to their aquatic life stage. Adults belonging to the orders Ephemeroptera, Plecoptera, and Trichoptera (EPT; mayflies, stoneflies, caddisflies) were collected, if observed at the study sites, and then sent to Aquabug (Pascal Stucki) for further identification (Chapter 3.2.2).

648 samples of 54 study sites were used for further analysis. These samples encompassed a total of 110,647 specimens, with approximately 57% (n=62,597) belonging to the EPT (Table 6; Annex 8.1).

Table 6. Field-screening identification level of taxa found (≥ 1 specimen) and used for final analyses. In brackets: number of specimens belonging to the orders Ephemeroptera, Plecoptera, and Trichoptera (EPT; mayflies, stoneflies, caddisflies). GR: species group.

Taxonomic level	Taxon
Phylum	Nemathelminthes
Class	Oligochaeta, Copepoda
Order	Plecoptera (4 specimens), Trichoptera (36 specimens), Diptera
Superfamily	Plecoptera: Perloidea (4 specimens)
Family	Seriata: Planariidae Arhynchobdellida: Hirudinidae Pulmonata: Lymnaeidae Coleoptera: Gyrinidae, Hydraenidae, Scirtidae Diptera; Athericidae, Blephariceridae, Ceratopogonidae, Chironomidae, Empididae, Limoniidae/Pediciidae, Psychodidae, Simuliidae, Stratiomyidae, Tabanidae, Tipulidae Ephemeroptera: Baetidae (5 specimens), Heptageniidae (2 specimens), Leptophlebiidae (12 specimens) Plecoptera: Chloroperlidae (677 specimens), Nemouridae (79 specimens), Perlidae (48 specimes), Perlodidae (83 specimens), Taeniopterygidae (1073 specimens) Trichoptera: Glossosomatidae (8 specimens), Goeridae (1 specimen), Limnephilidae (15 specimens),
Subfamily	Philopotamidae (24 specimens), Polycentropodidae, (50 specimens), Psychomyiidae (23 specimens), Rhyacophilidae (9 specimens) Diptera Chironomidae: Diamesinae
Tribe	Diptera: Eriopterini
	Myida Dreissenidae: Dreissena*
	Amphipoda Gammaridae: Gammarus
	Coleoptera Elmidae: Elmis
	Heteroptera Corixidae: Micronecta
	Diptera Limoniidae /Pediciidae: Antocha, Dicranota, Hexatoma
C	Ephemeroptera Ephemerellidae: Ephemerella (46 specimens)
Genus	Ephemeroptera Ephemeridae: Ephemera (10 specimens)
	Ephemeroptera Heptageniidae: Ecdyonurus (2184 specimens), Epeorus (86 specimens), Rhithrogena (12621 specimens)
	Ephemeroptera Leptophlebiidae: Habroleptoides (58 specimens)
	Plecoptera Leuctridae: Leuctra (9151 specimens)
	Plecoptera Nemouridae: Amphinemura (199 specimens), Nemoura (52 specimens), Protonemura (286

	specimens)
	Plecoptera Perlidae: Dinocras (29 specimens), Perla (58 specimens)
	Plecoptera Perlodidae: Perlodes (42 specimens), Isoperla (817 specimens)
	Plecoptera Taeniopterygidae: Rhabdiopteryx (1 specimen)
	Trichoptera Hydropsychidae: Hydropsyche (419 specimens)
	Trichoptera Lepidostomatidae: Lepidostoma (5 specimens)
	Trichoptera Limnephilidae: Allogamus (8060 specimens)
	Trichoptera Rhyacophilidae: Rhyacophila (140 specimens)
	Trichoptera Sericostomatidae: Sericostoma (58 specimens)
	Isopoda Asellidae: Asellus aquaticus
	Ephemeroptera Baetidae: Baetis alpinus (16229 specimens), Baetis rhodani (9090 specimens)
Species	Ephemeroptera Ephemerellidae: Torleya major (4 specimens)
Species	Ephemeroptera Heptageniidae: Epeorus alpicola (3 specimens)
	Trichoptera Rhyacophilidae: Rhyacophila GR sensu str. (503 specimens), Rhyacophila torrentium
	(276 specimens), Rhyacophila tristis (12 specimens)
Unranked	Hydracarina (general term for many families of water mites)

^{*} Neozoon

3.2.2 Laboratory

Despite the promising results obtained through field-screening methods, also in hydropeaked rivers (Auhser et al., in prep), it's important to acknowledge their limitations. These methods may lead to underestimated abundances of certain taxa and could potentially miss small individuals and taxa with low abundances (Humphrey et al., 2000; Metzeling et al., 2003; Nichols & Norris, 2006; Gillies et al., 2009). Therefore, for quality control and evaluation of the field-screening method, the 12 individual samples from approximately 57% of the study sites were fixed with about 80% non-denatured ethanol in the field. A total of 370 samples (excluding two samples from the Plessur, P1-T3-3 and P1-T4-3, which were lost) from 31 study sites were then transported to the ZHAW laboratory (Table 5). There, samples were separated from any remaining organic and inorganic material. Macroinvertebrates were then identified using the identification key of Tachet et al. (2000) and subsequently counted. After the laboratory determination at the ZHAW, EPT-taxa underwent further identification by Aquabug. Like for the field-screening dataset, pupae and larvae were counted together (Chapter 3.2.1). Except for Chironomidae (4364 pupae) and Simuliidae (133 pupae), pupae were rarely (Heteroptera 1 pupa, Rhyacophilidae 2 pupae) or not found for all other taxa. Terrestrial invertebrates were excluded from further analyses. Adult Elmidae were counted together with Elmidae larvae. Adult-EPT served for the identification of the EPT-larvae. At the Aquabug laboratory, they were determined, whenever possible, at the species level. Early larval stages, poor preservation conditions of individuals, or missing characteristics have in some cases led to identification of EPT-taxa at the genus level or, rarely, at the family or superfamily level (Table 7).

370 samples of 31 study sites were used for further analysis. These samples encompassed a total of 210,547 specimens, with approximately 49% (n=103,864) belonging to the EPT (Table 7; Annex 8.1).

Table 7. Laboratory identification level of taxa found (≥ 1 specimen) and used for final analyses. In brackets: number of specimens belonging to the orders Ephemeroptera, Plecoptera, and Trichoptera (EPT; mayflies, stoneflies, caddisflies). CX: species complexes, i.e., 2-3 species that cannot, or not yet, be distinguished. GR: species group.

Taxonomic level	Taxon
Phylum	Nemathelminthes
Class	Hirudinea, Oligochaeta, Ostracoda, Copepoda
Order	Heteroptera
	Seriata: Planariidae Arhynchobdellida: Erpobdellidae
··	Pulmonata: Lymnaeidae, Planorbidae
Family	Sphaeriida: Sphaeriidae
	Amphipoda: Gammaridae
	Coleoptera: Dryopidae, Dytiscidae, Gyrinidae, Haliplidae, Hydraenidae, Hydrophilidae, Scirtidae

	Diptera: Ceratopogonidae, Chironomidae, Empididae, Psychodidae, Simuliidae, Stratiomyidae, Tabanidae, Tipulidae
	Plecoptera: Chloroperlidae (35 specimens), Perlidae (116 specimes), Perlodidae (1 specimen) Trichoptera: Glossosomatidae (31 specimens), Leptoceridae (14 specimens), Limnephilidae (13 specimens), Rhyacophilidae (2 specimens)
Subfamily	Diptera Chironomidae: Diamesinae, Orthocladiinae, Tanypodinae
Subfamily	Trichoptera Glossosomatidae: Agapetinae (2 specimens)
Tribe	Diptera Chironomidae: Tanytarsini, Chironomini
	Coleoptera Elmidae: Elmis, Esolus, Limnius, Oulimnius, Riolus
	Diptera Chironomidae: Pseudodiamesa
	Diptera Blephariceridae: Blepharicera, Liponeura, Hapalothrix Diptera Limoniidae /Pediciidae: Antocha, Hexatoma, Molophilus, Rhabdomastix, Rhypholophus, Dicranota, Eloeophila
	Ephemeroptera Heptageniidae: Ecdyonurus (1923 specimens), Rhithrogena (6907 specimens)
	Plecoptera Chloroperlidae: Chloroperla (250 specimens)
	Plecoptera Leuctridae: Leuctra (745 specimens)
	Plecoptera Nemouridae: Nemoura (14 specimens), Protonemura (788 specimens)
Genus	Plecoptera Perlidae: Dinocras (30 specimens), Perla (16 specimens)
Genus	Plecoptera Perlodidae: Isoperla (420 specimens)
	Plecoptera Taeniopterygidae: Brachyptera (106 specimens), Rhabdiopteryx (698 specimens)
	Trichoptera Goeridae: Silo (1 specimen)
	Trichoptera Hydroptilidae: Hydroptila (19 specimens)
	Trichoptera Limnephilidae: Potamophylax (2 specimens)
	Trichoptera Philopotamidae: Wormaldia sp. (1 specimen)
	Trichoptera Polycentropodidae: Polycentropus (86 specimens)
	Trichoptera Psychomyiidae: Tinodes (1 specimen)
	Trichoptera Rhyacophilidae: Rhyacophila (37 specimens)
	Trichoptera Sericostomatidae: Sericostoma (71 specimens)
	Littorinimorpha Hydrobiidae (Tachet): Potamopyrgus antipodarum*
	Isopoda Asellidae: Asellus aquaticus Diptera Athericidae: Atherix ibis, Ibisia marginata
	Ephemeroptera Baetidae: Acentrella sinaica (7 specimens), Alainites muticus (249 specimens), Baetia alpinus (20689 specimens), Baetis GR fuscatus (1 specimen), Baetis GR lutheri (87 specimens), Baetis lutheri (835 specimens), Baetis rhodani (19199 specimens), Baetis vardarensis (108 specimens)
	Ephemeroptera Caenidae: <i>Caenis macrura</i> (2 specimens)
	Ephemeroptera Ephemerellidae: Ephemerella mucronata (28 specimens), Torleya major (10
	specimens), Serratella ignita (11 specimens)
	Ephemeroptera Ephemeridae: Ephemera danica (20 specimens)
	Ephemeroptera Heptageniidae: Ecdyonurus alpinus (1 specimen), Ecdyonurus helveticus (755 specimens), Ecdyonurus GR helveticus (223 specimens), Ecdyonurus picteti (91 specimens), Ecdyonurus torrentis (18 specimens), Ecdyonurus GR venosus (154 specimens), Ecdyonurus venosu (1228 specimens), Electrogena lateralis (42 specimens), Epeorus alpicola (85 specimens), Epeorus assimilis (118 specimens), Heptagenia sulphurea (15 specimens), Rhithrogena allobrogica (460
	specimens), Rhithrogena GR alpestris (219 specimens), Rhithrogena alpestris (1461 specimens),
Species	Rhithrogena carpatoalpina (3 specimens), Rhithrogena corcontica (3 specimens), Rhithrogena
	degrangei (160 specimens), Rhithrogena germanica (4 specimens), Rhithrogena gratianopolitana (121 specimens), Rhithrogena GR hybrida (7 specimens), Rhithrogena hybrida (44 specimens), Rhithrogena GR hybrida spK10 (1281 specimens), Rhithrogena landai (3 specimens), Rhithrogena puthzi (256 specimens), Rhithrogena GR semicolorata (10721 specimens), Rhithrogena semicolorata (979 specimens), Rhithrogena savoiensis (15 specimens), Rhithrogena beskidensis (13 specimens)
	Ephemeroptera Leptophlebiidae: <i>Habroleptoides confusa</i> (86 specimens), <i>Habrophlebia lauta</i> (13 specimens), <i>Habrophlebia eldae</i> (3 specimens), <i>Paraleptophlebia submarginata</i> (7 specimens)
	Ephemeroptera Oligoneuriidae: Oligoneuriella rhenana (55 specimens)
	Ephemeroptera Siphlonuridae: Siphlonurus lacustris (49 specimens)
	Plecoptera Capniidae: Capnia nigra (2 specimens), Capnioneura nemuroides (5 specimens)
	Plecoptera Chloroperlidae: Chloroperla susemicheli (62 specimens), Chloroperla tripunctata (263 specimens), Siphonoperla CV torrentium (5 specimens)
	specimens), Siphonoperla CX torrentium (5 specimens) Plecoptera Leuctridae: Leuctra GR fusca (16622 specimens), Leuctra alpina (1 specimen), Leuctra inermis (8 specimens), Leuctra nigra (1 specimen), Leuctra biellensis (1 specimen), Leuctra hippopu (4 specimens)
	Plecoptera Nemouridae: Amphinemura CX sulcicollis (681 specimens), Amphinemura sulcicollis (8 specimens), Amphinemura triangularis (2 specimens), Nemoura flexuosa (2 specimens), Nemoura

marginata (1 specimen), Nemoura mínima (29 specimens), Nemoura mortoni (303 specimens), Nemurella pictetii (2 specimens), Protonemura intricata (28 specimens), Protonemura lateralis (1 specimen), Protonemura nimborum (5 specimens), Protonemura nitida (2 specimens)

Plecoptera Perlidae: Dinocras cephalotes (23 specimens), Perla grandis (36 specimens), Perla marginata (22 specimens)

Plecoptera Perlodidae: *Dictyogenus alpinus* (10 specimens), *Perlodes microcephalus* (23 specimens), *Isoperla carbonaria* (6 specimens), *Isoperla grammatica* (462 specimens), *Isoperla rivulorum* (63 specimens)

Plecoptera Taeniopterygidae: *Brachyptera risi* (90 specimens), *Rhabdiopteryx CX alpina* (42 specimens), *Rhabdiopteryx neglecta* (200 specimens)

Trichoptera Glossosomatidae: Agapetus nimbulus (15 specimens), Agapetus ochripes (2 specimens), Glossosoma CX conformis (16 specimens)

Trichoptera Goeridae: Silo nigricornis (2 specimens), Silo piceus (2 specimens)

Trichoptera Hydropsychidae: *Hydropsyche dinarica* (9 specimens), *Hydropsyche incógnita* (12 specimens), *Hydropsyche GR instabilis* (220 specimens), *Hydropsyche instabilis* (210 specimens), *Hydropsyche pellucidula* (1 specimen), *Hydropsyche siltalai* (122 specimens), *Hydropsyche tenuis* (3 specimens)

Trichoptera Lepidostomatidae: Lepidostoma hirtum (1 specimen)

Trichoptera Limnephilidae: Allogamus auricollis (9083 specimens), Chaetopterygini-Stenophilacini GR auricollis (1 specimen), Chaetopteryx villosa (6 specimens), Drusus biguttatus (446 specimens), Halesus GR digitatus (1 specimen), Halesus radiatus (2 specimens), Metanoea flavipennis (2 specimens). Metanoea rhaetica (1398 specimens), Potamophylax cingulatus (9 specimens)

Trichoptera Odontoceridae: Odontocerum albicorne (9 specimens)

Trichoptera Philopotamidae: Philopotamus ludificatus (26 specimens)

Trichoptera Polycentropodidae: Polycentropus flavomaculatus (12 specimens)

Trichoptera Psychomyiidae: Psychomyia pusilla (90 specimens)

Trichoptera Rhyacophilidae: Rhyacophila GR sensu str. (597 specimens), Rhyacophila CX torrentium (261 specimens), Rhyacophila torrentium (9 specimens), Rhyacophila tristis (12 specimens)

Unranked

Hydracarina (general term for many families of water mites)

3.2.3 Data structure for further analyses

Due to mixed levels of taxonomic resolution in the field-screening and laboratory datasets, all macroinvertebrate data were aggregated to the field-screening level for the comparison of the metrics (Table 10). However, further analyses were carried out to investigate similarities and differences between the different taxonomic levels in order to perform quality control. To minimize the influence of rare species on score calculations and to focus the analyses on dominant assemblage patterns, all taxa present in fewer than 5% of the study sites were excluded. As a result, only taxa occurring in at least three study sites for the field-screening dataset and at least two study sites for the laboratory dataset were considered. Consequently, nine out of 77 taxa were removed from the field-screening dataset, and 36 out of 191 taxa were excluded from the laboratory dataset for further analyses.

3.3 Environmental data

To assess the potential effects of hydro- and geomorphological as well as physico-chemical characteristics of the study site on macroinvertebrate communities, a comprehensive set of 42 environmental variables was selected (Table 8; Annex 8.2). 14 variables were collected at each of the 12 sampling points (Figure 3) within every study site. The exact location of each sampling point was determined using high-precision RTK-GPS (Trimble R10 GNSS; accuracy < 0.025 m horizontally and < 0.05 m vertically, manufacturer's specifications). Water depth and flow velocity were each measured three times around the sampling point, and the resulting measurements were averaged. Flow velocity, determined as the average over 30 seconds, was assessed using a micro propeller device (Flowatch Flowmeter; accuracy \pm 2%, manufacturer's specifications) positioned at approximately 40% of the water depth (above the streambed). Additionally, the distance from each sampling point to the water's edge was recorded using a measuring tape. Degree of substrate clogging and dominant mineral substrate type

^{*} Neozoon

(categories after FOEN, 2019a), density of algal cover, coverage of coarse particulate organic matter (CPOM) and mosses (categories after Thomas & Schanz, 1976; then reclassified into three categories after FOEN, 2019a) were determined by visual assessment of the substrate surface. The substrate data were used to calculate the variables "total number of different substrate types" and "relative proportion of each substrate types". Furthermore, quantitative measurements of conductivity (\pm 0.5 μ S/cm), water temperature (\pm 0.3°C), dissolved oxygen content (\pm 0.2 mg/L), and pH (\pm 0.002) were conducted using a multi-parameter probe (HQ40d / HQ4300, Hach Lange). Turbidity (measured in NTU, Nephelometric Turbidity Unit; \pm 2.0%) was recorded using a portable turbidity meter (2100Q, Hach Lange). These measurements were taken at each study site downstream of transect T1 (Figure 3) at three distinct time points, before macroinvertebrate sampling, and subsequent to sampling transects T2 and T4.

In addition to the 14 variables collected in the field, 28 variables were computed for each study site with ArcGis Pro and R tools based on geodata from third part sources/external providers (Table 8):

- Modeled mean annual natural discharge (reference period 1981-2000) and natural hydrological regime type (FOEN, 2013a) at the downstream transect (T1). The 16 regime types were grouped into four main types: glacial, nival, pluvial, and "jurassisch". All selected study sites belong to the nival (nivo-glaciaire, nival alpin, nival de transition, nival meridional) or pluvial (nivo-pluvial préalpin, pluvial supérieur, pluvial inférieur, nivo-pluvial méridional, pluvio-nival méridional, pluvial meridional) types.
- Eight hydrological variables calculated using the "hydropeak" package (Greimel et al., 2016; Grün et al., 2022) based on flow data with a 15-minute temporal resolution from the six months preceding macroinvertebrate sampling. This extended period ensures an adequate assessment of possible seasonal variations in the frequency and/or intensity of hydropeaking events prior to macroinvertebrate sampling. With respect to the annual life cycle of most sensitive hemilimnic organisms (e.g., EPT taxa), a longer monitoring period adequately captures the relationship between hydropeaking and its effects on the macroinvertebrate community, as the response to hydraulic stress varies between larval stages (Poff et al., 1991; Bacher & Waringer, 1996). All sub-daily flow fluctuations whose intensity exceeded 20% of the expected annual maximum intensity of natural events were retained, as this threshold has been demonstrated relevant for classifying ecologicalflow relationships (Greimel & Zeiringer, 2025). The flow data used for calculating these hydrological variables were obtained from federal and cantonal gauging stations, as well as from hydropower plant operators. For study sites lacking measured flow data in the immediate vicinity, data were reconstructed based on the nearest available flow data and by taking the effects of flow routing and the presence of tributaries with Strahler order ≥ 3 into account. Details on the computation of these flow data can be found in Chapter 3.3.1.
- In addition to the eight hydrological variables, a multimetric hydrological index (CNT_MAFR_RATIO) was computed. This index is designed to summarize hydrological characteristics into a single value, where low values are supposed to represent natural hydrologic conditions (events with high flow ratio (RATIO) and ramping rate (MAFR) occur rarely (CNT)). In contrast, high values represent unnatural conditions with high intensity of hydrological variability (events with high RATIO and MAFR occur frequently (CNT)). Hydrological events can be separated into the increasing (IC) and the decreasing (DC) wave phases. Although models that differentiate between affected and unaffected situations may treat these phases as interchangeable, natural events are typically right-skewed, with lower ramping rates during the decreasing phase compared to the increasing phase (Greimel et al., 2016). This asymmetry allows for better differentiation between natural and unnatural events when the decreasing (DC) wave is analyzed. Consequently, the multimetric hydrological index was based on the decreasing (DC) wave of the events.

$$CNT_MAFR_RATIO = \frac{\frac{CNT_{DC_tot}}{\sqrt{\frac{1}{n}\sum_{i=1}^{n}CNT_{DC_tot}}^2} + \frac{MAFR_{DC_median}}{\sqrt{\frac{1}{n}\sum_{i=1}^{n}MAFR_{DC_median}}^2} + \frac{RATIO_{DC_median}}{\sqrt{\frac{1}{n}\sum_{i=1}^{n}RATIO_{DC_median}}^2}$$

- Upstream distance to the closest hydropeaking water release, computed based on the swissTLM3d (©Swisstopo) using the "linear referencing" toolbox in ArcGis Pro (ESRI). Downstream distances (for example in the case of study sites in residual flow reaches) were assigned a negative value.
- Strahler stream order (FOEN, 2014) at the downstream transect (T1).
- Number of upstream tributaries with Strahler order ≥ 3 located between study sites and standardized by their distance. For study sites with no upstream study site, only tributaries located max. 5000 m (mean distance calculated over all study sites) upstream were considered.
- Swiss ecomorphology level F (FOEN, 2013c; categories after BUWAL, 1998) at the downstream transect (T1).
- Geological bedrock (category: carbonate or silicate; FOEN, 2013b), at the downstream transect (T1).
- Glacier cover and land use type in % of the catchment area upstream of the study site, derived from the Swiss land-use statistics (FSO, 2018; reference period 2013-2018). Land use types were further categorized into "settlement area" and potentially pesticide-intensive "agricultural area" (sum of arable crops, orchards, vineyards and horticultural land).
- Cumulative number of inhabitants, whose wastewater flows through the respective study site, and domestic wastewater discharge in % of the discharge in the receiving watercourse at low flow (Q₃₄₇). Calculations based on the assumption of 375-liter wastewater per person per day (Gulde & Wunderlin, 2024). Number of inhabitants and wasterwater discharge based on data of 2021, while Q₃₄₇ on data of 1999 (Staub et al., 2003) and calculations of 2007 (Schär, 2007, unpubl.). Calculated at the downstream transect (T1).
- Mean diffuse total nitrogen and diffuse total phosphorous inputs into waters (Hutchings et al., 2023) of the catchment area upstream of the study site. Modelled data based on the Swiss land-use statistics (FSO, 2018; reference period 2013-2018) and average climatic conditions with reference year 2020.
- Longitudinal and transversal slope at the study site (i.e., slope between first and last point at each transect) using the coordinates measured with the RTK-GPS.
- Elevation above sea level of the study site, calculated as mean of z-coordinates of all RTK-GPS measurements belonging to the 12 sampling points.
- Swiss biogeographical regions (FOEN, 2020). Since only three study sites (S1, SR, TH3; Figure 2) belong to Northern Alps region, they were regrouped into the Central Plateau region, which corresponds to the region of the other study site on the same river (Sitter, Thur).
- Catchment size upstream of the study site calculated through a hydrological analysis (i.e., computation of flow directions, flow accumulations, etc.) and validated against the topographical catchment areas of Swiss waterbodies 2 km² (FOEN, 2019b).

Table 8. List and description of the environmental variables, grouped into five overarching groups (hydrology, morphology, hydraulic, water quality and topography). The spatial scale describes the spatial representativeness of the variables. SD: Standard Deviation. CPOM: Coarse Particulate Organic Matter. NTU: Nephelometric Turbidity Unit. MI: macroinvertebrate. IC: increasing. DC: decreasing.

Overarching group	Variable	Unit or category	Spatial scale	Statistics or comment
	Mean annual nat. discharge	m ³ /s		
Hydrology	Not bridgelesiaal	■ nival	Reach	
	Nat. hydrological regime type	pluvial		
Hydrology	CNT _{IC_tot} CNT _{DC_tot}	-		Total count of all IC and DC events of the last six month before MI sampling
	$\begin{array}{c} AMP_{IC_median} \\ AMP_{DC_median} \end{array}$	$\frac{m^3/s}{m^3/s}$		Median event-based amplitude of all IC and DC events of the last six month before MI sampling
	$\begin{array}{l} MAFR_{IC_median} \\ MAFR_{DC_median} \end{array}$	m ³ /(s 15 min) m ³ /(s 15 min)	Reach	Median event-based maximum flow rate of all IC and DC events of the last six month before MI sampling
	$\begin{array}{c} RATIO_{IC_median} \\ RATIO_{DC_median} \end{array}$	-		Median event-based ratio of all IC and DC events of the last six month before MI sampling
	CNT_MAFR_RATIO	-		Multimetric hydrological index
Hydrology	Distance study site to HP release	km	Reach	
Hydrology	Strahler order	-	Reach	
Hydrology	Number of tributaries	nr/km 1: none	Reach	
Morphology	Clogging	2: slight/medium 3: strong	Study site	Mean, median and SD of the 12 sampling points
Morphology	Relative proportion (%) of each substrate type Number of substrate types	 mobile blocks > 250 mm natural and artificial surfaces > 250 mm larger mineral sediments 250 mm > x > 25 mm gravel 25 mm > x > 2.5 mm sand and silt < 2.5 mm 	Study site	
Morphology	Ecomorphology	1: natural/near natural 2: slightly modified 3: heavily modified 4: non-natural/artificial	Reach	
Morphology	Geological bedrock	carbonatesilicate	Catchment	
Hydraulic	Water depth	cm	Study site	Mean, median and SD of the 12 sampling points
Hydraulic	Flow velocity	cm/s	Study site	Mean, median and SD of the 12 sampling points
Hydraulic	Distance to water's edge	m	Study site	Mean, median and SD of the 12 sampling points
Water quality	Algae cover Moos cover CPOM cover	1: < 10% 2: 10-50% 3: > 50%	Study site	Mean, median and SD of the 12 sampling points
Water quality	Conductivity	μS/cm	Reach	Mean, median and SD of the three measurements
Water quality	Water temperature	°C	Reach	Mean, median and SD of the three measurements

Water quality	Oxygen	mg/l	Reach	Mean, median and SD of the three measurements
Water quality	рН	-	Reach	Mean, median and SD of the three measurements
Water quality	Turbidity	NTU	Reach	Mean, median and SD of the three measurements
	Glacier cover			
	Settlement area			
Water quality	Agricultural area	%	Catchment	
	(arable crops, orchards, vineyards,			
	horticultural land)			
	Number of	-		
Water quality	inhabitants		Catchment	
water quarity	Domestic wastewater discharge	%		
Water quality	Mean diffuse total			
	nitrogen Mean diffuse total phosphor	kg/ha a	Catchment	
Topography	Longitudinal slope			
	Transversal slope	% 0	Study site	Mean and SD
Topography	Elevation study site	masl	Study site	
Topography	Biogeographical region	Southern AlpsCentral PlateauEastern Central Alps	Catchment	
Topography	Catchment size upstream study site	km ²	Catchment	

3.3.1 Reconstruction of flow data

For 14 out of the total 54 study sites, measured flow data from gauging stations or from hydropower plant operators were available and therefore used for computing the hydrological variables outlined in Table 8. For additional 33 study sites, flow data had to be reconstructed using neighboring measurements and considering flow routing effects. The methodology for this reconstruction varied based on factors such as the presence of tributaries, the location of gauging stations relative to the study site (upstream or downstream), and the availability of cross-section data from the Federal Office for the Environment (FOEN). A decision tree outlining these methodologies is presented in Figure 5.

For tributaries with a Strahler order ≥ 3 located between the gauging station and the study site, their contribution to the total flow was accounted for. When dealing with ungauged tributaries, their hydrograph was estimated as a proportion of the main river's flow. This estimation relied on the monthly mean natural runoff data from the MQ-GWN-CH dataset (FOEN, 2013a) of the last reach of the tributary prior to its confluence, weighted accordingly. For gauged tributaries, the measured flow was routed from the gauging station location to the confluence. If cross-sectional data from the FOEN were available for the tributary, a hydraulic routing method was employed using the 1D version of BASEMENT (version 3.2.0; VAW-ETHZ, 2022). The roughness (Strickler) coefficients were estimated based on those derived for similar rivers in Switzerland by Spreafico et al. (2001). In cases where cross-sectional data were unavailable, a hydrologic routing approach was applied utilizing the Muskingum method (McCarty, 1938). In this case, the parameters K and X, associated with the wave's travel time and attenuation tendency, respectively, were estimated a priori based on the morphological characteristics of each tributary, including factors such as river channel type and the presence of river widenings.

Once the tributary flow was determined, or if there were no tributaries, the flow measurements were

routed along the main channel from the gauging station or hydropower release location to the study site. If the flow measurements were located upstream, the same criteria as for tributaries were followed: hydraulic routing with BASEMENT if FOEN cross sections were available in the modeled reach, or hydrological routing with the Muskingum method if not. In cases where flow measurements were available downstream of a study site, an inverse Muskingum method was employed to reconstruct the potential hydrograph at the study site (Gąsiorowski & Szymkiewicz, 2022). Where FOEN cross sections were available, the potential hydrograph was validated trough hydraulic routing with BASEMENT back to the flow measurement location. The flow contribution from the sub-catchment draining the river reach between the flow measurement location and the study sites was disregarded.

In cases where flow data measurements were not available along the river or its tributaries, no flow data reconstruction was feasible. This circumstance occurred in seven study sites (LR, L2, L4, VE2, VE3, GL5, GL6), for which no hydrological variable could be computed and only rough estimates were possible.

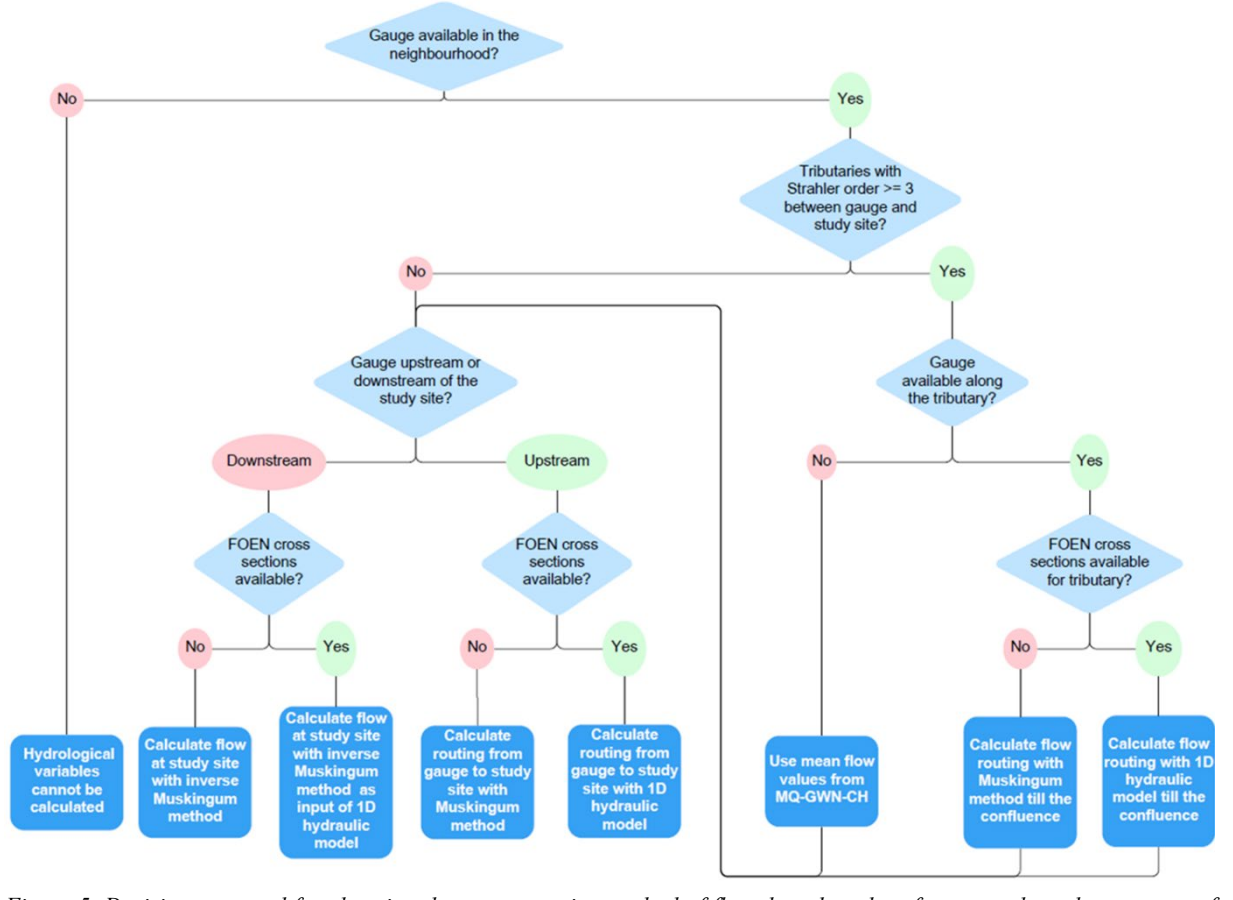


Figure 5. Decision tree used for choosing the reconstruction method of flow data, based on factors such as the presence of tributaries with Strahler order ≥ 3 , the location of gauging stations relative to the study site (upstream or downstream), and the availability of cross-section data from the Federal Office for the Environment (FOEN).

The reliability of the reconstructed flow data was evaluated for each study site, accounting for variations in data quality, availability, and the methodologies employed in the reconstruction process. This assessment was conducted according to the specific criteria outlined in Table 9. These reliability attributes can also be applied to evaluate the hydrological variables specified in Table 8.

Table 9: Overview of the classes and criteria used to assess the reliability of the reconstructed flow data, as well as the study sites belonging to each reliability class. For study site abbreviation and location see Figure 2 and Table 5.

Reliability class	Criteria	Study site
High	Flow data based on measurements from gauging stations or from hydropower releases located in the immediate vicinity (< 1 km from study site)	M7, S5, SA3, SA5, SA6, L3, PR, P3, GL1, SE3
Good	Modelled flow data in absence of tributaries or in presence of gauged tributaries between gauge and study site	TI1, SA1, SAR, SA2, SA4, P1, VE1, GL2, SE2
Moderate	Modelled flow data in presence of ungauged tributaries and/or on reaches without FOEN cross sections	M1, M2, MR, M4, M5, TI2, S1, S2, S3, S4, S6, SA7, L1, P2, VR1, VR2, VR3, VR5, VR6, GL3, GL4
Poor	Presence of uncertainties or inconsistencies either in the flow measurements or in the modelled flow data	M3, M6, TI3, SR, VR4, TH3, TH4
Not Applicable (NA)	Absence of flow measurements; flow data reconstruction not feasible	LR, L2, L4, VE2, VE3, GL5, GL6

3.3.2 Data structure for further analyses

Environmental data were further analyzed using Random Forest (RF), a widely applied machine learning algorithm. RF has been extensively used in ecosystem-related tasks (Pichler & Hartig, 2023), including the prediction of flow requirements for benthic macroinvertebrates (Theodoropoulos et al., 2018). It is known for achieving high prediction accuracy (Pichler & Hartig, 2023) and is less prone to overfitting compared to other ensemble models, such as boosted regression trees (Giri et al., 2019).

For the RF analysis, the environmental data were consolidated into a single set of variables. The empty cells (missing values) for the variables CNT_{IC_tot}, CNT_{DC_tot}, AMP_{IC_median}, AMP_{DC_median}, MAFR_{IC_median}, MAFR_{IC_median}, MAFR_{IC_median}, RATIO_{IC_median} and RATIO_{DC_median} (Table 8) at the study sites lacking flow measurements (LR, L2, L4, VE2, VE3, GL5, and GL6; Table 9) were filled based on the authors' expertise. Additionally, the missing data for the variable "Distance from study site to hydropeaking release" for sites with a (near-) natural flow regime were assigned the value 100,000 to represent the absence of influence from hydropeaking power-plant releases. Study sites in residual flow reaches were excluded from the RF analysis. Furthermore, three artificial variables (two numeric and one categorical), with no capacity to explain the metrics (Table 10), were created as a baseline to assess variable importance after the RF modeling.

Further details can be found in the master thesis by Wirth (2025).

4 Hydropeaking-sensitive assessment index (WP 3)

4.1 Introduction

Using macroinvertebrates for biomonitoring has become a widespread practice worldwide. Given the sensitivity of certain species or species assemblages to environmental changes, macroinvertebrate communities often exhibit dramatic alterations when human activities influence a watercourse. A common practice to assess changes in community structure is to define metrics (e.g., Hering et al., 2006; Birk et al., 2012). These metrics can then be used to assess and evaluate ecosystem impacts and further establish thresholds for implementing mitigation or restoration measures. Metrics can represent various aspects of macroinvertebrate communities, including community structure, diversity, and abundance of occurring taxa, as well as the sensitivity of taxa to specific influences and various ecological traits such as feeding type or locomotion type (Birk et al., 2012).

Human-induced alterations of the ecosystem can substantially affect metric values. For instance, hydropeaking can severely alter flow velocities, shear stress, and sediment composition in a watercourse, thereby affecting factors such as food source availability or reproduction habitats (Bunn & Arthington, 2002). If resident macroinvertebrate communities respond to these changes, it can be expected that corresponding metrics reflecting community adaptation to these habitat characteristics will change accordingly (Statzner & Holm, 1982), such as an increase in specifically rheobiont taxa (Schmutz et al., 2013). These shifts in metric values can subsequently serve as indicators to measure and assess the impact of anthropogenic alterations on river ecosystems.

Several studies from various countries have recently investigated the effects of anthropogenic flow fluctuations on macroinvertebrate communities using (multi-)metric-based assessment tools. Salmaso et al. (2021) provide a comprehensive overview of the latest methodologies from Europe, North America, and South America to support the design of monitoring plans aimed at assessing the ecological impacts of hydropeaking and the effects of possible mitigation strategies. For example, the Canadian Ecological Flow Index (CEFI), developed by Armanini et al. (2011), can be used as a valuable tool for assessing the ecological impact of peaking hydropower plants. It acts as a reliable indicator of flow alteration, making it useful for developing guidelines on ecological water management. In Austria, Leitner et al. (2025) recently introduced a guideline for a multimetric-based assessment tool that uses a combination of the mitigation measures approach and the reference approach to assess the good ecological potential (BMLRT, 2020). This guideline integrates the effects and efficiency of measures with target values for the cenoses based on pre- and post-monitoring of benthic macroinvertebrates. The good ecological potential is defined by the biological values observed when all measures with more than minor positive effects on the cenosis are implemented, while having no significant economic impact (BML, 2025). To classify and evaluate the effects of individual measures on the cenosis, the method uses benchmarks for selected metrics derived from watercourses with no or minimal influence from short-term flow fluctuations (reference sites) which were selected based on comparable typological criteria (e.g., biogeographical region, altitude, catchment areas). Finally, the Austrian multimetric index for assessing the influence of hydropeaking comprises five single metrics that provide a distinct indication regarding anthropogenic hydrological impact.

To implement such multimetric approaches in an assessment tool, standardized individual metrics have to be combined into a single value, integrating various community attributes to provide a comprehensive evaluation of a waterbody's condition. These combinations of single metrics are referred to as multimetric indices (MMIs). Given the diversity and natural variability of the macroinvertebrate cenoses, the use of MMIs is considered suitable. In principle, more than 100 different individual metrics are available to characterize a cenosis (Ofenböck et al., 2019). A crucial aspect in defining such MMIs

lies in the selection of candidate metrics. According to Ofenböck et al. (2004), candidate metrics should be (i) "ecologically relevant to the biological assemblage or community under study" and (ii) "sensitive to stressors and provide a response that can be discriminated from natural variation". In a final verification and reliability test of single metrics (as well as multimetric indices), their stressor-specificity should be examined. This entails determining whether they accurately indicate the influence of a particular stressor or if they are more responsive to general degradation (Vallefuoco, 2022). Therefore, environmental covariates, along with the results of habitat models, can be incorporated into the analysis to discern whether certain factors override the influence of the investigated hydropeaking stressor.

In this study, we developed hydropeaking-sensitive MMIs based on the response of the established aquatic macroinvertebrate community in both Swiss hydropeaked rivers and those that have a (near-) natural flow regime. The main focus was on (i) detecting differences induced by different macroinvertebrate sampling methodology and taxonomic identification levels (field-screening vs laboratory; Chapter 3.2), and (ii) comparing the MMIs with more classical and not stressor-specific methods which often rely on single metrics (e.g., abundance-related metrics, diversity metrics such as Shannon diversity, IBCH). For this purpose, suitable candidate metrics were pre-selected and calculated for each study site located in reaches with a hydropeaking or a (near-) natural flow regime (Chapter 4.2.1). These metrics were then evaluated based on their variability between laboratory and field-screening datasets, their indicative quality regarding hydropeaking sensitivity and natural variability, and how they were influenced by environmental variables such as hydromorphological alterations and pollution (Chapter 4.2.2). Based on these results, MMIs were proposed and calculated for each study site (Chapters 4.3.1 – 4.3.4) and subsequently validated (Chapter 4.3.5).

4.2 Material and methods

4.2.1 Candidate metrics

For the initial analysis, 25 candidate metrics were used to characterize the macroinvertebrate communities, focusing on their abundance, richness, structure, ecological characteristics (traits), and sensitivity to various anthropogenic influences (Table 10). The most common and suitable metrics for the taxonomic level of this study (field-screening level) were selected. However, some commonly used metrics in water quality assessment, such as feeding types and longitudinal zonation of river courses (Ofenböck et al., 2019), were excluded because trait classifications for these metrics are only available at the species level, which is beyond the field-screening scope.

The metrics were further grouped into three overarching groups (Table 10), based on how they represent the macroinvertebrate communities:

- 1. Community structure: Metrics describing fundamental aspects of the macroinvertebrate community, without incorporating trait classifications.
- 2. General ecological state: Metrics reflecting the ecological state in relation to hydromorphological or water quality alterations.
- 3. Hydropeaking sensitivity: Metrics indicating the sensitivity to hydrological alterations.

All metrics in Table 10 were calculated for each study site, whether located in hydropeaking reaches or (near-) natural river (reference) reaches. Study sites in residual flow reaches were excluded from the metric calculations and did not influence the metric selection process (Chapter 4.2.2).

Table 10. List of candidate metrics. Metric calculations according to Ofenböck et al. (2019) and metric classifications according to Fauna Aquatica Austriaca (Moog & Hartmann, 2017), except dom_inter, dom_lentic, dom_lotic, dom_surf, dom_surf_lenit and hp_sen (Working group RHEOPHYLAX (BOKU, Vienna), in prep.), CEFI_Arm (Armanini et al., 2011) and IBCH, DK_IBCH, IG_IBCH (FOEN, 2019a). Taxa classifications for hp_sen, interstitial-surface dwelling, lentic-lotic preference, flow optimum and tolerance (basis for CEFI and CEFI Arm) are reported in Annex 8.3.

Metric name	Overaching group	Description	
ab eph	Community structure	Number of Ephemeroptera – individuals per square meter	
ab ept	Community structure	Number of EPT – individuals per square meter	
ab_ple	Community structure	Number of Plecoptera – individuals per square meter	
ab tot	Community structure	Total number of individuals per square meter	
ab tri	Community structure	Number of Trichoptera – individuals per square meter	
dom ept	Community structure	Dominance (relative abundance) of EPT – individuals within the community	
mar_div	Community structure	Margalef diversity	
nr_eph_taxa	Community structure	Number of Ephemeroptera-taxa	
nr ept taxa	Community structure	Number of EPT-taxa	
nr ple taxa	Community structure	Number of Plecoptera-taxa	
nr taxa	Community structure	Total number of taxa	
nr tri taxa	Community structure	Number of Trichoptera-taxa	
sha div	Community structure	Shannon-Wiener diversity	
DI	General ecological state	Degradation index, based on sensitivity of individual taxa against hydromorphological alterations of the riverbed	
DK_IBCH	General ecological state	Weighted average of Diversity Class (DK), typically correlates well with habitat heterogeneity	
IBCH*	General ecological state	Swiss water quality index based on macroinvertebrates, calculated with <i>DK IBCH</i> and <i>IG IBCH</i>	
IG_IBCH	General ecological state	Most sensitive Indicator Group (IG), often shows a strong correlation with overall water quality	
CEFI	Hydropeaking sensitivity	Canadian ecological flow index modified according to an Austrian dataset	
CEFI Arm	Hydropeaking sensitivity	Canadian ecological flow index	
dom_inter	Hydropeaking sensitivity	Dominance (relative abundance) of interstitial-dwelling taxa within the community	
dom lentic	Hydropeaking sensitivity	Dominance (relative abundance) of lentic taxa within the community	
dom_lotic	Hydropeaking sensitivity	Dominance (relative abundance) of lotic taxa within the community	
dom_surf	Hydropeaking sensitivity	Dominance (relative abundance) of surface-dwelling taxa within the community	
dom_surf_lentic	Hydropeaking sensitivity	Dominance (relative abundance) of surface-dwelling, lentic taxa within the community	
hp_sen	Hydropeaking sensitivity	Hydropeaking sensitivity index based on sensitivity of individual taxa against hydrological alterations	

^{*} In this study, to compute the IBCH, we aggregated the 12 kick samples per study site for each taxon, thereby determining the total abundance per taxon and study site. Given that the IBCH method relies on a composite sample of eight kick samples, a corresponding correction was applied (Corrected abundance = $\frac{Totale\ Abundance}{12}$ * 8).

4.2.2 Metric selection

Laboratory and field-screening identification were used in this study (Chapter 3.2). Therefore, a first selection of metrics was made based on the discrepancy between the two datasets. The deviation of each metric between laboratory and field data was computed using the Metric Quality Ratio (MQR). The greater the deviation from one, the more variability exists between the two datasets. Metrics that showed the most stable MQR values were considered suitable for evaluation procedures using only the field-screening dataset.

In a next step, all metrics were investigated according to their indication quality in terms of hydropeaking sensitivity and natural variability for both the field and laboratory datasets. First, study sites in hydropeaking and (near-) natural river (reference) reaches were tested for differences (discrimination efficiency *sensu* Ofenböck et al., 2004) to evaluate which metrics best indicate the impact of hydropeaking. Second, the variability of the metrics within the hydrologically unaffected reference sites was investigated, based on the standard deviation (standardized by the 75th percentile), to identify metrics with minimal natural variability. Discrimination efficiency and variability were then combined into the multimetric "indication quality" by calculating the mean of these values, after

standardizing both between 0 and 1 and considering the reciprocal value of the standard deviation.

Finally, the influence of environmental variables (covariates) on the macroinvertebrate community, including stressors like hydromorphological alterations and pollution (Chapter 3.3), was evaluated using Random Forest (RF) (Chapter 3.3.2). For each RF model, the prediction error (root-mean-square error, RMSE) and variable importances were exported. To compare the importance of environmental variables across response metrics (macroinvertebrate metrics), those with lower importance than the artificial variables were excluded from each model separately. For the remaining variables, an effect on the macroinvertebrate community was assumed, and a ranking was created for each metric. Additionally, the number of environmental variables belonging to the overarching groups "Hydrology" and "Hydraulic" (as defined in Table 8) were calculated. These categories were selected to represent the direct influence of hydropeaking. Highly ranked variables of the overarching groups highlight metrics, which are strongly influenced by a variable belonging to those categories. Since different models may include varying numbers of predictors (environmental variables), the percentage of variables from these overarching groups was also calculated for each model. Given that RMSE depends on the range of values each macroinvertebrate metric can take, RMSE values were standardized by dividing them by the average value of each metric within the data used for each model. This RF analysis ensures that the macroinvertebrate metrics and resulting multimetric indices (MMIs) reliably reflect the influence of hydropeaking, especially hydrological and hydraulic effects. This is achieved by considering the absolute (number) and relative (%) contributions of hydrological and hydraulic predictors and the RMSE of the RF models.

Further details can be found in the master thesis by Wirth (2025).

4.2.3 Calculation and validation of multimetric indices

The calculation of the MMIs for the Swiss dataset are integral to this study's results and are described in detail in the Chapters 4.3.1 - 4.3.4. Further, to validate and compare with other projects, two additional MMIs were computed. One of these MMIs is part of the "Austrian Hydropeaking Guideline" (Leitner et al., 2025) and is calculated as follows:

$$MMI_HP_AT = \frac{dom_ept_{sc} + nr_taxa_{sc} + sha_div_{sc} + hp_sen_{sc} + dom_inter_{sc}}{5}$$

MMI_HP_AT Multimetric index Austria

dom_ept_{sc} EPT-dominance (scaled by division of the 75th percentile at reference sites)

nr_taxa_{sc} Number of taxa (scaled by division of the 75th percentile at reference sites)

sha_div_{sc} Shannon-Wiener diversity (scaled by division of the 75th percentile at reference sites)

hp_sen_{sc} Hydropeaking sensitivity index (scaled by division of the 75th percentile at reference sites)

dom intersc Dominance of interstitial-dwelling taxa (scaled by division of the 75th percentile at reference sites)

The second MMI is the k-index, a multimetric macroinvertebrate index from Greece (Theodoropolus et al., 2018):

$$k = 0.4 * \frac{n}{n_{-}max} + 0.3 * \frac{H}{H_{-}max} + 0.2 * \frac{EPT}{EPT_{-}max} + 0.1 * \frac{a}{a_{-}max}$$

k k-index

n Number of taxa

H Shannon-Wiener diversity
EPT Number of EPT-Taxa
a Absolute abundance

i max Maximum value of the metric within the dataset (study site)

In a subsequent validation step, all MMIs were initially tested by correlating the macroinvertebrate multimetric indices (Swiss MMIs as in Chapter 4.3.4, MMI_HP_AT, k-index) with the multimetric hydrological index CNT_MAFR_RATIO described in Chapter 3.3. Further, non-metric Multi-Dimensional Scaling (NMDS) was used to investigate how well the single metrics reflect actual changes between the macroinvertebrate communities. This method, recommended for datasets with many zero values (Leyer & Wesche, 2008), is well-suited to macroinvertebrate data from multiple study sites, as not all species are present at each site. NMDS was calculated using the laboratory dataset to show how the taxa differentiate between sites. Macroinvertebrate metrics were then fitted to the NMDS using the *envfit* function (Oksanen et al., 2022), illustrating their correlations with both ordination axes. In a final analysis, this approach was extended to include the results of an indicator species analysis (Dufrene & Legendre, 1997). This analysis identifies the most distinctive taxa for specific groups of sites (in this case, the river Verzasca) and was used to assess the influence of a potential covariate, geology – since Verzasca is the only river with a silicate bedrock (Annex 8.4).

4.3 Results

4.3.1 Metric selection – Comparison of field-screening and laboratory identification

All metrics listed in Table 10 were evaluated for their variability between laboratory and field-screening datasets using the Metric Quality Ratio (MQR) (Figure 6). Except for those metrics that represent the abundance of the entire community (ab_tot) or specific groups (ab_eph, ab_ept, ab_ple, ab_tri) and the dominance of surface-dwelling lentic taxa (dom_surf_lenit), none of the other metrics exhibited strong deviations between laboratory and field-screening datasets.

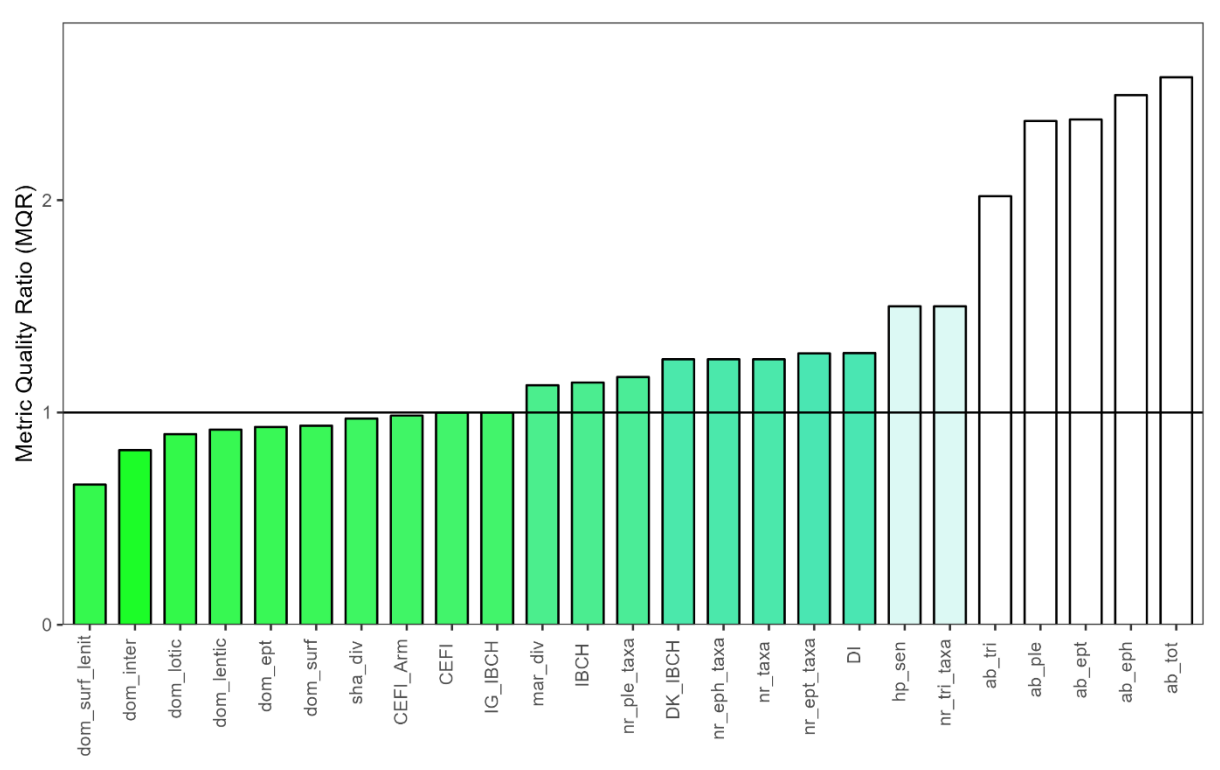


Figure 6. Metric Quality Ratio (MQR) showing the coherence between laboratory and field-screening datasets. MQR values of one indicate perfect coherence; the further they diverge from one, the less stable the metric. This graph displays the median deviation of the metrics across all study sites. The metrics showing the best MQR are highlighted in green. For metric abbreviation see Table 10.-This analysis replaces the preliminary analyses of Looser (2022) and Wirth (2023).

4.3.2 Metric selection – Indication quality

According to the multimetric "indication quality", the five highest-ranked metrics for the field-screening dataset were the number of EPT taxa (nr_ept_taxa), the degradation index (DI), the Shannon-Wiener diversity (sha_div), the number of Plecoptera taxa (nr_ple_taxa), and the total number of taxa (nr_taxa) (Figure 7, top panels). The weakest responses were observed for the IG_IBCH, DK_IBCH, and IBCH. Most metrics showed quite high discrimination efficiency, with the exceptions of IG_IBCH, DK_IBCH and IBCH, dom_ept, nr_eph_taxa, dom_surf, and nr_tri_taxa. Notably, dom_lentic and ab_tri exhibited high variability in the reference sites, while the variability of most other metrics remained relatively low.

For the laboratory dataset, slightly different metrics showed the best "indication quality". In this case, the five best-ranked metrics were the Canadian Ecological Flow Index (modified according to an Austrian dataset; CEFI), the dominance of lotic taxa (dom_lotic), the Weighted average of Diversity Class of the Swiss water quality index (DK_IBCH), the Margalef diversity (mar_div), and the Swiss water quality index (IBCH) (Figure 7, bottom panels). Like for the field-screening dataset, the IG_IBCH

exhibited the lowest discrimination efficiency, followed by nr_eph_taxa, nr_ept_taxa, dom_ept, and CEFI_Arm. Notably, dom_surf_lenit, dom_lentic, dom_inter, dom_surf, and ab_tri showed high variability in the reference sites, while the variability of most other metrics remained relatively low.

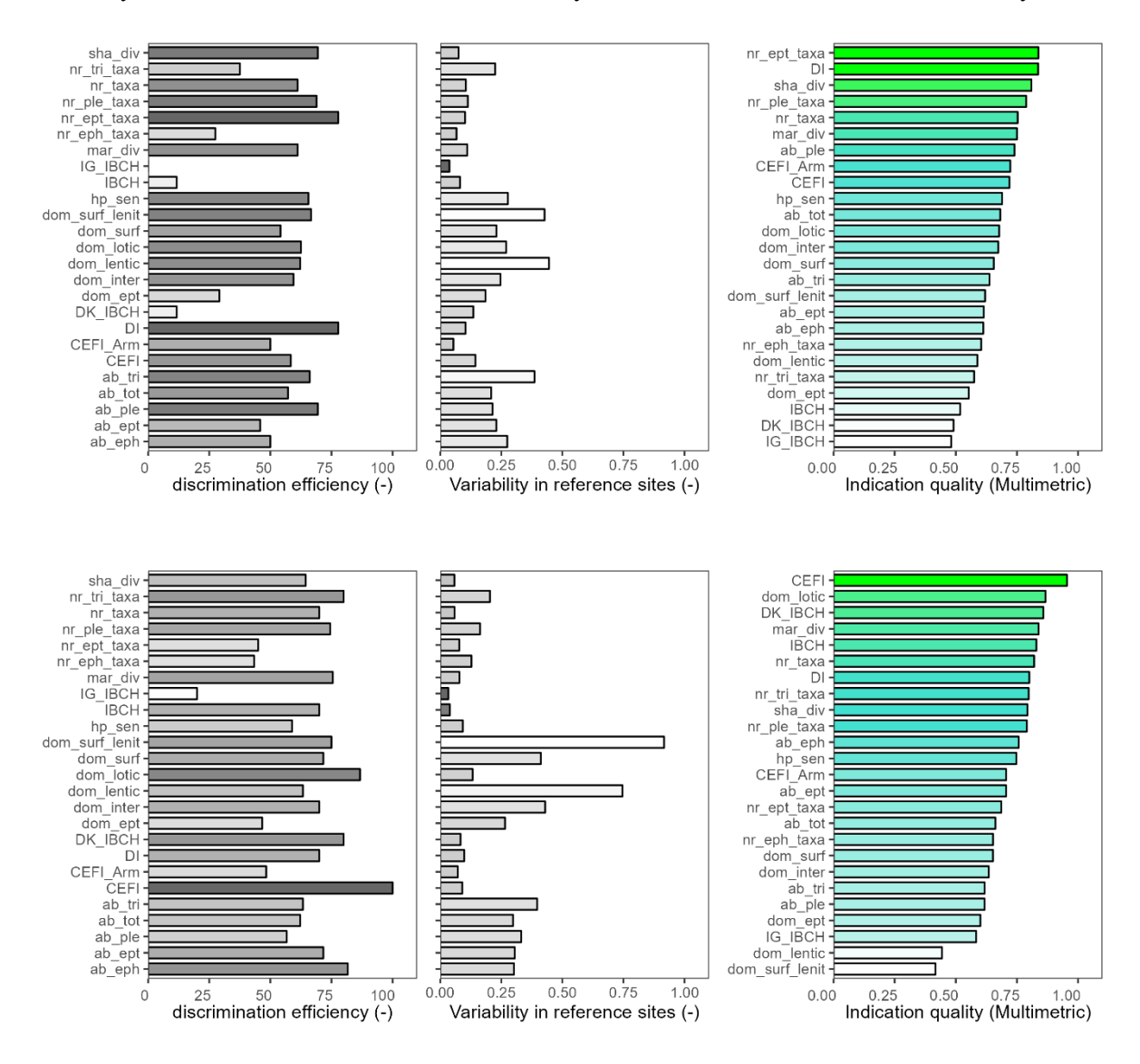


Figure 7. Indication quality, based on discrimination efficiency and natural variability (standard deviation, standardized by division through the 75th percentile), calculated using the field-screening dataset (top panels) and the laboratory dataset (bottom panels). For variability low values indicate suitable metrics, whereas for discrimination efficiency and indication quality, high values are suited. The metrics with the best indication quality are highlighted in green. For metric abbreviation see Table 10.

4.3.3 Metric selection – Influence of environmental covariates

The suitability of the metrics was additionally assessed using the results of the Random Forest (RF) models based on two main criteria: (i) the absolute amount and relative proportion of hydrological and hydraulic variables, and (ii) the standardized RMSE for both the field data-based RF models (fie) and the laboratory data-based RF models (lab). Of the initial 25 candidate metrics (Table 10), only 16 were retained for analysis. The remaining nine were discarded as they were deemed less relevant based on the findings in Chapters 4.3.1 and 4.3.2.

Several RF models included a considerable number of hydrological and hydraulic variables. Specifically, more than 10 hydrological variables were included in the models for lab nr ple taxa,

lab_mar_div, fie_nr_ple_taxa, lab_DI, and lab_dom_inter (Figure 8, left top panel). Similarly, ≥ 5 hydraulic variables were present in the models for lab_CEFI, lab_dom_inter, fie_nr_ple_taxa, lab_nr_ple_taxa, fie_DK_IBCH, lab_DI, lab_IBCH, lab_mar_div, lab_nr_taxa, and fie_sha_div (Figure 8, left middle panel).

There were also models in which hydrological variables (fie_dom_lentic, fie_dom_lotic, fie_IBCH, lab_CEFI_Arm, fie_dom_surf_lentic, lab_sha_div, fie_dom_surf, lab_DK_IBCH, and lab_dom_lotic) or hydraulic variables (lab_dom_lentic) accounted for $\geq 30\%$ of all variables (Figure 8, right panels). The standardized RMSE from the dominance-based models (dom) clearly exceeded that of all other models (Figure 8, lower panel).

Further details can be found in the master thesis by Wirth (2025).

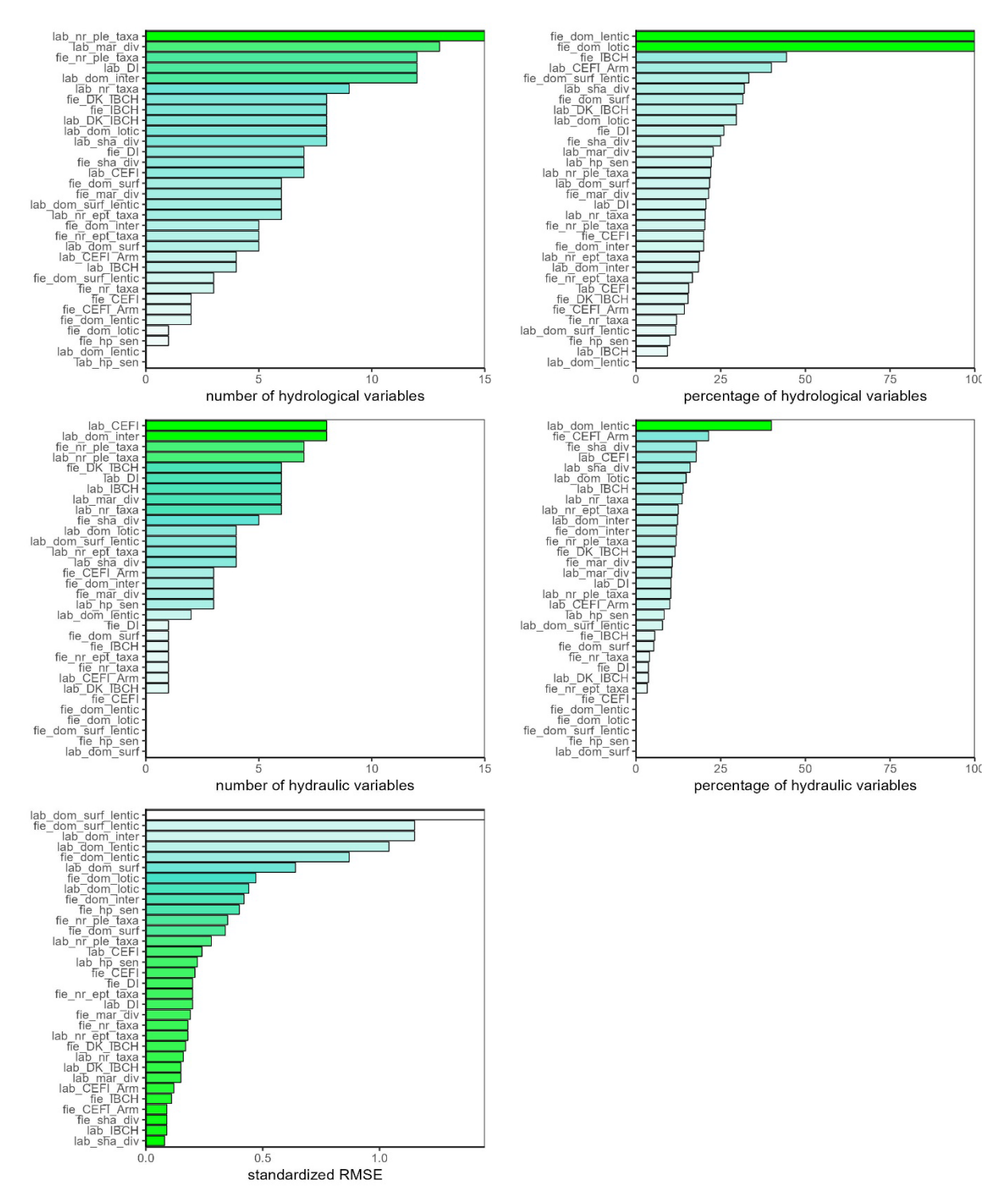


Figure 8: Absolute number (left top and middle panels) and relative proportion (right top and middle panels) of hydrological and hydraulic variables, as well as standardized RMSE (bottom panel) for each metric in both field data-based RF models (fie) and laboratory data-based RF models (lab). Only variables with higher variable importance than those of artificial (false) variables were used (3.3.2). A higher number or percentage of hydrological and/or hydraulic variables indicates a stronger association of the metric with these variables. The standardized RMSE, calculated by dividing the absolute RMSE by the average value of the metric within the data used for each model, allows for independent comparison of metrics regardless of their value ranges. Low values are better suited. The best metrics are highlighted in green. Of the initial 25 candidate metrics (Table 10), only 16 were retained for this analysis. For metric abbreviation see Table 10.

4.3.4 Metrics selection – Metrics suitable for multimetric indices

The selection of suitable metrics for constructing multimetric indices (MMIs) was guided by five main principles. First, the metrics should represent the macroinvertebrate community structure, and second, they should reflect the general ecological state (according to Table 10). Third, they should capture hydropeaking impact (according to Table 10 and/or high discrimination efficiency according to Figure 7) while minimizing the influence of natural variability on the macroinvertebrate community (low natural variability in Figure 7). Fourth, the metrics were required to primarily represent hydrological and hydraulic effects, rather than other environmental factors such as morphology, water quality, and topography. Additionally, they should be capable of being predicted with minimal error (RMSE) by Random Forest models (Figure 8). Fifth, metrics derived from the field-screening dataset were expected to show minimal deviation from those obtained using the laboratory dataset (high coherence in Figure 6).

MMI based on field-screening data

For the field-screening dataset, the number of EPT taxa (nr_ept_taxa), the degradation index (DI), and the Shannon-Wiener diversity (sha_div) emerged as the most effective metrics in terms of both discrimination efficiency and stability across reference study sites (Figure 7, top panels). The number of Plecoptera taxa (nr_ple_taxa), also showed high discrimination efficiency and low variability in the reference sites. Compared to the nr_ept_taxa, the nr_ple_taxa showed stronger association with hydrological (20.3% vs 16.7%) and hydraulic (11.9% vs 3.3%) variables, along with low standardized RMSE error (0.35 vs 0.20) (Figure 8). Consequently, we decided to include the nr_ple_taxa in the MMI instead of the nr_ept_taxa. DI and sha_div both exhibited \geq 25% association with hydrological variables and a standardized RMSE error \leq 0.2.

DI reflects the general ecological state (specifically hydromorphological alteration), whereas sha_div and nr_ple_taxa provide valuable insights into the community structure. As hydropeaking primarily alters flow characteristics in riverine ecosystems, and recognizing that the DI, sha_div and nr_ple_taxa, do not directly capture this impact, we considered the inclusion of two additional metrics in the MMI to better reflect the effects of hydropeaking intensity.

The Canadian Ecological Flow Index (CEFI_Arm) and the CEFI modified according to an Austrian dataset (CEFI) were the two top-performing metrics from the hydropeaking sensitivity group (according to Table 10), based on their strong indication quality shown in Figure 7 (top panels). Both metrics reflect the flow preferences and tolerances of the occurring taxa, representing those ecological adaptations of the community that are most likely to be altered by hydropeaking. We decided to include the CEFI in the MMI rather than the CEFI_Arm because it ranked as the top-performing metric in the laboratory dataset (Figure 7, bottom panels) and exhibited 20% association with hydrological variables, along with a standardized RMSE error of 0.21 (Figure 8).

The second additional metric included in the MMI was the dominance of interstitial-dwelling taxa (dom_inter), which ranked similarly as the hydropeaking sensitivity index (hp_sen) in terms of indication quality within the hydropeaking sensitivity group (Figure 7, top panels). In addition, this metric showed a stronger association with hydrological (20.0% vs 10.0%) and hydraulic (12.0% vs 0.0%) variables, while maintaining a comparable standardized RMSE error (0.42 vs 0.40) (Figure 8).

All five metrics – sha_div, nr_ple_taxa, DI, dom_inter, and CEFI – showed an acceptable level of deviation between the laboratory and field-screening datasets (Figure 6). These metrics were subsequently combined into a MMI for hydropeaking based on the field-screening dataset, referred to as MMI HP FIE.

$$\label{eq:mmi_hamiltonian} \text{MMI_HP_FIE} = \frac{\text{sha_div}_{\text{sc}} + \text{nr_ple_taxa}_{\text{sc}} + \text{DI}_{\text{Sc}} + \text{dom_inter}_{\text{sc}} + \text{CEFI}_{\text{sc}}}{5}$$

MMI HP FIE Swiss multimetric index for hydropeaking based on field-screening data

sha_div_{sc} Shannon-Wiener diversity (scaled by division of the 75th percentile at reference sites; Annex 8.5)

nr_ple_taxa_{sc} Number of Plecoptera-taxa (scaled by division of the 75th percentile at reference sites; Annex 8.5)

DI_{sc} Degradation index (scaled by division of the 75th percentile at reference sites; Annex 8.5)

dom_intersc Dominance of interstitial-dwelling taxa (scaled by division of the 75th percentile at reference sites; Annex

8.5)

CEFI_{sc} Canadian ecological flow index modified according to an Austrian dataset (scaled by division of the 75th

percentile at reference sites; Annex 8.5)

MMI based on laboratory data

Considering discrimination efficiency and variability in the reference sites, the CEFI emerged as the most effective metric for the laboratory dataset (Figure 7, bottom panels). Moreover, the CEFI exhibited a good association with hydraulic (17.8%) and hydrological variables (15.6%), along with a standardized RMSE error of 0.24 (Figure 8). Therefore, it was selected as the top-performing metric belonging to the hydropeaking sensitivity group (according to Table 10).

The Weighted average of Diversity Class of the Swiss water quality index based on macroinvertebrates (DK_IBCH) and the Margalef diversity (mar_div) were selected as the top-performing metrics in terms of indication quality (Figure 7, bottom panels) from the general ecological state group and the community structure group, respectively. Both metrics also exhibited > 22% association with hydrological variables and a standardized RMSE error of 0.15 (Figure 8).

As with the MMI_HP_FIE, we considered the inclusion of two additional metrics in the MMI based on the laboratory dataset. The first was the Shannon-Wiener diversity (sha_div), which showed high discrimination efficiency and low variability at reference sites (Figure 7, bottom panels), providing further insight into community structure beyond what mar_div captures. Additionally, sha_div showed a strong association with both hydrological (32%) and hydraulic (16%) variables. along with a low standardized RMSE error (0.08) (Figure 8).

The second additional metric included in the MMI was the dominance of lotic taxa (dom_lotic). This metric ranked second in indication quality within the hydropeaking sensitivity group (Figure 7, bottom panels) and showed a 29.6% association with hydrological variables and 14.8% with hydraulic variables, along with an acceptable standardized RMSE error (0.44) (Figure 8).

All five metrics – sha_div, mar_div, DK_IBCH, CEFI, and dom_lotic were subsequently combined into a MMI for hydropeaking based on the laboratory dataset, referred to as MMI_HP_LAB.

$$MMI_HP_LAB = \frac{sha_div_{sc} + mar_div_{sc} + DK_IBCH_{sc} + CEFI_{sc} + dom_lotic_{sc}}{5}$$

MMI HP Lab Swiss multimetric index for hydropeaking based on laboratory data

sha_div_{sc} Shannon-Wiener diversity (scaled by division of the 75th percentile at reference sites; Annex 8.5)

mar_div_{sc} Margalef diversity (scaled by division of the 75th percentile at reference sites; Annex 8.5)

DK_IBCH_{sc} Weighted average of Diversity Class (DK) of the Swiss water quality index based on macroinvertebrates

(IBCH) (scaled by division of the 75th percentile at reference sites; Annex 8.5)

CEFI_{sc} Canadian ecological flow index modified according to an Austrian dataset (scaled by division of the 75th

percentile at reference sites; Annex 8.5)

dom lotic_{sc} Dominance of lotic taxa (scaled by division of the 75% quantile at reference sites; Annex 8.5)

MMI based on both datasets (field-screening and laboratory)

The metrics considered most reliable, based on both datasets, were then combined into a MMI (MMI_HP_ALL) that incorporates the evaluation of the two distinct datasets (field and laboratory) and three different assessment methods: discrimination efficiency, natural variability, and sensitivity to hydrological and/or hydraulic variables. The only difference between the MMI_HP_ALL and the MMI_HP_FIE is that in MMI_HP_ALL the metric DI from the MMI_HP_FIE has been replaced by the metric DK_IBCH.

$$\label{eq:mmi_hall} \begin{aligned} \text{MMI_HP_ALL} = & \frac{\text{sha_div}_{\text{sc}} + \text{nr_ple_taxa}_{\text{sc}} + \text{DK_IBCH}_{\text{sc}} + \text{dom_inter}_{\text{sc}} + \text{CEFI}_{\text{sc}}}{5} \end{aligned}$$

MMI_HP_ALL Swiss multimetric index for hydropeaking based both datasets (field-screening and laboratory)

sha_div_sc Shannon-Wiener diversity (scaled by division of the 75th percentile at reference sites; Annex 8.5)

nr_ple_taxa_sc Number of Plecoptera-taxa (scaled by division of the 75th percentile at reference sites; Annex 8.5)

DK_IBCH_sc Weighted average of Diversity Class (DK) of the Swiss water quality index based on macroinvertebrates (IBCH) (scaled by division of the 75th percentile at reference sites; Annex 8.5)

dom_inter_sc Dominance of interstitial-dwelling taxa (scaled by division of the 75th percentile at reference sites; Annex 8.5)

CEFI_sc Canadian ecological flow index modified according to an Austrian dataset (scaled by division of the 75th percentile at reference sites; Annex 8.5)

4.3.5 Validation of the multimetric indices

Validation 1: Correlation of MMIs and hydrology

As an initial validation step, the MMI_HP_ALL was calculated separately using the field-screening and the laboratory datasets. The results were then correlated with the multimetric hydrological index CNT_MAFR_RATIO (Chapter 3.3). This analysis was conducted for the three investigated biogeographical regions: Central Plateau/Northern Alps, Eastern Central Alps, and Southern Alps.

Both calculations revealed similar negative relationships between the MMI_HP_ALL and the CNT_MAFR_RATIO (Figure 9). The strongest correlation was observed for the Central Plateau/Northern Alps ($R^2 = 0.17/0.076$), followed by the Southern Alps ($R^2 = 0.082/0.032$) and the Eastern Central Alps ($R^2 = 0.00067/0.911$). However, none of these correlations were significant ($R^2 = 0.005$). The lowest p-value was found for the field-screening dataset of the Central Plateau/Northern Alps ($R^2 = 0.005$).

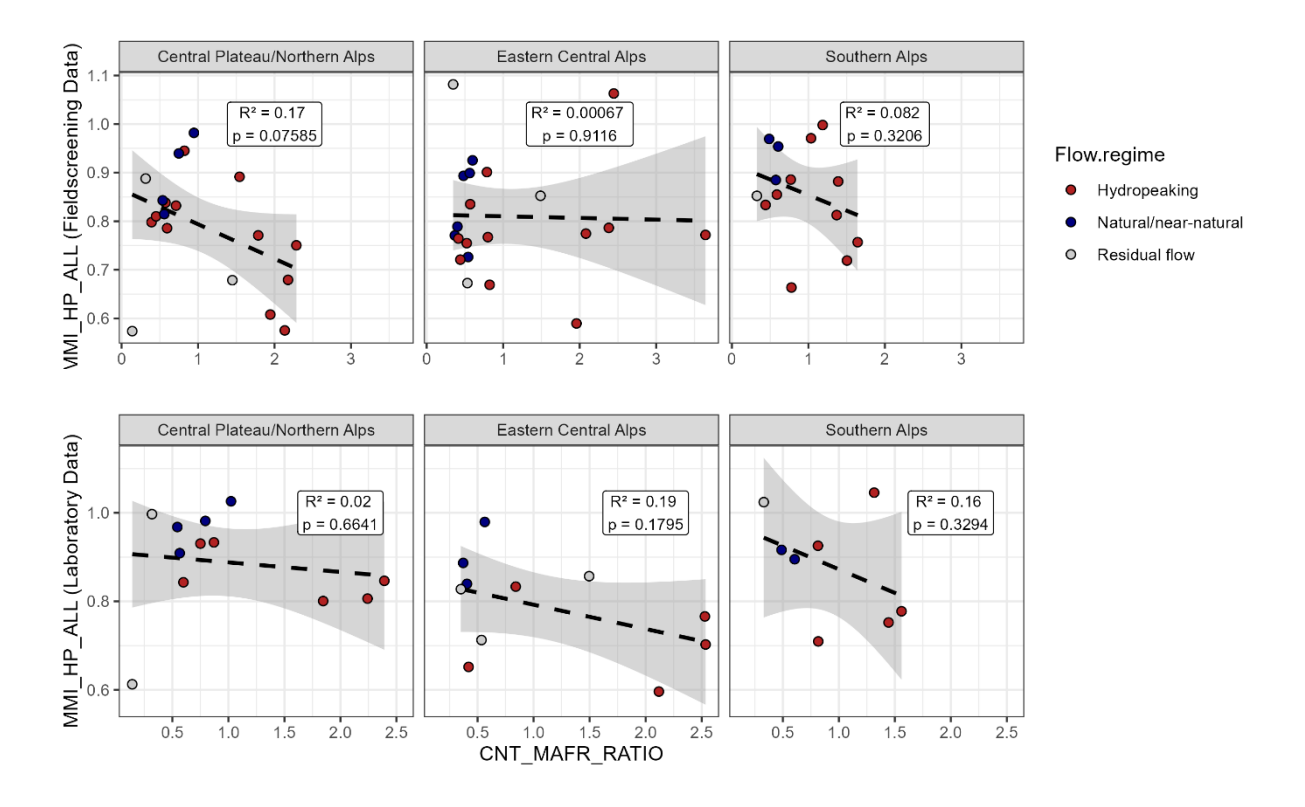


Figure 9. Correlation between the MMI_HP_ALL and the multimetric hydrological index (CNT_MAFR_RATIO) within the different biogeographical regions Central Plateau/Northern Alps, Eastern Central Alps, and Southern Alps. The correlation is depicted for the field-screening dataset (top panels) and the laboratory dataset (bottom panels).

A similar pattern emerged when using the Austrian macroinvertebrate multimetric index for the assessment of hydropeaked rivers (MMI_HP_AT) calculated using the field-screening dataset (Figure 10, top panels). The strongest correlation with the CNT_MAFR_RATIO was found in the Southern Alps ($R^2 = 0.160$), whereas weaker correlations were found in the Eastern Central Alps ($R^2 = 0.110$) and the Central Plateau/Northern Alps ($R^2 = 0.052$). However, none of these correlations were significant (p < 0.05).

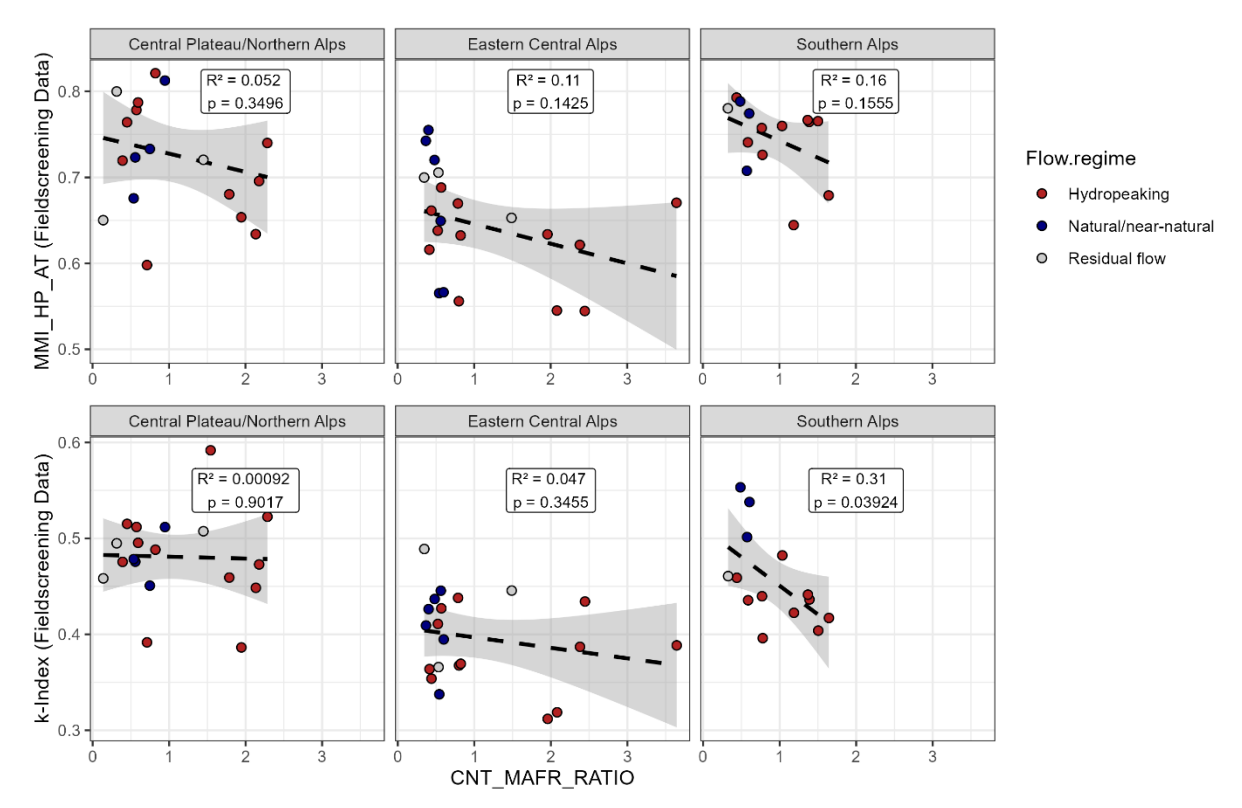


Figure 10. Correlation between the MMI_HP_AT (top panels; calculated with the field-screening dataset) respectively the k-index (bottom panels; calculated with the field-screening data) and the multimetric hydrological index (CNT_MAFR_RATIO) within the different biogeographical regions Central Plateau/Northern Alps, Eastern Central Alps, and Southern Alps.

Comparable to the MMI_HP_AT, the k-index showed varying relationships with the CNT_MAFR_RATIO (Figure 10, bottom panels). The strongest correlation was observed for the Southern Alps ($R^2 = 0.310$), while the correlations in the Eastern Central Alps ($R^2 = 0.047$) and Central Plateau/Northern Alps ($R^2 = 0.00092$) were notably weaker. Only the correlation for the k-index in the Southern Alps was significant (p < 0.05). For all other biogeographical regions, the correlations were not significant.

MMI_HP_ALL was chosen for both datasets (field-screening and laboratory) due to its independence from the sample processing method (Chapter 3.2). Although the coefficient of determination would be generally higher for each method if the corresponding MMI (MMI_HP_FIE vs MMI_HP_LAB) were used (Annex 8.6.1), this approach would require two separate evaluation methods, which do not appear essential for the final refinement of the results.

Separated correlations between individual biological and hydrological metrics are provided in Annex 8.6.2. Additionally, Annex 8.6.3 presents the hydrological variables across the investigated rivers and biogeographical regions, while Annex 8.6.4 illustrates the effect of the reliability of the reconstructed flow data (Chapter 3.3.1) on the MMI HP ALL.

Validation 2: Representativeness for the actual macroinvertebrate community

The macroinvertebrate community, based on taxa identified during laboratory analysis, provides a more detailed representation of the actual community at each study site compared to the field-screening method. To visualize similarities and differences among these communities, a non-metric multidimensional scaling (NMDS) analysis was performed, revealing a clear separation between the three biogeographical regions (Central Plateau/Northern Alps, Eastern Central Alps, Southern Alps (Figure 11).

Several metrics, calculated from the field-screening dataset significantly (p < 0.05) explained variations within the actual macroinvertebrate communities (Figure 11). This analysis provided information on whether the metrics derived from the field-screening dataset reliably reflected the differences observed in the more detailed laboratory dataset. Metrics such as dom ept and nr eph taxa primarily captured community differences along the NMDS1 axis, which represented variation between biogeographical regions. In contrast, some of the selected metrics used in the multimetric indices significantly (p < 0.05) explained variations within biogeographical regions. Notably, the MMI HP ALL, along with some of the individual metrics used in its calculation, effectively captured changes along the NMDS2 axis (e.g., associated with hydrological alteration). In this context, study sites affected by hydropeaking were distinctly separated from (near-) natural reference sites in the Southern Alps and in the Central Plateau/Northern Alps (where 2 out of 4 reference sites were distinctly separated from the hydropeaking sites). However, this finding was only partially supported by the correlation plots in Validation 1, which showed the strongest relationships for the Central Plateau/Northern Alps biogeographical region (Figure 9). In the Eastern Central Alps, hydropeaking sites separated from reference sites rather along the NMDS1 axis, suggesting that typologically driven differences may have influenced the separation, as the biogeographical regions also split along this axis

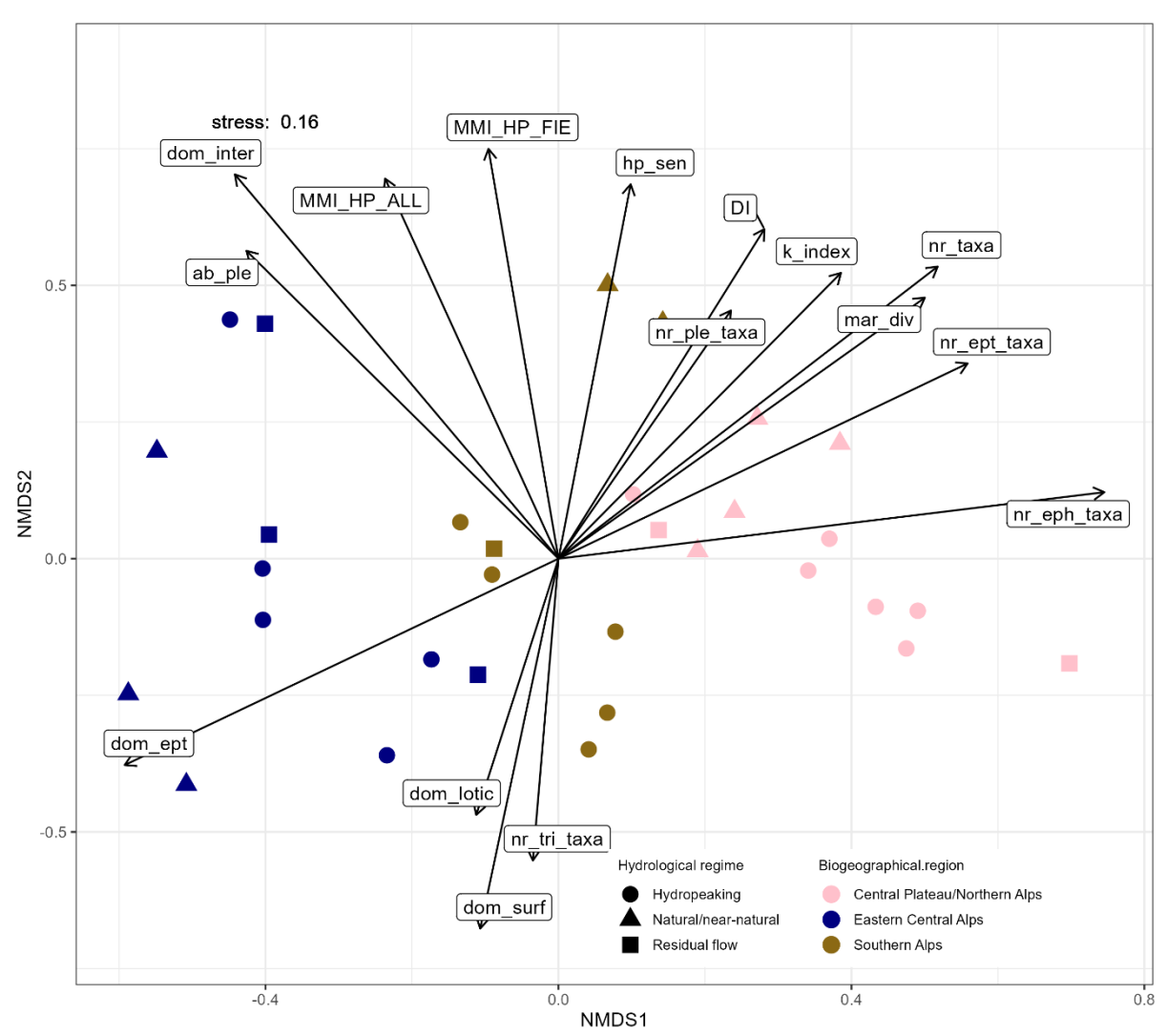


Figure 11. NMDS reflecting the clustering of study sites based on abundances of taxa using the laboratory dataset. Arrows indicate the significant relationships (p< 0.05) of metrics calculated based on the field-screening dataset with the clustering of the laboratory dataset. Colors represent the biogeographical regions and shapes the hydrological regime. Each study site is represented as a point on the graph. For metric abbreviation see Table 10 and Chapter 4.3.4.

4.4 Discussion

Since national standard methods for evaluating the ecological status class based on the Biological Quality Elements (BQE) "benthic macroinvertebrates" as employed in the Water Framework Directive (WFD), as well as the Swiss water quality index based on macroinvertebrates (IBCH; FOEN, 2019a), are not suitable for assessing hydropeaked river sections (as also mentioned in Ofenböck et al., 2019), a hydropeaking-specific approach is essential to evaluate this anthropogenic stressor.

The assumptions underlying this study and the development of the multimetric indices were based on numerous previous studies that have clearly demonstrated the effects of hydropeaking on macroinvertebrate communities. One of the most commonly used metrics in these studies was total abundance, which often showed a clear decline with increasing hydropeaking intensity (e.g., Moog, 1993; Lauters et al., 1996; Céréghino et al., 2002; Leitner et al., 2017; Elgueta et al., 2021). However, a review by Baumann & Klaus (2003) highlighted that approximately 20% of the studies examined reported no significant changes in biomass or abundance due to hydropeaking. This underscores the importance of site comparability when using these metrics, as local differences can be substantial. Therefore, the development of a hydropeaking assessment approach must carefully consider the suitability of non-abundance-related metrics. In this context, a multimetric approach that integrates various individual metrics is particularly valuable.

Following the recently developed methodological approach for Austria (Leitner et al., 2025), a hydropeaking-specific metric selection was also conducted for Switzerland as part of this study, forming the basis for defining a multimetric index (MMI). The multimetric approach offers the advantage of integrating individual metrics into an index that captures various aspects, such as faunal structure and ecological status, while specifically reflecting hydropeaking-related impacts in terms of hydrological and hydraulic effects. Additionally, it is designed to minimize sensitivity to other environmental factors, such as morphology, water quality, or topography. To achieve this, the selected metrics were tested for their responsiveness along hydropeaking-specific gradients – such as the hydropeaking multimetric hydrological index CNT_MAFR_RATIO (Chapter 3.3) – and their suitability was evaluated accordingly. It is essential to incorporate diverse metrics that capture the relevant aspects mentioned while avoiding highly redundant metrics (according to Ofenböck et al., 2004; Hering et al., 2006) to prevent an artificial overemphasis on a specific signal.

The development of the hydropeaking-specific assessment was designed to apply a time- and cost-efficient field-screening approach (based on the screening method according to Ofenböck et al., 2019 and Leitner et al., 2025). This approach includes a subsequent laboratory post-determination for validation, where macroinvertebrate samples are further determined to the highest possible taxonomic level and quantified in detail. The comparison between field and laboratory analyses revealed differences, particularly in abundance-related metrics – an expected outcome that justifies the need for distinct metric selections for each processing method (field-screening *vs* laboratory). Accordingly, 25 metrics were tested for their suitability for either the field-screening method (screening taxa level) or the laboratory method (highest possible taxonomic level). The selection process considered their indicative value in terms of hydropeaking sensitivity, as well as their methodological and natural variability. Additionally, the metrics' responses to hydrological and hydraulic variables were assessed using Random Forest models, comparing them against other environmental factors such as morphological and water quality alterations.

The results indicate that most of these metrics can be effectively integrated into a MMI for hydropeaking assessment. The final metric selection was guided by the principles outlined in Ofenböck et al. (2004) rather than strictly predefined rules. Following various analyses, the five most meaningful metrics

(representing community structure, ecological adaptations, and sensitivity to hydrological/hydraulic changes) – calculated from both the field and laboratory datasets – were selected for inclusion in the MMI. The validation process included correlations with hydrological metrics (which were also combined into the hydropeaking multimetric hydrological index CNT_MAFR_RATIO) and multivariate analyses to assess the representativeness of individual metrics for the entire macroinvertebrate community. Due to differences in taxonomic resolution between the field-screening and laboratory approaches, some metrics responded differently between datasets. As a result, two method-specific core sets of metrics were defined, leading to the development of two corresponding MMIs: MMI_HP_FIE for field-screening data and MMI_HP_LAB for laboratory data. In both cases, the number of selected core (best responding) individual metrics was maintained at five.

Correlations with hydrological parameters showed that MMI_HP_FIE and MMI_HP_LAB values decrease as hydrological intensity (CNT_MAFR_RATIO) increases across all biogeographical regions. However, these correlations were weak and, in most cases, not statistically significant. Similar patterns were observed for other tested multimetric indices, such as MMI_HP_AT and the k-index (Chapter 4.3.5). These results suggest that macroinvertebrate communities respond to hydrological alterations, a pattern also reflected in the multivariate NMDS analysis. However, the strength of these responses varies by biogeographical region. Despite this variability, multimetric indices can still be developed to capture the effects of hydrological variability on macroinvertebrate communities. Since the differing responses of MMI_HP_FIE and MMI_HP_LAB were relatively minor, given their low correlation with the hydropeaking gradient, a unified index (MMI_HP_ALL) was developed. This combined index incorporates matching individual metrics (sha_div and CEFI) as well as the best-fit metrics for both methods (nr_ple_taxa, DK_IBCH, and dom_inter). The MMI_HP_ALL ensures consistency in hydropeaking impact assessments, making the results independent of the chosen method (Chapter 4.3.4).

Despite the unexpectedly weak response of macroinvertebrate communities to hydrological alterations – observed not only in abundance-based metrics but also in the most sensitive indices – it remains crucial to monitor their responses to hydropeaking mitigation and restoration measures. Therefore, further studies are needed to determine whether the implemented measures are substantial enough to induce changes in the multimetric indices (e.g., through pre- and post-monitoring). Monitoring the effectiveness of measures is essential for gaining deeper insights into how this complex group of organisms responds to hydrological changes. The metrics tested and the multimetric indices developed offer a simplified yet representative way to capture and visualize the key sensitive characteristics of macroinvertebrate communities.

In summary, the results of this study suggest that multimetric indices can detect the potential impacts of mitigation/restoration measures on macroinvertebrate communities, supporting the hypotheses defined in Chapter 1. Specifically, while the methodology (field-screening vs laboratory) and the corresponding responses of individual metrics show some divergence, the overall impact on assessment remains minor, allowing the derivation of a common multimetric index (MMI_HP_ALL). Accordingly, a time- and cost-efficient field-screening method is sufficient to evaluate the effects of hydropeaking (hypothesis 1). Furthermore, compared to standard methods for assessing hydropeaked rivers – which often rely on abundance-based metrics – hydropeaking-specific metrics provide additional advantages. When integrated into a multimetric index, these metrics improve the ability to effectively assess anthropogenic hydrological/hydraulic alterations (hypothesis 2).

Compared to the Swiss results, the Austrian approach (Leitner et al., 2025) showed a clearer distinction between hydropeaked and reference sites based on the Austrian dataset. Although both studies aimed to minimize the influence of non-hydrological factors by focusing sampling along gravel bars, differences in morphology or water quality may still have affected the results, potentially explaining certain

ambiguities in the Swiss findings. Morphology appears particularly decisive, as sediment composition and transport may vary greatly between rivers and substantially influence habitat quality. This variability may also account for the differing results regarding sediment transport and its effects in hydropeaking studies across various eco- or bioregions worldwide (as summarized in Bipa et al., 2024). Additionally, water quality parameters such as organic pollution (e.g., Buffagni et al., 2009) and land use (e.g., Larsen et al., 2021) have been shown to affect benthic communities. In the present study, mean diffuse total nitrogen and the proportion of settlement area in the catchment had a substantial impact on the metrics (Wirth, 2025 – results of the Random Forest models). Finally, the effects of climate change cannot be ruled out, as they may drive shifts in faunal structure, leading to an increase in euryecious taxa or altitudinal shifts in macroinvertebrate cenoses due to global warming (Durance & Ormerod, 2007; Domisch et al., 2011).

Further research is therefore needed to clarify these questions and deepen our understanding of macroinvertebrate community responses to hydropeaking across different biogeographical regions.

5 Habitat modeling (WP 4)

5.1 Introduction

Habitat models serve as a valuable tool for linking flow-ecology relationships with hydrological scenarios, enabling the prediction of how mitigation or restoration measures may affect potential macroinvertebrate distribution. While most existing approaches such as the habitat simulation models CASiMiR (Schneider et al., 2017), PHABSIM (Bovee, 1982), or HABBY (Royer et al., 2022) primarily focus on fish, some have been adapted and implemented for macroinvertebrates in rivers impacted by hydropower (e.g., Tanno, 2012; Leitner et al., 2017; Theodoropoulos et al., 2018).

The most commonly used habitat modeling approach relies on habitat suitability curves (HSC), which provide results as habitat suitability values ranging from 0 (no suitability) to 1 (absolute suitability) (e.g., Person, 2013; Leitner et al., 2017). Typically, one or more river-specific target species are selected, requiring the development of taxa-specific HSC. Using these curves, habitat suitability at different flow can then be calculated based on outputs from hydrodynamic models. However, biotic and abiotic factors vary over time, necessitating season-, taxa- and location-specific adaptation of the HSC. Additionally, the expert-based selection of target species introduces a degree of subjectiveness, which can impact modeling outcomes (Ahmadi-Nedushan et al., 2006). To address this, Schmidlin et al. (2023) proposed a simplified, univariate modeling approach that uses a generalized HSC for the entire macroinvertebrate community, based on flow velocity classes and associated habitability classes.

In this study, we tested the approach of Schmidlin et al. (2023) with a focus on (i) validating the approach against the data collected in this study, (ii) detecting changes in the availability of suitable habitats induced by hydropeaking based on this approach, and (iii) comparing the habitat modeling outcomes with the multimetric index based on both datasets (MMI_HP_ALL) developed in WP 3 (Chapter 4.3.4). For this purpose, eight study sites were selected for the creation of 2D hydrodynamic models (Chapter 5.2.1). At each study site, topographical and hydraulic data were collected in the field, and a hydrodynamic model was set up, calibrated and validated (Chapter 5.2.2). Based on the results of the hydrodynamic simulations, the generalized HSC was applied on seven study (Chapter 5.2.3) sites and compared to the MMI_HP_ALL (Chapter 5.3).

5.2 Material and methods

5.2.1 Selected study sites and field survey

A total of eight study sites along six different rivers were selected for habitat modeling (Figure 2; Table 11). Site selection was based on two main criteria: the representativeness of hydropeaked and reference rivers as well as the availability of macroinvertebrate sampling data identified in the laboratory (Table 5). For each study site, topographic (elevation and bathymetry) as well as hydraulic data (water depths, flow velocities and grain sizes) were collected in the field (Table 11). The surveys were conducted primarily in winter and spring, to minimize vegetation cover and avoid snow/glacier melt. Two GNSS systems (Trimble R10 and R2; accuracy < 0.025 m horizontally and < 0.05 m vertically, manufacturer's specifications) were used to record cross-section wise approximately 2'400 GPS points in Real Time Kinematic (RTK) mode. Within the wetted area, water depths were read from the GPS stick and recorded on the GPS controller. Water surface elevations were also derived by adding the water depths to the correspondent z coordinates. In addition, along cross-sections with favorable hydraulic conditions (i.e., geometrically homogeneous and with low turbulences), flow velocities were measured using a micropropeller device (Flowatch Flowmeter; accuracy ± 2%, manufacturer's specifications) positioned at

approximately 40% of the water depth (above the streambed). Furthermore, points along the water's edge as well as on the sediment bars were measured with RTK-GPS. These data were then used for both model calibration and validation. For all study sites except those at the Sitter River (S1, S2), drone flights were conducted with an Ebee plus (SenseFly) equipped with a S.O.D.A. camera. At least three ground control points (GCP) were set during each flight and geolocated using RTK-GPS for orthorectification. Drone images were processed with Pix4D mapper (Pix4D, 2023) to extract a digital elevation model (DEM). At the Moesa study site (M1), a GCP was incorrectly positioned and flushed away by a hydropeaking wave. Its original position was reconstructed from the orthophoto but is subject to some uncertainty.

Table 11. Overview of the field survey date, measured discharge during the survey, GPS points surveyed as well as water depth (h) and velocity (v) measurements, availability of drone imagery, number of ground control points, mesh elements, and mean size of mesh elements. For study site abbreviation and location see Figure 2 and Table 5.

Study site	Date of field survey	Discharge [m ³ /s]	GPS points (h, v)	Drone flight (dd.mm.yy)	GCP	Mesh elements	Mean size of mesh elements [m²]
S1	04.01.2023	3.7	588 (307; 41)	no	-	104'129	0.65
S2	08.12.2022	3.2	361 (267; 47)	no	-	30'797	0.95
TH4	18.03.2023	25.0	194 (110; 22)	yes (18.03.2023)	7	293'399	0.32
L2	25.11.2022	7.0	337 (205; 30)	yes (07.12.2022)	5	38'694	0.97
GL1	04.05.2023	_1	116 (49; 0)	yes (09.05.2023)	4	216'666	0.33
GL2	04.05.2023	11.0	272 (85; 61)	yes (09.05.2023)	6	312'694	0.33
VR3	04.05.2023	18.8	488 (87; 81)	yes (04.05.2023)	8	303'766	0.65
M1	23.03.2023	0.6	40 (26; 0)	yes (23.03.2023)	3	257'430	0.33

 $[\]overline{\ }$ No direct discharge measurement was possible at GL1 due to high flow velocities. However, it can be assumed that the discharge was the same as that measured in GL2.

5.2.2 Pre-processing – Hydrodynamic modeling

The habitat modeling approach selected for this study requires information on the spatial distribution of flow velocities as input. This information can either be measured directly or provided by hydrodynamic models. In this study, the hydrodynamic models of the selected study sites were created using BASEMENT (version 3.2.0; VAW-ETHZ, 2022), which solves the 2D shallow water equations with a finite volume method on unstructured computational meshes (Vanzo et al., 2021). The pre-processing workflow consisted of three steps, which differed slightly depending on the available data at the different study sites. The first step was to obtain the topographic data of the river reaches. Where drone imagery was available, the DEM generated with Pix4D mapper (Pix4D, 2023) was corrected to account for the refraction effect of underwater pixels. This was done with a simplified approach based on the one proposed by Woodget et al. (2015). The resulting bathymetric data were validated with the z coordinates of the GPS points. For those two study sites for which drone imagery was not available (i.e., S1 and S2; Table 11), elevation data from the GPS cross sections were spatially interpolated using the elevation meshing tool of the BASEMesh plugin (version 2.0.0; VAW-ETHZ, 2022) in QGIS (version 3.28). In a second step, the computational mesh for each study site was created using BASEMesh. To avoid boundary condition effects, each model perimeter was defined in a way that the four transects of each study site were located approximately in the middle third of the computational mesh. In a third step, measured discharges and Strickler's roughness coefficient (K_{st}) of the riverbeds were calculated for each hydrodynamic model (Table 12). Discharge represents the boundary conditions in the inflow zone of the model and was calculated based on the water depth and flow velocity measurements using the velocity area method (Herschy, 1993). K_{st} was estimated using following equation (Garbrecht, 1961):

$$K_{st} = 26/d_{90}(1/6)$$
 [m^{1/3}/s]

K_{st} Strickler's roughness coefficient

d₉₀ The particle size at which 90% of the material is finer

In this study, d_{90} was calculated based on the grain size analysis (GSA) proposed by Fehr (1987). In the last step, the model was calibrated against (i.e., the K_{st} values are modified to best fit) the water depths measured in the field and validated against the cross-sectional flow velocity measurements. The computational meshes created contained between 30'000 and 312'000 elements (triangles), with a mean size ranging between 0.32 and 0.97 m² (Table 11).

Overall, the measured water depths, water surface elevations and flow velocities were well reproduced by the hydrodynamic models (Table 12). The root mean square errors (RMSE) of water depths ranged between 0.09 m and 0.22 m, whereas the correspondent mean absolute errors (MAE) were even lower (between 0.07 m and 0.17 m). The RMSEs and MAEs related to the water surface elevations were in a similar range (between 0.01 m and 0.20 m). The K_{st} were only slightly changed during the calibration process according to the overall form roughness parameter, except for L2, where the best simulation results were reached with a K_{st} of 11.5 m^{1/3}/s, that is conspicuously lower than the grain roughness estimated from the GSA (35 m^{1/3}/s). Very likely, the sediment bar (form roughness), where the GSAs were performed, was not representative of the grain size distribution (grain roughness) dominating in the riverbed. The calibrated K_{st} allowed flow velocities to be satisfactorily simulated, as the correspondent RMSEs ranged between 0.14 m/s and 0.29 m/s and the MAEs between 0.11 m/s and 0.21 m/s. Considering all sources of uncertainty in the input data, in the calibration procedure (roughness may change under hydropeaking conditions, as shown by Hauer et al., 2013), as well as in the model structure and parameters, such errors can be considered acceptable. Therefore, the models were used to simulate the spatial distributions of flow velocity at different discharges as input for habitat modeling. The only study site which was poorly modelled was GL2 at the Glenner, where the high water turbidity (due to unexpected snow melt) during the drone flight led to large uncertainties in the topographic data (RMSE wse = 0.35 m). These uncertainties propagated into the numerical simulations, leading to large errors in the simulated flow velocities (RMSE v = 0.93 m/s). For this reason, the GL2 model was not used as input for habitat modeling.

Table 12. Overview of the d_{90} (i.e., the particle size at which 90% of the material is finer), the Strickler's roughness coefficients estimated from the grain size analysis (K_{st} _GSA) and after the calibration (K_{st} _cali), including root mean square error (RMSE) and mean absolute error (MAE) of simulated water depths (h), water surface elevation (wse) and flow velocities (v). For study site abbreviation and location see Figure 2 and Table 5.

Study site	d90 [m]	K_{st} GSA $[m^{1/3}/s]$	K _{st_} cali [m ^{1/3} /s]	RMSE h [m]	MAE h [m]	RMSE wse [m]	MAE wse [m]	RMSE v [m/s]	MAE v [m/s]
S1	0.06	41.6	33.0	0.12	0.10	0.17	0.11	0.20	0.16
S2	0.07	40.5	36.0	0.20	0.17	0.20	0.17	0.17	0.13
TH4	0.07	40.5	42.0	0.18	0.13	0.14	0.10	0.29	0.20
L2	0.17	35.0	11.5	0.13	0.10	0.10	0.06	0.14	0.11
GL1	0.13	36.5	38.0	0.17	0.13	0.18	0.14	-	-
GL2	0.09	38.8	38.0	0.22	0.17	0.35	0.35	0.93	0.77
VR3	0.08	39.6	35.0	0.14	0.10	0.16	0.07	0.28	0.21
M1	0.11	37.6	35.0	0.09	0.07	0.02	0.01	-	-

5.2.3 Univariate habitat modeling

The univariate modeling approach based on the generalized preference curve developed by Schmidlin et al. (2023) was used, which defines habitability classes for the entire macroinvertebrate community based on flow velocity classes (Table 13). For each flow velocity (i.e., habitability) class, a habitat suitability index (HSI) was defined, where HSI close to 1 indicate best suitability whereas HSI close to 0 correspond to a not suitable habitat.

Table 13. Flow velocity classes according to Schmedtje & Colling (1996), the Swiss macroinvertebrate guideline (FOEN, 2019a), and additional literature references. Habitability classes 1 to 5 correspond to the expected habitability suggested by FOEN (2019a). For instance, class 5 can be colonized by most lotic taxa, while class 1 remains only suitable for few taxa. The class "rheobiont+" and "unsuitable" were added by Limnex AG. v40: mean flow velocity at 40% of the water depth (above the streambed).

	Flow velocity class		Habitability class	Habitat Suitability Index (HSI) ¹
Limnophilic (lip)	Standing to slow flowing	v40 < 0.05 m/s	1	0.2
Limno-rheophilic (lrp)	Slow flowing	$0.05 \le v40 < 0.25 \text{ m/s}$	3	0.6
Rheo-limnophilic (rlp) and rheophilic (rhp)	Slow to fast flowing	$0.25 \le v40 < 0.75 \text{ m/s}$	5	1.0
Rheobiont (rhb)	Fast to very fast flowing	$0.75 \le v40 < 1.5 \text{ m/s}$	4	0.8
Rheobiont+ (rhb+)	Very fast flowing	$1.50 \le v40 < 2.5 \text{ m/s}$	2	0.4
Unsuitable (uns)	Extremely fast current	$v40 \ge 2.5 \text{ m/s}$	-	0.0

 $[\]overline{}^{1}$ Habitat Suitability Indices (HIS) were adapted from Schmidlin et al. (2023) to range between 0 and 1.

As the HSI is a spatial distributed index (one value for each mesh element), the weighted usable area (WUA) was calculated as an aggregated index for each study site and simulated discharge:

$$WUA(Q) = \sum_{i=1}^{n} HSI_{i}(Q) \cdot A_{i}$$
 [m²]

WUA(Q) Weighted usable area. Discharge dependent

Ai Area of the i-th wetted mesh element

n Number of wetted mesh elements

 $HSI_i(Q)$ Habitat suitability index for A_i . Discharge dependent

In addition, to allow different study sites and discharge scenarios to be compared with each other, the unitless hydraulic habitat suitability (HHS) was calculated by dividing WUA by the total wetted area (WA).

$$HHS(Q) = \frac{WUA(Q)}{WA(Q)}$$
 [-]

HHS(Q) Hydraulic habitat suitability. Discharge dependent

WUA(Q) Weighted usable area. Discharge dependent.

WA(Q) Total wetted area, i.e. the sum of the areas of the single wetted mesh elements. Discharge dependent

River reaches with the best suitability show *HHS* values close to 1, while those with low suitability result in *HHS* values close to 0.

The habitat modeling approach was applied to different discharge scenarios (Table 14). For each study site modelled, a discharge range was defined based on available data. For reference rivers (Glenner, Thur), their mean annual natural discharge, as well as their minimum and maximum monthly mean natural discharges were defined based on FOEN (2013a). For hydropeaked rivers, the base and peak flow were reconstructed based on ANU (2014a), ANU (2014b) AFU & ANJF (2014). Additional discharges were simulated, including the discharge during the field survey, the mean annual natural discharge, and minimum and maximum monthly mean natural discharge of the hydropeaked river reaches. To increase the resolution of the habitat modeling results, additional scenarios were simulated within each discharge range. The aim was to put the hydraulic characteristics of the hydropeaked rivers in perspective to the natural variability of discharge. In addition, this approach allows a better comparison with the approach of Schmidlin et al. (2023).

Table 14. Simulated discharge range (values between Q_{min} and Q_{max}) for the seven study sites modelled. Between five and 16 additional discharges were simulated within each discharge range to increase the resolution of the habitat modeling results. Discharge ranges were obtained from ANU (2014a), ANU (2014b) AFU & ANJF (2014) and FOEN (2013a). Q_{min} : base flow for hydropeaked rivers resp. minimum monthly mean natural flow for natural/near-natural rivers. Q_{max} : peak flow for hydropeaked rivers resp. maximum monthly mean natural flow for reference rivers. For study site abbreviation and location see Figure 2 and Table 5.

Study sites	Flow regime	Qmin [m ³ /s]	$Q_{max} [m^3/s]$	Additional Q scenarios [m ³ /s]
S1	Hydropeaking	2.0	20.0	3.7, 6.5, 8.5, 10.7, 13, 15, 18
S2	Hydropeaking	2.0	20.0	3.2, 6.5, 8.5, 10.9, 13, 15, 18
TH4	Natural/Near-natural	11.5	36.3	15, 18, 20, 22.5, 25, 27, 30, 33, 35
L2	Hydropeaking	2.4	18.9	3.9, 7, 9.5, 13.3, 16.5
GL1	Natural/Near-natural	3.3	31.8	6, 9, 12.7, 16, 19, 22, 25, 28
VR3	Hydropeaking	2.9	52.9	6, 9, 12, 15, 18.8, 22, 25, 28, 31, 34, 37,
VKS	пушореакті	2.9	32.9	40, 43, 46, 48, 50
M1	Hydropeaking	0.5	22.8	1.5, 4, 6, 8, 10, 12, 1, 16, 18.9

For all discharge scenarios except for the Q_{min} ones, the WUA and the HHS were additionally calculated for the permanently wetted zone, defined as only those mesh elements that are wetted also during Q_{min} conditions.

$$WUA_perm(Q) = \sum_{i=1}^{n} HSI_i(Q) \cdot A_i|_{Omin}$$
 [m²]

WUA_perm(Q) Weighted usable area in the permanently wetted zone. Discharge dependent

 $A_i|_{Qmin}$ Area of the i-th mesh element that is wetted during Q_{min}

n Number of wetted mesh elements

HSI_i(Q) Habitat suitability index for A_i. Discharge dependent

$$HHS_perm(Q) = \frac{WUA_perm(Q)}{WA|_{Qmin}}$$
 [-]

HHS_perm(Q) Hydraulic habitat suitability in the permanently wetted zone. Discharge dependent

WUA_perm(Q) Weighted usable area. Discharge dependent

 $WA|_{Qmin}$ Permanently wetted zone, i.e. the sum of the areas of the mesh elements that were wetted during Q_{min} conditions

To validate the results of the habitat modeling, the spatial distributions of velocity classes were compared with the macroinvertebrate sampling data identified in the laboratory (further details can be found in Scheib, 2023). To inspect whether the results from the habitat modeling correlate with the multimetric index defined in Chapter 4.3.4, all the spectrum of HHS and HHS_perm values obtained for each study site modelled was plotted against the MMI HP ALL of the correspondent study site.

5.3 Results

The spatial distribution of the flow velocity classes at Q_{min} showed in most study sites a clear alignment with the spatial distribution of the macroinvertebrate taxa sampled (Figure 12a; Annex 8.7). At the study site L2, for example, the highest number of taxa sampled on 11.4.2022 was primarily found within the flow velocity class with the highest habitability (0.25 \leq v₄₀ < 0.75 m/s; Table 13). Under Q_{max} conditions, the spatial distribution of taxa within the permanently wetted zone continued to align with the flow velocity classes, with the highest number of taxa found in the velocity class with the highest habitability, as well as in the second most favorable class (0.75 \leq v₄₀ < 1.50 m/s) (Figure 12c).

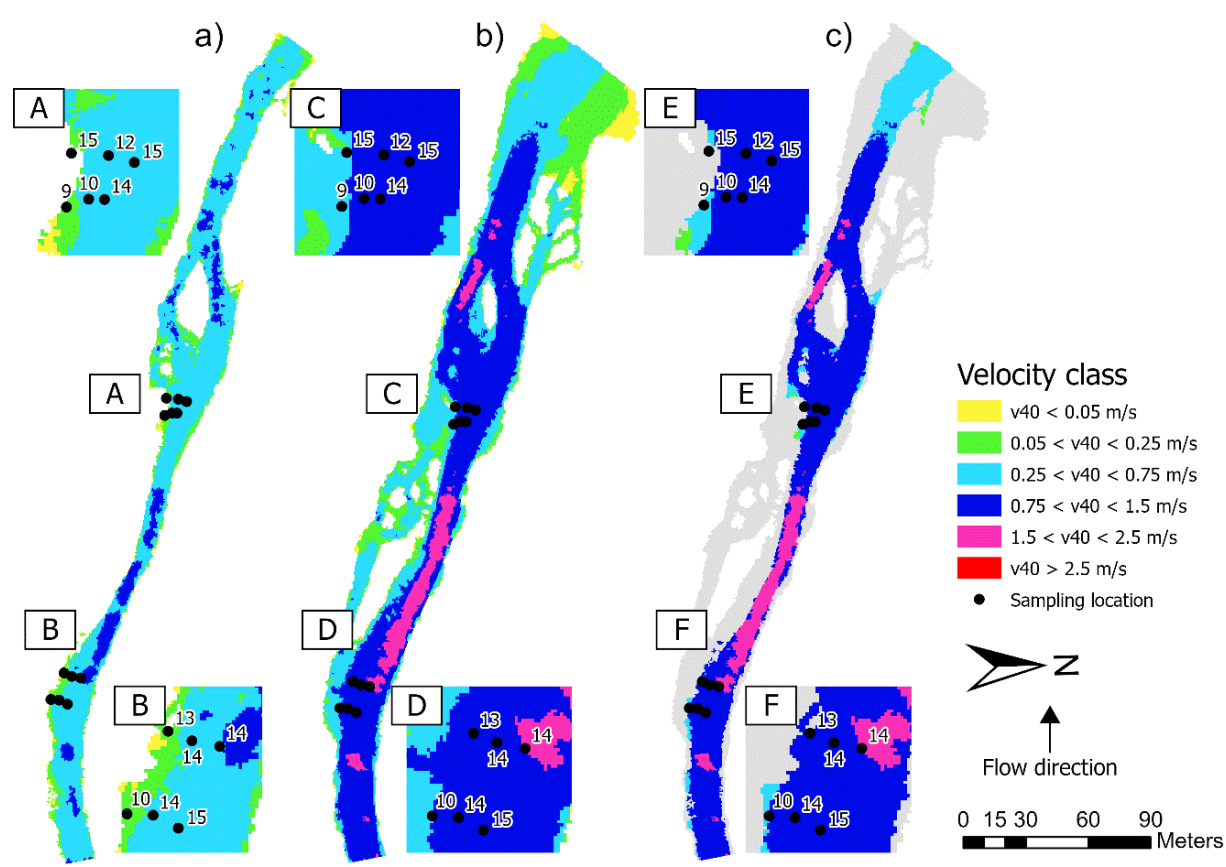


Figure 12. Spatial distribution of flow velocity classes in the L2 study site. a) Q_{min} scenario (2.4 m^3/s); b) Q_{max} scenario (18.9 m^3/s); c) Q_{max} scenario considering only the permanently wetted zone. The dewatering area is shaded grey. A-F represent an enlarged view of the locations (black dots), where macroinvertebrates were sampled, whereas the numbers indicate the different macroinvertebrate taxa found with the laboratory identification. The spatial distributions of flow velocity classes for the other study sites can be found in Annex 8.7. For study site abbreviation and location see Figure 2 and Table 5.

The spatial distribution of velocity classes varied considerably across study sites and discharges scenarios (Figure 13a). During Q_{min} , the most represented velocity classes were the one characterized by slow to fast flowing water $(0.25 \le v_{40} < 0.75 \text{ m/s})$; predominant at L2, S2, and VR3) and that one characterized by slow flowing water $(0.05 \le v_{40} < 0.25 \text{ m/s})$; predominant at S1and M1). In the two study sites with a (near-) natural flow regime, TH4 and GL1, the fast to very fast class $(0.75 \le v_{40} < 1.5 \text{ m/s})$ dominated over the other classes. At GL1, the second fastest velocity class $(1.5 \le v_{40} < 2.5 \text{ m/s})$ was present even under Q_{min} conditions, and velocities exceeding 2.5 m/s emerged at discharges of 9 m³/s. As discharge increased, the spatial extent of the two fastest velocity classes expanded, ultimately covering 72% of the wetted area at Q_{max} . In contrast, L2 remained dominated by velocities below 1.5 m/s. The fastest velocity class did not occur even at Q_{max} , and the second fastest class $(1.5 \le v_{40} < 2.5 \text{ m/s})$ was predicted to cover a maximum of only 7% of the wetted area during Q_{max} . As discharge increased, slow-flowing areas $(0.05 \le v_{40} < 0.25 \text{ m/s})$ in L2 slightly increased due to the activation of two side channels (Figure 13a).

With respect to the permanently wetted zone, standing water and area with slow-flowing water (v_{40} < 0.25 m/s) generally decreased as discharge increased (Figure 13b). The dominance of fast to very fast velocity classes ($v \ge 0.75$ m/s) became apparent in most scenarios, except at GL1 and under very high discharges at M1 and VR3, where even higher velocities dominated. Within the permanently wetted zone, areas with slow to fast flowing water (0.25 m/s $\le v_{40} < 0.75$ m/s) tended to persist even under higher discharges at most study sites. However, they tend to diminish with increasing discharge. In general, the areas with velocities associated with the best three habitability classes (0.05 m/s $\le v_{40} < 1.5$ m/s) were present in more than 50% of the permanently wetted zones area under all discharge scenarios.

However, an exception is observed at GL1, where these velocity classes declined to less than 40% of the permanently wetted area as soon as a discharge of 12.7 m³/s is reached (Figure 13b).

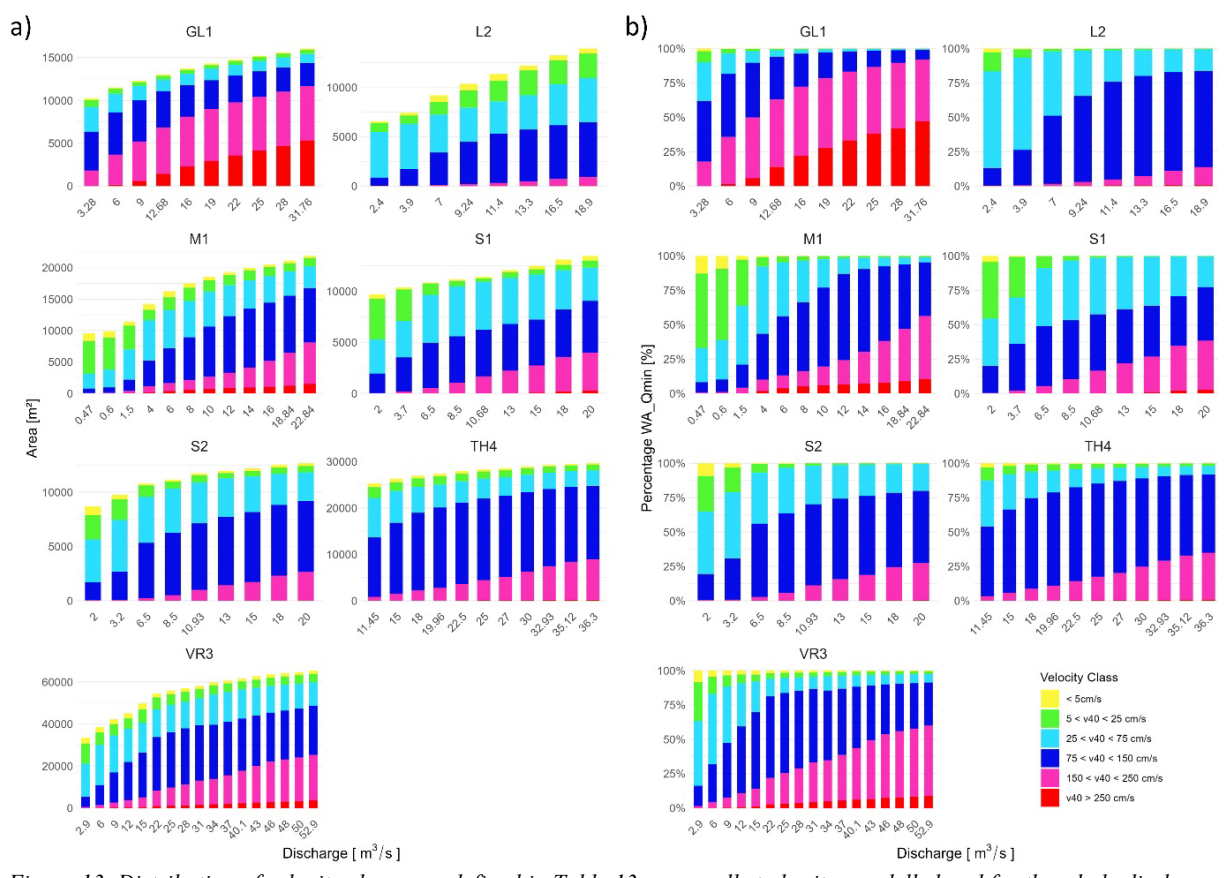


Figure 13. Distribution of velocity classes as defined in Table 13 across all study sites modelled and for the whole discharge spectrum as defined in Table 14. a) Area values in m^2 considering the whole wetted area. b) Percentage of permanently wetted zone (wetted area during Q_{min} conditions). For study site abbreviation and location see Figure 2 and Table 5.

The wetted area (WA) increased with increasing discharge across all study sites (Figure 14, top panels). The most pronounced increases were simulated in VR3 and M1, where the WA nearly doubled its extension when passing from Q_{min} to Q_{max}. The weighted usable area (WUA) exhibited site-specific trends (Figure 14, middle panels). For most study sites, it increased with increasing discharge. Exceptions were observed in TH4, where the WUA remained constant, and GL1, where it slightly decreased with higher discharges. When considering only the permanently wetted zone, WUA_perm decreased at nearly all study sites as discharge increased. This decline was most pronounced in VR3. Exceptions were observed in M1 and S1, where WUA_perm initially increased slightly before starting to decrease with higher discharge.

The hydraulic habitat suitability (HHS) constantly decreased in GL1 and TH4, whereas at M1, S1, S2, and VR3, it initially increased at lower discharges before decreasing at higher discharges, creating therefore local knickpoints (at 4 m³/s for M1, 6.5 m³/s for S1 and S2, and 6 m³/s for VR3) (Figure 14, bottom panels). At L2, HHS initially decreased until a discharge of 12 m³/s, after which it stabilized. Across all sites, the highest HHS values were simulated at L2, whereas the lowest were at GL1. The trend of HHS_perm closely mirrored that of HHS at S1, S2, and TH4. At VR3 and GL1, HHS_perm decreased more rapidly than HHS with increasing discharge (Figure 14, bottom panels). At L2 it remained higher than HHS across the entire discharge spectrum. At M1, HHS_perm exceeded HHS up to a discharge of 9 m³/s, with a maximum near 4 m³/s, after which it dropped below HHS. As with HHS, the highest HHS perm values were simulated at L2, while the lowest values occurred at GL1 and VR3.

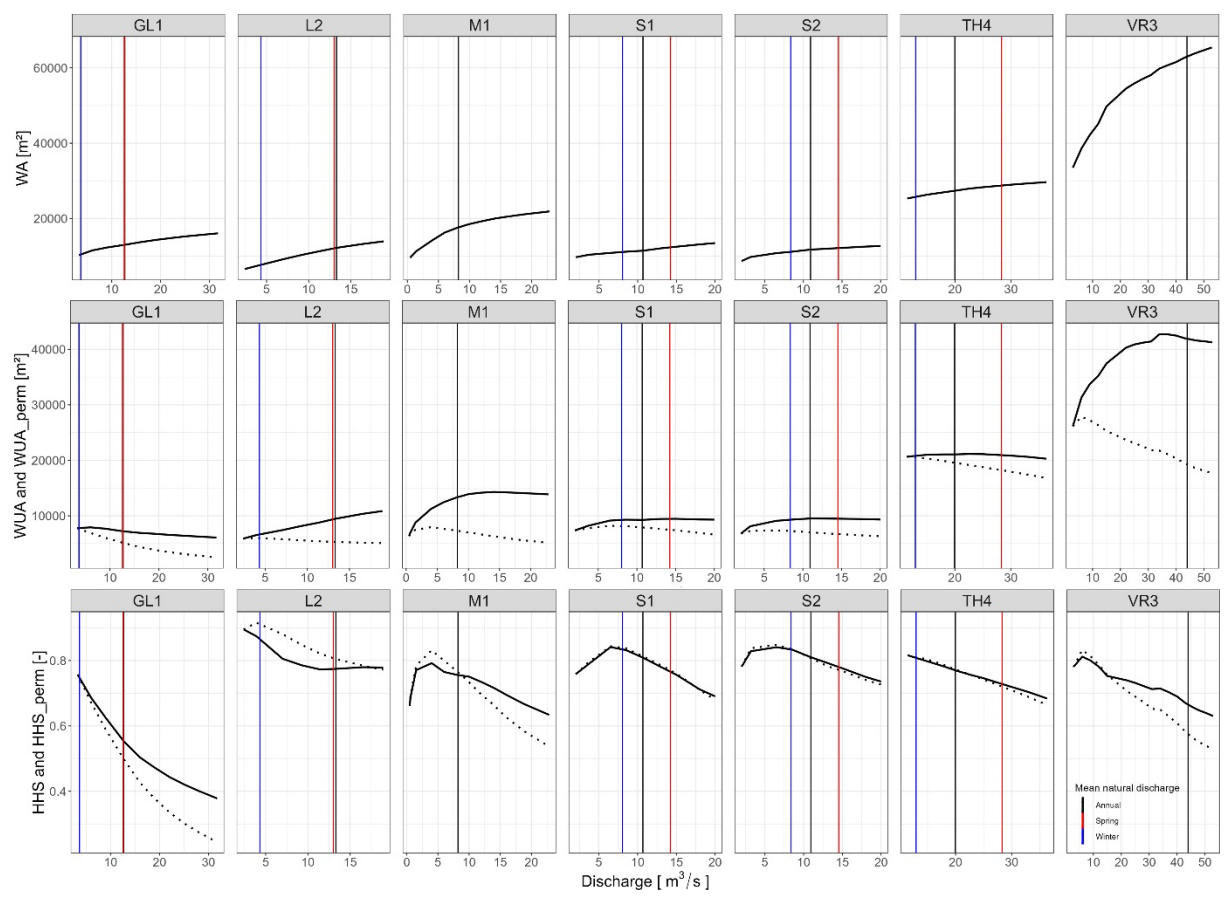


Figure 14. Wetted area (WA) weighted usable area (WUA) and hydraulic habitat suitability (HHS) of the seven study sites modelled with the univariate approach of Schmidlin et al. (2023). Solid lines refer to the total wetted areas, whereas dotted lines refer to the permanently wetted zone (i.e., wetted areas during Q_{min} conditions). The mean natural annual, spring (March-May) and winter (December-February) discharges are displayed as vertical lines. For M1 and VR3 the mean monthly natural discharges were not available. For study site abbreviation and location see Figure 2 and Table 5.

The comparison between the results of the univariate habitat modeling (HHS_perm) and the multimetric index based on both datasets from this study (MMI_HP_All; Chapter 4.3.4) revealed only weak to moderate correlations between the two metrics (Figure 15). The correlation was stronger with the field-screening data (r = 0.53 considering the HHS_perm values of the whole discharge spectrum resp. 0.32 when considering the weighted HHS_perm) than with the laboratory data (r = 0.10 in both cases). Notably, the study site with the highest mean HHS_perm across the entire discharge spectrum (L2) exhibited one of the lowest MMI_HP_All values when considering the laboratory data. Conversely, the site M1 had the highest MMI_HP_All value based on both field-screening and laboratory data but ranked only fifth in in terms mean HHS_perm.

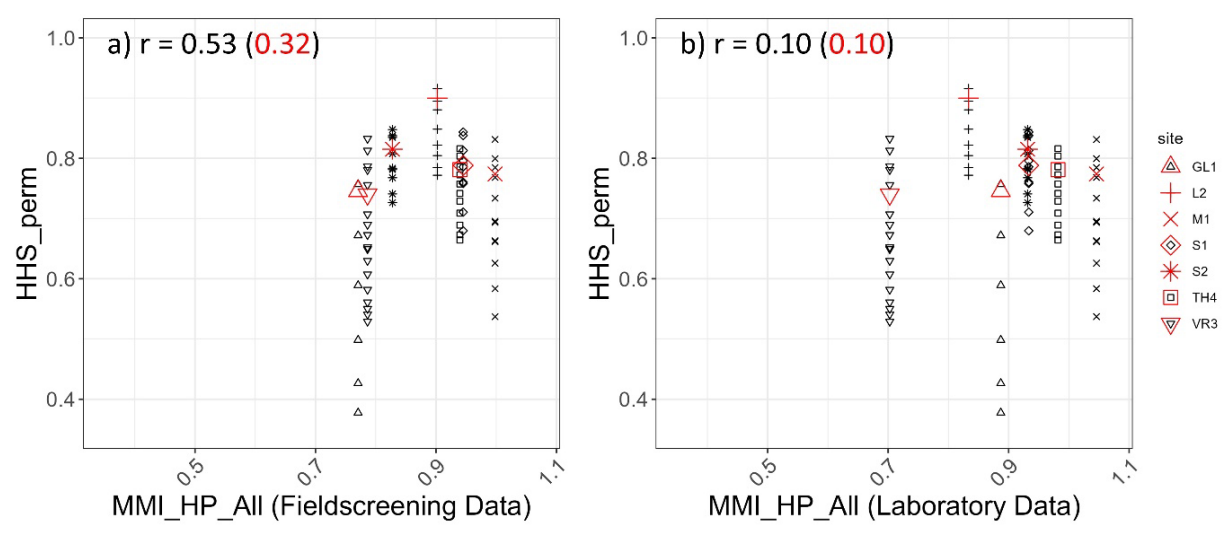


Figure 15. Comparison between the hydraulic habitat suitability (calculated for the permanently wetted zone; HHS_perm) and the Swiss multimetric index for hydropeaking based on both datasets (MMI_HP_ALL; Chapter 4.3.4) for each study site modelled. a) MMI_HP_ALL calculated with the field data; b) MMI_HP_ALL calculated with the laboratory data. Black symbols represent HHS_perm values calculated across the entire discharge spectrum, whereas red symbols correspond to the mean HHS_perm values weighted with the discharge of the last six month before macroinvertebrate sampling. r: Pearson correlation coefficient. Black values refer to the entire discharge spectrum, whereas red values were calculated with the weighted HHS perm values. For study site abbreviation and location see Figure 2 and Table 5.

5.4 Discussion

The univariate habitat modeling approach based on the generalized HSC for the entire macroinvertebrate community (Schmidlin et al., 2023) was successfully validated against the sampling data collected at study site L2, as the highest number of taxa was found where the highest habitability classes were predicted (supporting the hypothesis 3 defined in Chapter 1). As effects of further environmental parameters (e.g., substrate, water depths, as well as their temporal variation) were not considered, the spatial extent of suitable habitats modelled with this approach may be overestimated (Schmidlin et al., 2023). However, flow velocity is widely recognized in the literature as a reliable proxy for habitat suitability. For example, the hydrologically sensitive invertebrate community index (LIFENZ, Greenwood et al., 2016) also utilizes flow velocity preference categories, which closely align with those proposed by Schmidlin et al. (2023). Similarly, the Canadian Ecological Flow Index (CEFI) is based on flow velocity preferences of 55 common invertebrate taxa (Armanini et al., 2011).

The distribution of velocity classes reflected the interplay between the hydrological and morphological characteristics of the study sites. At nearly all study sites, slow-flowing areas (preferred by lentic taxa) decreased substantially as discharge increased. The only exception was at L2, where a slow-flowing side channel became activate at a discharge between 3.9 and 7 m³/s. When considering only the permanently wetted zone, study sites with greater morphological complexity (e.g., M1 and VR3) exhibited higher flow heterogeneity also at higher discharges. In contrast, velocities at GL1 were uniformly high, as the study site is characterized by a narrow channel with very steep banks.

Hydropeaking-induced changes in the availability of suitable habitats were detected at all modelled study sites. Discharge thresholds, at which the availability of suitable habitats reached a maximum or exhibited a trend change were identified (Figure 14). Therefore, this approach allows the effects of mitigation or restoration measures to be estimated, such as an increase of Q_{min} or a reduction in the magnitude of Q_{max}. The highest mitigation/restoration effects can be expected at study sites showing steep HHS curves (e.g., M1, VR3), whereas sites with a smaller gradient (e.g., L2) would show minor changes.

Considering habitat persistency when interpreting modeling outcomes is essential for assessing habitat

conditions for sessile organism such as macroinvertebrates. The modeling results indicated that, in some cases (e.g., at S1, S2, and TH4), the interaction between the river morphology and discharge led to a similar spatial distribution of suitable habitats between the permanently wetted zone and the dewatering area. Consequently, the HHS and the HHS_perm curves were nearly overlapping. In general, metrics such as WUA and HHS have the drawback of not explicitly accounting for the spatial distribution of suitable habitats at the patch scale (i.e., individual microhabitats within the habitat mosaic) and the distance between them (Bruder et al., 2016; Bätz et al., 2024). Thus, for a comprehensive analysis, these metrics should always be complemented by habitat suitability distribution maps. Additionally, a promising refinement of the approach by Schmidlin et al. (2023) could involve quantifying temporal variations in habitat composition. As both Q_{min} and Q_{max} occur less frequently in rivers with a (near-) natural flow regime compared to hydropeaked rivers, their frequency of occurrence may lead to markable differences in potential impacts (Hayes et al., 2024). This aspect could be addressed, for example, by incorporating additional metrics such as the "habitat probability" and the "habitat shift" within patches, as recently proposed by Bätz et. al. (2024), or by identifying persistent suitable habitats in the context of hydropeaking, as demonstrated in Hauer et al. (2024).

The comparison between the outcomes of the univariate habitat modeling (HHS perm) and the multimetric index developed in this study (MMI HP ALL) revealed a moderate correlation with the field-screening data but only a weak correlation with the laboratory data. This weak correlation may be attributed to uncertainties in the macroinvertebrate datasets and the numerically simulated flow velocities. Additional factors, such as the occurrence of preceding flood events, the potential influence of grain roughness on macroinvertebrates (which is not captured in the model's surface roughness representation), different spatial aggregation of the two metrics – HHS perm being calculated for the entire river reach, whereas macroinvertebrates sampling is performed at the patch scale – and seasonal variations (only partially accounted for in the univariate modeling approach used here) may also contribute to this uncertainty. However, increasing the complexity of the modeling approach did not automatically lead to improved predictive performance. In the master thesis of Scheib (2024), machine learning techniques (e.g., random forests and boosted regression trees) were applied to quantify the availability of suitable habitats based on different combinations of environmental predictors. Yet, the predictive accuracy of these models remained unsatisfactory. This finding aligns with the weak response of macroinvertebrate communities to hydrological alterations discussed in Chapter 4.4. Additional environmental factors, such as those related to morphology and sediment (Bipa et al., 2024) as well as water quality (Buffagni et al., 2009; Larsen et al., 2021; Wirth, 2025 - results of the Random Forest models), play a non-negligible role in shaping the macroinvertebrates community. Consequently, the univariate habitat modeling approach applied here – based solely on flow velocity – may not fully explain the variability in the macroinvertebrate community composition. Extending the univariate habitat modeling approach to additional study sites, particularly those with low MMI_HP_ALL values between 0.55 and 0.75 (as the MMI HP ALL value-range in Figure 15 is quite limited: 0.77-1.00), could improve the assessment of a potential trend between these two methods.

6 General discussion and conclusions

Aquatic macroinvertebrates are widely recognized as crucial bioindicators for assessing anthropogenic alterations in freshwaters (Hering et al., 2003; Lear et al., 2009; FOEN, 2019a). However, the specific effects of hydropeaking on these organisms are diverse and complex, as different taxa exhibit varying degrees of vulnerability to the multiple impacts associated with frequent flow fluctuations. Numerous studies have explored both the short- and long-term consequences of hydropeaking on benthic macroinvertebrates, considering a range of intensity-related parameters such as up- and down-ramping rates, flow velocity, flow amplitude, and event frequency. Hydropeaking-induced hydrological and hydraulic changes alters hydromorphological habitat conditions, which trigger passive drift especially during up-ramping phases (e.g., Bruno et al., 2010, 2013; Schülting et al., 2016, 2023; Friese et al., 2025) and increase the risk of stranding between the permanently wetted zone and the dewatered area during down-ramping phases (e.g., Tanno et al., 2016; Tonolla et al., 2023). The resulting reduction in permanently suitable habitats (e.g., Bätz et al., 2023, 2024) alters colonization dynamics and can lead to long-term shifts in the faunal composition of macroinvertebrate communities in hydropeaked rivers (Cushman, 1985; Bretschko & Moog, 1990; Schmutz et al., 2013; Leitner et al., 2017; Kjaerstad et al., 2018).

6.1 Methodological approach for assessing the response of macroinvertebrates to hydropeaking – drift, stranding, changing habitat conditions

The impact of hydropeaking on aquatic macroinvertebrates can be assessed through drift and stranding analyses, as well as benthic habitat sampling. Drift and stranding analyses are relatively complex and provide a snapshot of the short-term effects of individual hydropeaking events (Tonolla et al., 2023). However, these methods do not offer insights into the overall community structure within a river reach. In contrast, benthic habitat sampling is well suited to detect long-term changes in faunal composition resulting from cumulative hydropeaking effects. Accordingly, **drift and stranding analyses are valuable for evaluating the immediate response of benthic communities to discrete flow variables, whereas benthic sampling is more appropriate for assessing broader, long-term impacts of hydropeaking on population structure (Salmaso et al., 2021)**. In this context, and as applied in the present study, we recommend assessing hydrological variables over six months preceding macroinvertebrate sampling. This period is deemed sufficient to capture potential seasonal variations in the intensity and/or frequency of hydropeaking events. It also allows for the detection of long-term effects of anthropogenic flow fluctuations on macroinvertebrate communities, particularly given the unequal life cycles of sensitive hemilimnic organisms, including various larval stages of EPT taxa (Poff et al., 1991; Bacher & Waringer, 1996; Leitner et al., 2017).

As the focus of the present study was on a methodology for recording the influence of hydropeaking on the benthic community, a **benthic sampling method** was employed based on the newly developed Austrian hydropeaking assessment approach (Leitner et al., 2025), which represents a **time- and cost-saving field method** (**field-screening method**; Chapter 3.2.1). The **multimetric indices** developed from the obtained data reflects the current ecological status of the given river reach, **based on the established aquatic macroinvertebrate community using the selected core metrics** (Chapter 4.3.4). This method allows for the comparison of different river reaches regardless of river type and can therefore be applied not only to assess hydropeaking impacts, but also to evaluate the effectiveness of hydrological and/or morphological mitigation or restoration measures through **a pre- and post-implementation comparison of the benthic macroinvertebrate community** – serving, in this sense, as an **efficient monitoring tool**.

6.2 Evaluation and effects of hydropeaking variables on macroinvertebrates

For the Biological Quality Element (BQE) "fish," as defined in the Water Framework Directive (WFD), as well as for the fish-related metrics "fish stranding" and "habitat suitability" in the "Swiss mitigation guideline" (Tonolla et al., 2017; Tonolla, 2023), relatively specific conclusions can already be drawn regarding the influence of various hydropeaking-related hydrological and hydraulic variables. This is much more challenging for benthic macroinvertebrates due to the varying sensitivities of taxa to anthropogenic influences. For instance, Schmutz et al. (2015) demonstrated that fish are most strongly affected by a combination of hydropeaking event frequency, ramping rate, and morphological habitat conditions. Ramping rates exceeding 15 cm/h were identified as particularly harmful, especially when occurring more than 20 times per year. More recently, Hayes et al. (2024) found that, for example for juvenile grayling, stranding becomes a significant concern when three or more hydropeaking events occur per day, regardless of the ramping rate's intensity. Moreover, fish responses are species-specific, and it is well established that larval and juvenile fish are at greater risk of stranding than adults (e.g., Nagrodski et al., 2012; Harby & Noack, 2013; Moreira et al., 2019).

With regard to aquatic macroinvertebrates, drawing precise conclusions about the effects of specific hydropeaking-related hydrological and hydraulic variables is more complex than for fish. This complexity arises from the much higher taxonomic and trait diversity among macroinvertebrates and their correspondingly diverse habitat preferences (e.g., Schmidlin et al., 2023). These preferences not only vary between taxa but often also between different larval stages within the same taxon (e.g., Bacher & Waringer, 1996). Moreover, the experimental drift study by Schülting et al. (2023), has shown that the magnitude of macroinvertebrate responses to hydropeaking depends strongly on physiological and behavioral adaptations. For instance, interstitial and current-tolerant taxa generally exhibit significantly less drift compared to current-sensitive taxa or those dwelling on the substrate surface. Their findings also identified flow amplitude as the primary driver of increased drift, while up-ramping rates only lead to increased drift when specific discharge-related thresholds, such as flow velocity, are exceeded. Tanno et al. (2021) and Tonolla et al. (2023) further demonstrated that macroinvertebrate stranding is positively correlated with drift, particularly during the up-ramping phase. The risk of stranding also increases with greater fluctuations in the wetted area between base and peak flows – driven by the flow ratio – and is further amplified by higher down-ramping rates (Kroger, 1973; Perry & Perry, 1986; Tanno et al., 2016; Tonolla et al., 2023). The findings of Tonolla et al. (2023) further highlighted that current-sensitive taxa, such as the Trichoptera family Limnephilidae, are particularly vulnerable to hydropeaking, whereas more current-tolerant taxa, like the Ephemeroptera family Heptageniidae, appear more resistant to both short- and long-term effects. Interestingly, despite showing high levels of drift and stranding, highly resilient taxa such as Chironomidae and Baetidae remained dominant in the benthic community, and no significant reduction in overall benthic density was observed in their experimental field study. In addition, Friese et al. (2025) revealed that drift responses vary significantly between habitats characterized by fast (> 0.5 m/s) and slow (< 0.5 m/s) currents, with the latter being more susceptible to hydraulic stress. Collectively, these studies suggest that flow velocity, which integrates the hydrological and morphological characteristics of a site, is a reliable proxy for assessing hydropeaking impacts on macroinvertebrates (Schmidlin et al., 2023; Schülting et al., 2023; Tonolla et al., 2023; Friese et al., 2025). Accordingly, the generalized preference curve developed by Schmidlin et al. (2023) – which defines habitat suitability classes for the entire macroinvertebrate community based on flow velocity classes – represents a robust approach for modeling the effects of mitigation measures on these communities. Furthermore, Bätz et al. (2023, 2024) emphasized the importance of evaluating the spatiotemporal variability of habitats. They proposed novel metrics such as "habitat shifts within patches", which quantify the frequency of habitat condition changes in a given patch over time, as a mean of assessing habitat persistence for sessile organisms like macroinvertebrates. Despite these promising approaches, case-specific factors – such as substrate composition, water depth, water quality, and the influence of tributaries – must still be considered to ensure accurate ecological assessments.

In the present study, we developed a multimetric index (MMI HP ALL) to assess the specific influence of hydropeaking on macroinvertebrate communities. This index integrates individual metrics that best represent community structure (including diversity) and ecological status, while specifically reflecting hydropeaking-related hydrological and hydraulic impacts. MMI HP ALL was also designed to minimize the influence of natural variability and other environmental factors – such as morphology, water quality, or topography – by accounting for 42 covariates (Chapter 3.3). The five most reliable metrics ultimately selected and combined into the MMI HP ALL were: (i) Shannon-Wiener diversity, (ii) the number of Plecoptera taxa, (iii) the weighted average of Diversity Class (DK) of the Swiss water quality index based on macroinvertebrates (IBCH), (iv) the dominance of interstitial-dwelling taxa, and (5) a modified version of the Canadian Ecological Flow Index (CEFI), (Chapter 4.3.4). We tested (Chapter 4.3.5) both the individual macroinvertebrate metrics and the composite MMI HP ALL using correlation analyses against single hydrological variables (e.g., up-ramping flow rate, event frequency) and a multimetric hydrological index (CNT MAFR RATIO), which summarizes hydropeaking-specific hydrological characteristics into a single value (Chapter 3.3; according to Greimel et al., 2016; Greimel & Zeiringer, 2025). The results indicate that macroinvertebrate communities do respond to hydrological and hydraulic alterations. However, the strength of these responses was relatively weak and varied across No consistent correlation patterns were observed between biogeographical regions. CNT MAFR RATIO and MMI HP ALL, nor between individual hydrological variables and their corresponding macroinvertebrate metrics (Annex 8.2). Despite the heterogeneity of results, we consider the MMI HP ALL to be a more targeted and effective tool for assessing hydropeaking effects on macroinvertebrate communities than traditional indices not specifically designed for this purpose - such as the Swiss IBCH (FOEN, 2019a), which was primarily developed to assess deficits in water quality and microhabitat diversity.

In summary, we argue that **changes in MMI_HP_ALL values can serve as a meaningful index for evaluating the effectiveness of hydrological mitigation or restoration measures based on before-and-after comparisons (Wirkungskontrolle)**. This is particularly valid when comparing the effects of mitigation at the same study site over time. We expect that computing the MMI_HP_ALL at a specific site or reach – before and after implementation of mitigation measures – will reduce signal variability and noise. Consequently, this approach should yield stronger correlations than comparisons across sites with differing hydrological regimes and macroinvertebrate communities.

6.3 Conclusions and recommendations

As discussed in Chapter 6.1, the influence of hydropeaking on macroinvertebrates can be demonstrated through drift analyses, which show clear correlations with individual hydropeaking-related hydrological and hydraulic variables – particularly flow velocity. However, while drift data provide valuable insights, they only allow for a limited assessment of the broader ecological consequences. In some cases, such as the studies by Tanno et al. (2021) and Tonolla et al. (2023), no strong effects were observed on key community parameters such as benthic density of certain dominant taxa. This indicates that **drift alone** is not a reliable predictor of hydropeaking-related impacts on benthic communities. Moreover, the context-dependent nature of these experimental studies, often limited by (field)-specific constraints, prevents the derivation of universally applicable stressor thresholds (e.g., for the number of prior hydropeaking events).

In contrast to previous approaches, the present study adopts a broader ecological perspective by evaluating the established aquatic macroinvertebrate community in the context of long-term hydropeaking effects. Overall, macroinvertebrate responses to hydropeaking were generally weak, both for abundance-based metrics and for the most hydropeaking-sensitive indices. This contrasts with recent Austrian studies (Leitner et al., 2025; Auhser et al., in prep.), which reported stronger correlations between macroinvertebrate communities and hydropeaking intensity. The weaker relationships observed here likely reflect the greater complexity of assessing hydropeaking impacts at larger spatial scales, where interacting factors such as river type, channel gradient, sediment dynamics, and water quality introduce significant variability in macroinvertebrate responses (Bipa et al., 2024).

Morphological and sedimentological conditions are key determinants of faunal composition. To minimize their confounding influence and better isolate hydrological and hydraulic drivers shaping macroinvertebrate communities, the sampling design of our study focused on gravel bars, which represent relatively unaltered morphological units (Chapter 3.1). In addition, both the relative proportion and diversity of substrate types were considered as environmental covariates during the selection of macroinvertebrate metrics (Chapters 3.3 and 4.2.2). However, unlike most Austrian rivers included in the hydropeaking guideline by Leitner et al. (2025), not all Swiss study sites featured gravel bars, and sediment composition was generally more heterogeneous. As a result, morphological and sedimentological effects could not be entirely excluded in the present study.

The Austrian study sites likely experience greater fine sediment accumulation, potentially due to lower channel gradients, differing geology, enhanced sediment inputs, or differences in power plant operation regimes. Morphological features, especially substrate heterogeneity and particle size, directly influence habitat stability and suitability. Fine sediment accumulation leads to more homogeneous substrates, which tend to support less diverse and more uniform faunal assemblages (Beisel et al., 2000). Hydropeaking can exacerbate these effects by disrupting sediment supply, causing selective bed mobility and hydraulic habitat instability (Vericat et al., 2020; Bätz et al., 2023), which negatively affect benthic diversity (Death & Winterbourn, 1995). In contrast, coarser substrates – such as those dominated by macro- and megalithal particles – offer more stable microhabitats and provide essential hydraulic refugia and flow shelter, particularly for lentic taxa during frequent water-level fluctuations. For instance, Swiss sites like the Moesa (M4), Plessur (P1), Landquart (L1), and Verzasca (V1) were characterized by substrates in which blocks larger than 250 mm comprised over 50% of the riverbed (Annex 8.2), potentially offering more favorable microhabitat conditions. These findings highlight the need to assess hydropeaking impacts on macroinvertebrate communities at the habitat patch scale and to consider sedimentological and morphological site characteristics in the development of effective, sitespecific river management and restoration strategies (Bätz et al., 2023; Friese et al., 2025).

It can therefore be cautiously inferred that the more natural morphological conditions observed at many of the assessed Swiss study sites may enhance their resistance and resilience to hydropeaking compared to the more morphologically impaired Austrian study sites. However, this conclusion is subject to several uncertainties. In particular, hydropeaking intensity (at least for certain hydropeaking-related hydrological variables) in our study may have been underestimated due to missing or incomplete hydrological data (Chapter 3.3.1). Additionally, habitat modeling often struggles to accurately reproduce the hydraulic conditions of complex microhabitats, such as those found at many study sites with steep slopes and predominantly coarse sediment, which limits the accuracy of model predictions.

Water quality also plays a significant role in shaping macroinvertebrate communities (Buffagni et al., 2009; Larsen et al., 2021). Its interaction with hydropeaking, morphology, and sediment composition further complicates ecological interpretation. In the present study, for example, total nitrogen concentrations and the proportion of settlement area in the catchment emerged as key drivers influencing

macroinvertebrate metrics (Wirth, 2025). In addition, the spatial location within the river network can have a strong influence on species richness, with headwater systems generally supporting lower species diversity than higher-order rivers (Ward, 1998). Spatial position within the river network adds another layer of complexity. Headwater systems generally support lower species richness than higher-order streams (Ward, 1998). This effect was partially controlled for by selecting study sites based on Strahler stream order and discharge regime, and by sampling along longitudinal gradients within the same reach (Chapters 2.1.2 and 2.2). Nonetheless, some residual influence of specific site location on taxonomic diversity cannot be excluded.

Other potential drivers potentially influencing macroinvertebrate communities – such as biotic interactions (e.g., predation, competition), colonization history, recolonization potential (Dudley et al., 1990; Mackay 1992; Wallace & Webster, 1996; Schuwirth et al., 2016), and climate change (Durance & Ormerod, 2007; Domisch et al., 2011) – were not incorporated into the MMI, as they are difficult to quantify. Their exclusion may further limit the explanatory power of our analyses.

Additionally, the trait classifications of taxa in surface/interstitial or lentic/lotic, which are partly included in the Swiss MMIs, were adopted from the Austrian hydropeaking guideline (Leitner et al., 2025) without modification to avoid statistical overfitting. However, refining these classifications using the current dataset could improve indices sensitivity, especially for river types that differ substantially from Austrian systems, such as those in the biogeographical region of the Southern Alps (Moesa, Ticino, Verzasca). Moreover, the current classification does not adequately account for taxa that exhibit both surface-dwelling behavior and current tolerance, as exemplified by the Ephemeroptera genus *Rhithrogena* or the Diptera families Blephariceridae and Simuliidae. In contrast, other surface dwellers, such as most taxa of the Trichoptera family Limnephilidae, are highly sensitive to strong currents. A combined metric incorporating both habitat preference and flow tolerance could improve the diagnostic precision and ecological relevance of the assessment.

In conclusion, effective mitigation and restoration of hydropeaked rivers require an integrated approach that considers hydrology, morphology, sedimentology, and water quality in concert. Tools such as the generalized preference curves by Schmidlin et al. (2023), the habitat metrics proposed by Bätz et al. (2024), and the multimetric indices developed in this study offer valuable guidance. However, due to methodological simplifications and/or data limitations, their application and interpretation should be guided by expert judgement and embedded within a multifactorial, site-specific framework. In our view, particular attention should be paid to grain size, water quality, and the spatial location of the site within the river network.

7 References

- Abernethy EF, Muehlbauer JD, Kennedy TA, Tonkin JD, Van Driesche R, & Lytle DA. 2021. Hydropeaking intensity and dam proximity limit aquatic invertebrate diversity in the Colorado River Basin. *Ecosphere* 12, e03559. https://doi.org/10.1002/ecs2.3559
- AFU & ANJF. 2014. Sanierung Wasserkraft Kanton St. Gallen. Strategische Planung zur Wiederherstellung der Fischwanderung, zur Sanierung von Schwall und Sunk und zur Sanierung des Geschiebehaushaltes. Amt für Umwelt und Energie & Amt für Natur, Jagd und Fischerei.
- Ahmadi-Nedushan B, St-Hilaire A, Bérubé M, Robichaud É, Thiémonge N, & Bobée B. 2006. A review of statistical methods for the evaluation of aquatic habitat suitability for instream flow assessment. *River Research and Applications* 22, 503–523. https://doi.org/10.1002/rra.918
- Alp M, Batalla RJ, Bejarano MD, Boavida I, Capra H, Carolli M, ... & Bruno MC. 2023. Introducing HyPeak: An international network on hydropeaking research, practice, and policy. *River Research and Applications* 39, 283–291. https://doi.org/10.1002/rra.39966
- ANU. 2014a. Strategische Planung Sanierung Schwall und Sunk: Defizitanalyse, Massnahmenplanung Kanton Graubünden. Koordinationsgebiet: Alpenrhein und Zuflüsse. Amt für Natur und Umwelt Graunbünden.
- ANU. 2014b. Strategische Planung Sanierung Schwall und Sunk: Defizitanalyse, Massnahmenplanung Kanton Graubünden. Koordinationsgebiet: Misox. Amt für Natur und Umwelt Graubünden.
- Armanini DG, Horrigan N, Monk WA, Peters DL, & Baird DJ. 2011. Development of a benthic macroinvertebrate flow sensitivity index for Canadian rivers. *River Research and Applications* 27, 723–737. https://doi.org/10.1002/rra.1389
- Arthington AH, Bhaduri A, Bunn SE, Jackson SE, Tharme RE, Tickner D, ... & Ward S. 2018. The Brisbane declaration and global action agenda on environmental flows. *Frontiers in Environmental Science* 6. https://doi.org/10.3389/fenvs.2018.00045
- Auhser A, Leitner P, Merl K, Hayes D, Tonolla D, Greimel F, & Graf W. in prep. Evaluating the impact of hydropeaking on macroinvertebrates using the Austrian "fieldscreening method".
- Bacher I, & Waringer JA. 1996. Hydraulic microdistribution of cased caddis larvae in an Austrian mountain brook. *Internationale Revue der Gesamten Hydrobiologie* 81, 541–554. https://doi.org/10.1002/iroh.19960810408
- Bätz N, Judes C, & Weber C. 2023. Nervous habitat patches: The effect of hydropeaking on habitat dynamics. *River Research and Applications* 39, 349–363. https://doi.org/10.1002/rra.4021
- Bätz N, Judes C, Vanzo D, Lamouroux N, Capra H, Baumgartner J, ... & Weber C. 2024. Patch-scale habitat dynamics: three metrics to assess ecological impacts of frequent hydropeaking. *Journal of Ecohydraulics* 10, 79–106. https://doi.org/10.1080/24705357.2024.2426790
- Baumann P, & Klaus I. 2003. Gewässerökologische Auswirkungen des Schwallbetriebes: Ergebnisse einer Literaturstudie. *Mitteilungen zur Fischerei*. 75. Herausgegeben vom Bundesamt für Umwelt, Bern.
- Beisel JN, Usseglio-Polatera P, & Moreteau J.C. 2000. The spatial heterogeneity of a river bottom: a key factor determining macroinvertebrate communities. *Hydrobiologia* 422, 163–171. https://doi.org/10.1023/A:1017094606335
- Bipa NJ, Stradiotti G, Righetti M, & Pisaturo GR. 2024. Impacts of hydropeaking: A systematic review. *Science of The Total Environment* 912, 169251. https://doi.org/10.1016/j.scitotenv.2023.169251
- Birk S, Bonne W, Borja A, Brucet S, Courrat A, Poikane S, ... & Hering D. 2012. Three hundred ways to assess Europe's surface waters: An almost complete overview of biological methods to implement the Water Framework Directive. *Ecological Indicators* 18, 31–41. https://doi.org/10.1016/j.ecolind.2011.10.009
- BML. 2025. Einleitung. Leitfaden zur Bewertung und Minderung der Auswirkungen von

- Schwallbelastungen. Bundeministerium für Land- und Forstwirtschaft, Regionen und Wasserwirtschaft, Wien.
- BMLRT. 2020. Leitfaden zur Ableitung und Bewertung des ökologischen Potentials bei erheblich veränderten Wasserkörpern, Wien.
- Boes R, Burlando P, Evers F, Felix D, Hohermuth B, Schmid M, ... & Manso P. 2021. Swiss potential for hydropower generation and storage. ETH Zurich, Zurich, Switzerland: Synthesis report.
- Bovee KD. 1982. A guide to stream habitat analysis using the instream flow incremental methodology. In *Instream Flow Information Paper 12*, USDI Fish and Wildlife Services, Office of Biology Services, Washington DC.
- Bretschko G, & Moog O. 1990. Downstream effects of intermittent power generation. *Water Science & Technology* 22, 127–135. https://doi.org/10.2166/wst.1990.0020
- Bruder A, Tonolla D, Schweizer SP, Vollenweider S, Langhans SD, & Wüest A. 2016. A conceptual framework for hydropeaking mitigation. *Science of the Total Environment* 568, 1204–1212. https://doi.org/10.1016/j.scitotenv.2016.05.032
- Bruno MC, Maiolini B, Carolli M, & Silveri L. 2010. Short time-scale impacts of hydropeaking on benthic invertebrates in an Alpine stream (Trentino, Italy). *Limnologica*, 40, 281-290. https://doi.org/10.1016/j.limno.2009.11.012
- Bruno MC, Siviglia A, Carolli M, & Maiolini B. 2013. Multiple drift responses of benthic invertebrates to interacting hydropeaking and thermopeaking waves. *Ecohydrology*, 6, 511–522. https://doi.org/10.1002/eco.1275
- Bruno MC, Cashman MJ, Maiolini B, Biffi S, & Zolezzi G. 2016. Responses of benthic invertebrates to repeated hydropeaking in semi-natural flume simulations. *Ecohydrology* 9, 68–82. https://doi.org/10.1002/eco.1611
- Buffagni A, Armanini DG, & Erba S. 2009. Does the lentic-lotic character of rivers affect invertebrate metrics used in the assessment of ecological quality? *Journal of Limnology* 68, 92–105 https://doi.org/10.4081/jlimnol.2009.92
- Bunn SE, & Arthington AH. 2002. Basic principles and ecological consequences of altered flow regimes for aquatic biodiversity. *Environmental Management* 30, 492–507. https://doi.org/10.1007/s00267-002-2737-0
- BUWAL. 1998. Methoden zur Untersuchung und Beurteilung der Fliessgewässer in der Schweiz. Ökomorphologie Stufe F (flächendeckend). *Mitteilungen zum Gewässerschutz*: 27.
- Céréghino, R, Cugny P, & Lavandier P. 2002. Influence of intermittent hydropeaking on the longitudinal zonation patterns of benthic invertebrates in a mountain stream. *International Review of Hydrobiology* 87: 47-60. <a href="https://doi.org/10.1002/1522-2632(200201)87:1<47::AID-IROH47>3.0.CO;2-9">https://doi.org/10.1002/1522-2632(200201)87:1<47::AID-IROH47>3.0.CO;2-9
- Cushman RM. 1985. Review of ecological effects of rapidly varying flows downstream from hydroelectric facilities. *North American Journal of Fisheries Management* 5, 330–339. https://doi.org/10.1577/1548-8659(1985)5<330:ROEEOR>2.0.CO;2
- Death RG, & Winterbourn MJ. 1995. Diversity patterns in stream benthic invertebrate communities: the influence of habitat stability. *Ecology*, 765, 1446-1460. https://doi.org/10.2307/1938147
- Domisch S, Jähnig SC, & Haase P. 2011. Climate-change winners and losers: stream macroinvertebrates of a submontane region in Central Europe. *Freshwater Biology* 56, 2009–2020. https://doi.org/10.1111/j.1365-2427.2011.02631.x
- Dudley TL, D'Antonio CM, & Cooper SD. 1990. Mechanisms and consequences of interspecific competition between two stream insects. The Journal of Animal Ecology 59, 849–866. https://doi.org/10.2307/5018
- Dufrene M, & Legendre P. 1997. Species assemblages and indicator species: the need for a flexible asymmetrical approach. *Ecological Monographs* 67, 345–366. https://doi.org/10.1890/0012-9615(1997)067[0345:SAAIST]2.0.CO;2

- Durance I, & Ormerod SJ. 2007. Climate change effects on upland stream macroinvertebrates over a 25-year period. *Global Change Biology* 13, 942–957. http://dx.doi.org/10.1111/j.1365-2486.2007.01340.x
- Elgueta A, Górski K, Thoms M, Fierro P, Toledo B, Manosalva A, & Habit E. 2021. Interplay of geomorphology and hydrology drives macroinvertebrate assemblage responses to hydropeaking. *Science of the Total Environment* 768, 144262. https://doi.org/10.1016/j.scitotenv.2020.144262
- Fehr R. 1987. Einfache Bestimmung der Korngrössenverteilung von Geschiebematerial mit Hilfe der Linienzahlanalyse. *Schweizer Ingenieur und Architekt* 105, 1104–1109. https://doi.org/10.5169/seals-76710
- FOEN. 2013a. Mean runoff and flow regime types for the river network of Switzerland. Swiss Federal Office for the Environment.
- FOEN. 2013b. River Typology for Switzerland. Swiss Federal Office for the Environment.
- FOEN. 2013c. Ecomorphology Level F River reaches. Swiss Federal Office for the Environment.
- FOEN. 2014. Strahler stream order. Swiss Federal Office for the Environment.
- FOEN. 2019a. Methoden zur Untersuchung und Beurteilung von Fliessgewässern (IBCH_2019). Makrozoobenthos Stufe F. Swiss Federal Office for the Environment. Umwelt-Vollzug, 1026.
- FOEN. 2019b. Topographical catchment areas of Swiss waterbodies 2 km². Swiss Federal Office for the Environment.
- FOEN. 2020. Biogeographical regions of Switzerland. Swiss Federal Office for the Environment.
- Friese N, Mathers KL, Weber C, Tonolla D, Bätz N. 2025. Habitat-specific response of macroinvertebrate drift to rapid flow pulses: implications for hydropeaking management. *Freshwater Biology* (submitted).
- FSO. 2018. Swiss land use statistics. Swiss Federal Statistical Office.
- Garbrecht G. 1961. Abflussberechnung für Flüsse und Kanäle. *Die Wasserwirtschaft* 51, 40–45 and 72–77.
- Gąsiorowski D, Szymkiewicz R. 2022. Inverse flood routing using simplified flow equations. *Water Resources Management* 36, 4115–4135. https://doi.org/10.1007/s11269-022-03244-8
- Gibbins CN, Vericat D, Batalla RJ, & Buendia C. 2016. Which variables should be used to link invertebrate drift to river hydraulic conditions? *Fundamental and Applied Limnology* 187, 191–205. https://doi.org/10.1127/fal/2015/0745
- Gillies CL, Hose GC, & Turak E. 2009. What do qualitative rapid assessment collections of macroinvertebrates represent? A comparison with extensive quantitative sampling. *Environmental Monitoring and Assessment* 149, 99–112. https://doi.org/10.1007/s10661-008-0186-9
- Giri S Zhang Z, Krasnuk D, Lathrop RG. 2019. Evaluating the impact of land uses on stream integrity using machine learning algorithms. *Science of The Total Environment* 696, 133858. https://doi.org/10.1016/j.scitotenv.2019.133858
- Graf W, Leitner P, Moog O, Steidl C, Salcher G, Ochsenhofer G, & Müllner K. 2013. Schwallproblematik an Österreichs Fließgewässern Ökologische Folgen und Sanierungsmöglichkeiten. Vienna, Austria: Datenerhebung und Analyse Benthische Invertebraten.
- Greenwood MJ, Booker DJ, Smith BJ, & Winterbourn MJ. 2016. A hydrologically sensitive invertebrate community index for New Zealand rivers. *Ecological Indicators* 61, 1000–1010. https://doi.org/10.1016/j.ecolind.2015.10.058
- Greimel F, Zeiringer B, Höller N, Grün B, Godina R, & Schmutz S. 2016. A method to detect and characterize sub-daily flow fluctuations. *Hydrological Processes* 30, 2063–2078. https://doi.org/10.1002/hyp.10773
- Greimel F, & Zeiringer B. 2025. Teil B Hydrologische Maßnahmen-Bewertung und Monitoring von kurzfristigen Abflussregimen. Leitfaden zur Bewertung und Minderung der Auswirkungen von Schwallbelastungen. Bundeministerium für Land- und Forstwirtschaft, Regionen und Wasserwirtschaft, Wien.

- Greimel F, Neubarth J, Zeiringer B, Leitner P, Holzapfel P, Graf W, Hauer C, Schmutz S, & Ofenböck G. 2025. Teil A Maßnahmenfindung und -bewertung. Leitfaden zur Bewertung und Minderung der Auswirkungen von Schwallbelastungen. Bundeministerium für Land- und Forstwirtschaft, Regionen und Wasserwirtschaft, Wien.
- Grün B, Haider J, & Greimel F. 2022. Hydropeak Detect and characterize sub-daily flow fluctuations. https://cran.r-project.org/web/packages/hydropeak/index.html
- Gulde R, & Wunderlin P. 2024. Grenzwertüberschreitungen im Gewässer mit ARA-Ausbau beseitigen Stoffflussanalyse identifiziert betroffene ARA. VSA, Glattbrugg.
- Harby A, & Noack M. 2013. Rapid flow fluctuations and impacts on fish and the aquatic ecosystem. *In* Ecohydraulics: An Integrated Approach. Maddock J, Harby A, Kemp P, & Wood P (Eds), John Wiley & Sons, 323–335. https://doi.org/10.1002/9781118526576.ch19
- Hauer C, Schober B, & Habersack H. 2013. Impact analysis of river morphology and roughness variability on hydropeaking based on numerical modeling: *Hydrological Processes* 27, 2209–2224. https://doi.org/10.1002/hyp.9519
- Hauer C, Unfer G, Holzapfel P, & Tritthart M. 2024. Habitat persistency analysis with HEM-PEAK: A novel approach for the assessment of hydropeaking impacts and mitigation measure design. *River Research and Applications* 40, 1296–1313. https://doi.org/10.1002/rra.4291
- Hayes DS, Schülting L, Carolli M, Greimel F, Batalla RJ, & Casas-Mulet R. 2022. Hydropeaking: Processes, effects, and mitigation. *In* Mehner T, & Tockner K (Eds.), *Encyclopedia of Inland Waters* (Second Edition), Elsevier.
- Hayes S, Bruno MC, Alp M, Boavida I, Batalla RJ, Bejarano MD, ... & Venus TE. 2023. 100 key questions to guide hydropeaking research and policy. *Renewable and Sustainable Energy Reviews* 187, 113729. https://doi.org/10.1016/j.rser.2023.113729
- Hayes DS, Bätz N, Tonolla D, Merl K, Auer S, Gorla L, ... & Greimel F. 2024. Why hydropeaking frequency matters: effects of recurring stranding on fish. *Journal of Ecohydraulics*, 1–17. https://doi.org/10.1080/24705357.2024.2426820
- Hering D, Buffagni A, Moog O, Sandin L, Sommerhäuser M, Stubauer I ... & Zahrádková S. 2003. The development of a system to assess the ecological quality of streams based on macroinvertebrates Design of the sampling programme within the AQEM Project. *International Review of Hydrobiology* 88, 345–361. https://doi.org/10.1002/iroh.200390030
- Hering D, Feld CK, Moog O, & Ofenböck T. 2006. Cook book for the development of a multimetric index for biological condition of aquatic ecosystems: experiences from the European AQEM and STAR projects and related initiatives. *Hydrobiologia* 566, 311–324. https://doi.org/10.1007/s10750-006-0087-2
- Herschy R. 1993. The velocity-area method. *Flow Measurement and Instrumentation* 4, 7–10. https://doi.org/10.1016/0955-5986(93)90004-3
- Horne AC, Nathan R, Poff NL, Bond NR, Webb JA, Wang J, & John A. 2019. Modeling flow-ecology responses in the Anthropocene: Challenges for sustainable riverine management. *BioScience* 69, 789–799. https://doi.org/10.1093/biosci/biz087
- Humphrey CL, Storey AW, & Thurtell L. 2000. AUSRIVAS: operator sample processing errors and temporal variability implications for model sensitivity. *In*: Wright JF, Sutcliffe DW, & Furse MT (Eds.) Assessing the biological quality of fresh waters. *RIVPACS and other Techniques*, 143–163. Freshwater Biological Association, Ambleside, UK.
- Hutching, C, Spiess E, & Prasuhn V. 2023. Abschätzung diffuser Stickstoff- und Phosphoreinträge in die Gewässer der Schweiz mit MODIFFUS 3.1. Stand 2020. Agroscope, Zurich. https://doi.org/10.34776/as155g
- Ilg C, Flury R, Küng M, Wittmer I, Maurer V, Menetrey N, ... & Albert R. 2022. Abwasserbewirtschaftung bei Regenwetter. Modul Gewässeruntersuchung, Bestimmungshilfe Makroinvertebraten. Verband Schweizer Abwasser- und Gewässerschutzfachleute (VSA),

- Glattbrugg.
- Kasssambara A, & Mundt F. 2020. Factoextra: Extract and visualize the results of multivariate data analyses. R package version 1.0.7. https://CRAN.R-project.org/package=factoextra
- Kjærstad G, Arnekleiv JV, Speed JDM, & Herland, AK. 2018. Effects of hydropeaking on benthic invertebrate community composition in two central Norwegian rivers. *River Research and Applications* 34, 218–231. https://doi.org/10.1002/rra.3241
- Krell B, Röder N, Link M, Gergs R, Entling MH, & Schäfer RB. 2015. Aquatic prey subsidies to riparian spiders in a stream with different land use types. *Limnologica* 51, https://doi.org/10.1016/j.limno.2014.10.001
- Kroger RL. 1973. Biological effects of fluctuating water levels in the Snake River, grand Teton National Park, Wyoming. *The American Midland Naturalist* 89, 478–481. https://doi.org/10.2307/2424055.
- Larsen S, Majone B, Zulian P, Stella E, Bellin A, Bruno MC, & Zolezzi G. 2021. Combining hydrologic simulations and stream-network models to reveal flow-ecology relationships in a large Alpine catchment. *Water Resources Research*, e2020WR028496. https://doi.org/10.1029/2020WR028496
- Lauters F, Lavandier P, Lim P, Sabaton C, & Belaud A. 1996. Influence of hydropeaking on invertebrates and their relationship with fish feeding habits in a Pyrenean River. *Regulated Rivers: Research and Management* 12, 563–573. <a href="https://doi.org/10.1002/(sici)1099-1646(199611)12:6<563::aid-rrr380>3.0.co;2-m">https://doi.org/10.1002/(sici)1099-1646(199611)12:6<563::aid-rrr380>3.0.co;2-m
- Le S, Josse J, & Husson F. 2008. FactoMineR: An R Package for Multivariate Analysis. *Journal of Statistical Software* 25, 1–18. https://doi.org/10.18637/jss.v025.i01
- Lear G, Boothroyd IKG, Turner SJ, Roberts K, & Lewis GD. 2009. A comparison of bacteria and benthic invertebrates as indicators of ecological health in streams. *Freshwater Biology* 54, 1532–1543. https://doi.org/10.1111/j.1365-2427.2009.02190.x
- Leathwick JR, Elith J, & Hastie T. 2006. Comparative performance of generalized additive models and multivariate adaptive regression splines for statistical modeling of species distributions. *Ecological Modeling* 199, 188–196. https://doi.org/10.1016/j.ecolmodel.2006.05.022
- Leitner P, Hauer C, & Graf W. 2017. Habitat use and tolerance levels of macroinvertebrates concerning hydraulic stress in hydropeaking rivers A case study at the Ziller River in Austria. *Science of the Total Environment* 575, 112–118. https://doi.org/10.1016/j.scitotenv.2016.10.011
- Leitner P, Auhser A, Schülting L, Dossi F, Hartmann A, Greimel F, & Graf W. 2025. Teil E Methodik zur Durchführung des benthosökologischen Prä- und Postmonitorings an schwallbeeinflussten Gewässern. Leitfaden zur Bewertung und Minderung der Auswirkungen von Schwallbelastungen. Bundeministerium für Land- und Forstwirtschaft, Regionen und Wasserwirtschaft, Wien
- Leyer I, & Wesche K. 2008. Multivariate Statistik in der Ökologie. (Ed. L.-T.J.S.& V.G. Leipzig), Springer Verlag Berlin Heidelberg, Berlin.
- Looser D. 2022. Entwicklung eines Schwallbewertungsindexes auf Basis aquatischer Makroinvertebraten. Bachelor Thesis. Zurich University of Applied Sciences ZHAW, Wädenswil.
- Mackay RJ. 1992. Colonization by lotic macroinvertebrates: a review of processes and patterns. *Canadian Journal of Fisheries and Aquatic Sciences* 49, 617–628. https://doi.org/10.1139/f92-071
- McCarthy GT. 1938. The unit hydrograph and flood routing. *Conference of North Atlantic Division*, US Army Corps of Engineers, New London, CT. US Engineering.
- McCullagh P, & Nelder JA. 1990. Generalised linear models. *The Mathematical Gazette* 74, 320–321. https://doi.org/10.2307/3619865
- Metzeling L, Chessman B, Hardwick R, & Wong V. 2003. Rapid assessment of rivers using macroinvertebrates: the role of experience, and comparisons with quantitative methods. *Hydrobiologia* 510, 39–52. https://doi.org/10.1023/B:HYDR.0000008500.34301.a0
- Milner VS, Yarnell SM, & Peek RA. 2019. The ecological importance of unregulated tributaries to macroinvertebrate diversity and community composition in a regulated river. *Hydrobiologia* 829, 291–305. https://doi.org/10.1007/s10750-018-3840-4

- Moog O. 1993. Quantification of daily peak hydropower effects on aquatic fauna and management to minimize environmental impacts. *Regulated Rivers: Research & Management* 8, 5–14. https://doi.org/10.1002/rrr.3450080105
- Moog O, & Hartmann A. 2017. Fauna Aquatica Austriaca, 3. Edition 2017. BMLFUW, Wien.
- Moreira M, Hayes DS, Boavida I, Schletterer M, Schmutz S, & Pinheiro A. 2019. Ecologically-based criteria for hydropeaking mitigation: a review. *Science of the Total Environment* 657, 1508–1522. https://doi.org/10.1016/j.scitotenv.2018.12.107
- Nagrodski A, Raby GD, Hasler CT, Taylor MK, & Cooke SJ. 2012. Fish stranding in freshwater systems: sources, consequences, and mitigation. *Journal of Environmental Management* 103, 133–141. https://doi.org/10.1016/j.jenvman.2012.03.007
- Naman SM, Rosenfeld JS, & Richardson JS. 2016. Causes and consequences of invertebrate drift in running waters: From individuals to populations and trophic fluxes. *Canadian Journal of Fisheries and Aquatic Sciences* 73, 1292–1305. https://doi.org/10.1139/cjfas-2015-0363
- Nichols SJ, & Norris RH. 2006. River condition assessment may depend on the sub-sampling method: Field live-sort versus laboratory sub-sampling of invertebrates for bioassessment. *Hydrobiologia* 572, 195–213. https://doi.org/10.1007/s10750-006-0253-6
- Ofenböck T, Moog O, Gerritsen J, & Barbour M. 2004. A stressor specific multimetric approach for monitoring running waters in Austria using benthic macro-invertebrates. *Hydrobiologia* 516, 251–268. https://doi.org/10.1023/B:HYDR.0000025269.74061.f9
- Ofenböck T, Moog O, Hartmann A, Schwarzinger I, & Leitner P. 2019. Leitfaden zur Erhebung der biologischen Qualitätselemente Teil A Makrozoobenthos. Bundesministerium für Nachhaltigkeit und Tourismus, Wien.
- Oksanen J, Simpson G, Blanchet FG, Kindt R, Legendre P, Minchin P, ... & Weedon J. 2022. Vegan community ecology package. *R package* version 2.6-2.
- Perry SA, & Perry WB. 1986. Effects of experimental flow regulation on invertebrate drift and stranding in the Flathead and Kootenai Rivers, Montana, USA. *Hydrobiologia* 134, 171–182. https://doi.org/10.1007/BF00006739
- Person E. 2013. Impact of hydropeaking on fish and their habitat. Phd Thesis. EPFL, Lausanne.
- Pichler M, & Hartig F. 2023. Machine learning and deep learning A review for ecologists. *Methods in Ecology and Evolution* 14, 994–1016. https://doi.org/10.1111/2041-210X.14061
- Pix4D. 2023. PIX4Dmapper: Professional photogrammetry software for drone mapping.
- Poff NL, DeCino RD, & Ward JV. 1991. Size-dependent drift responses of mayflies to experimental hydrologic variation: Active predator avoidance or passive hydrodynamic displacement? *Oecologia* 88, 577–586. https://doi.org/10.1007/BF00317723
- Poff N L. 2018. Beyond the natural flow regime? Broadening the hydro-ecological foundation to meet environmental flows challenges in a non-stationary world. *Freshwater Biology* 63, 1011–1021. https://doi.org/10.1111/fwb.13038
- R Core Team. 2023. R: A language and environment for statistical computing. R Foundation for Statistical Computing, Vienna, Austria.
- Rader RB. 1997. A functional classification of the drift: Traits that influence invertebrate availability to salmonids. *Canadian Journal of Fisheries and Aquatic Sciences* 54, 1211–1234. https://doi.org/10.1139/f97-025
- Royer Q, Gunten, DV, Le Coarer Y, Lamouroux N, Capra H, Sagnes P, & Zaoui F. 2022. HABBY: A new open-source software to estimate hydraulic habitat suitability. *In* IAHR 2022 from Snow to Sea, Granada, Spain.
- Ruhi A, Dong X, McDaniel CH, Batzer DP, & Sabo JL. 2018. Detrimental effects of a novel flow regime on the functional trajectory of an aquatic invertebrate metacommunity. *Global Change Biology* 24, 3749–3765. https://doi.org/10.1111/gcb.14133
- Salmaso F, Servanzi L, Crosa G, Quadroni S, & Espa P. 2021. Assessing the impacts of hydropeaking

- on river benthic macroinvertebrates: A state-of-the-art methodological overview. *Environments* 8, 67. https://doi.org/10.3390/environments8070067
- Schär P. 2007. Projektdokumentation Modellstudie Schweiz (GIS-Teil). Swiss Federal Office for the Environment. Unpublished.
- Scheib M. 2023. Comparing habitat modeling approaches for the assessment of macroinvertebrate response to hydropeaking. Project Work. Zurich University of Applied Sciences ZHAW, Wädenswil.
- Scheib M. 2024. Predicting hydropeaking effects on spatiotemporal macroinvertebrate distribution by using machine learning algorithms. Master Thesis. Zurich University of Applied Sciences ZHAW, Wädenswil.
- Schmedtje U, & Colling M. 1996. Ökologische Typisierung der aquatischen Makrofauna. *Informationsberichte des Bayerischen Landesamtes für Wasserwirtschaft*, 4/96.
- Schmidlin S, Tanno D, Baumgartner J, Berger B, & Tonolla D. 2023. Habitateignung Makrozoobenthos (B5). *In* Tonolla D (Ed.). Erarbeitung und Beurteilung von Schwall-Sunk Massnahmen Neue Erkenntnisse aus Forschung und Praxis. Report commissioned by the Swiss Federal Office for the Environment.
- Schmutz S, Fohler N, Friedrich T, Fuhrmann M, Graf W, Greimel F, ... & Zeiringer B. 2013. Schwallproblematik an Österreichs Fließgewässern Ökologische Folgen und Sanierungsmöglichkeiten. BMFLUW, Wien.
- Schmutz S, Bakken TH, Friedrich T, Greimel F, Harby A, Jungwirth M, ... & Zeiringer, B. 2015. Response of fish communities to hydrological and morphological alterations in hydropeaking rivers of Austria. *River Research and Applications*, 31, 919–930. https://doi.org/10.1002/rra.2795
- Schneider M, Kopecki I, Tuhtan J, Sauterleute JF, Zinke P, Bakken TH, ... & Merigoux S. 2017. A fuzzy rule-based model for the assessment of macrobenthic habitats under hydropeaking impact. *River Research and Applications* 33, 377–387. https://doi.org/10.1002/rra.3079
- Schülting L, Feld CK, & Graf W. 2016. Effects of hydro- and thermopeaking on benthic macroinvertebrate drift. *Science of the Total Environment* 573, 1472–1480. https://doi.org/10.1016/j.scitotenv.2016.08.022
- Schülting L, Dossi F, Graf W, & Tonolla D. 2023. Flow amplitude or up-ramping rate? Quantifying single and combined effects on macroinvertebrate drift during hydropeaking simulations, considering sensitive traits. *River Research and Applications* 39, 412–426. https://doi.org/10.1002/rra.3963
- Schuwirth N, Dietzel A, & Reichert P. 2016. The importance of biotic interactions for the prediction of macroinvertebrate communities under multiple stressors. *Functional Ecology* 30, 974–984. https://doi.org/10.1111/1365-2435.12605
- SFOE. 2024. Status of hydropower utilization in Switzerland on the 31st December 2023. Swiss Federal Office of Energy.
- Spreafico M, Hodel HP, & Kaspar H. 2001. Rauheiten in ausgesuchten schweizerischen Fliessgewässern. Berichte des BWG, Serie Wasser Bern.
- Statzner B, & Holm TF. 1982. Morphological adaptations of benthic invertebrates to stream flow an old question studied by means of a new technique (Laser Doppler Anemometry). *Oecologia* 53, 290–292. https://doi.org/10.1007/BF00389001
- Staub E, Blardone M, Droz M, Hertig A, Meier E, Soller E, ... & Zulliger D. 2003. Angelfang, Forellenbestand und Einflussgrössen: Regionalisierte Auswertung mittels GIS. Fischnetz, Netzwerk Fischrückgang Schweiz. BUWAL, EAWAG.
- Tachet H, Richoux P, Bournaud M, & Usseglio-Polatera P. 2000. Invertébrés d'eau douce, systématique, biologie, écologie. Paris: CNRS Editions.
- Tanno D. 2012. Physical habitat modeling for the assessment of macroinvertebrate response to hydropeaking. Master-Thesis, University of Zurich, Zurich.
- Tanno D, Wächter K, & Schmidlin S. 2016. Stranden von Wasserwirbellosen bei Schwallrückgang -

- Ergebnisse einer Pilotstudie. Wasser Energie Luft 108, 277-284.
- Tanno D, Wächter K, & Gerber R. 2021. Stranden von Wasserwirbellosen bei Schwallrückgang Fallstudie am Hinterrhein. *Wasser Energie Luft* 113, 89–96.
- Theodoropoulos C, Vourka A, Skoulikidis N, Rutschmann P, & Stamou A. 2018. Evaluating the performance of habitat models for predicting the environmental flow requirements of benthic macroinvertebrates. *Journal of Ecohydraulics* 3 30–44. https://doi.org/10.1080/24705357.2018.1440360
- Thomas EA, & Schanz F. 1976. Beziehungen zwischen Wasserchemismus und Primärproduktion in Fliessgewässern, ein limnologisches Problem. *Vierteljahresschriften der Naturforschenden Gesellschaft Zürich* 121, 309–317.
- Tonolla D, Chaix O, Meile T, Zurwerra A, Büsser P, Oppliger S, & Essyad K. 2017. Schwall-Sunk Massnahmen. Ein Modul der Vollzugshilfe Renaturierung der Gewässer. Bundesamt für Umwelt, Bern. *Umwelt-Vollzug* 1701.
- Tonolla D. 2023. Erarbeitung und Beurteilung von Schwall-Sunk Massnahmen Neue Erkenntnisse aus Forschung und Praxis. Report commissioned by the Swiss Federal Office for the Environment.
- Tonolla D, Dossi F, Kastenhofer O, Doering M, Hauer C, Graf W, & Schülting L. 2023. Effects of hydropeaking on drift, stranding and community composition of macroinvertebrates: A field experimental approach in three regulated Swiss rivers. *River Research and Applications* 39, 427–443. https://doi.org/10.1002/rra.4019
- Vallefuoco F. 2022. Advancing quantitative understanding of flow-ecology relations in Alpine rivers. Phd Thesis. Università degli Studi di Trento, a.y. 2018/2019, Civil, Environmental and Mechanical Engineering, XXXIV Cycle.
- Vanzo, D, Peter S, Vonwiller L, Bürgler M, Weberndorfer M, Siviglia A, ... & Vetsch DF. 2021. BASEMENT v3: A modular freeware for river process modeling over multiple computational backends. *Environmental Modeling & Software* 143, 105102. https://doi.org/10.1016/j.envsoft.2021.105102
- VAW-ETHZ. 2022. BASEMENT Basic simulation environment for computation of environmental Fflows and natural hazard simulation. Version 3.2.0, ETH Zurich, VAW.
- Vericat D, Ville F, Palau-Ibars A, & Batalla RJ. 2020. Effects of hydropeaking on bed mobility: Evidence from a Pyrenean River. *Water* 12,178. https://doi.org/10.3390/w12010178
- Wallace JB, & Webster JR. 1996. The role of macroinvertebrates in stream ecosystem function. *Annual Review of Entomology* 41, 115–139. https://doi.org/10.1146/annurev.en.41.010196.000555
- Ward JV. 1998. Riverine landscapes: Biodiversity patterns, disturbance regimes, and aquatic conservation. *Biological Conservation* 83, 269–278. https://doi.org/10.1016/S0006-3207(97)00083-9
- Wirth S. 2023. Vergleich von Labor- und Felddaten aus der Erhebung der Makroinvertebraten-Zönose. Project Work. Zurich University of Applied Sciences ZHAW, Wädenswil.
- Wirth S. 2025. Einfluss abiotischer Faktoren auf Makroinvertebraten-Metriken: Analyse mit Random Forest Modellen. Master Thesis. Zurich University of Applied Sciences ZHAW, Wädenswil.
- Woodget AS, Carbonneau PE, Visser F, & Maddock IP. 2015. Quantifying submerged fluvial topography using hyperspatial resolution UAS imagery and structure from motion photogrammetry. *Earth Surface Processes and Landforms* 40, 47–64. https://doi.org/10.1002/esp.3613
- Working group RHEOPHYLAX (BOKU, Vienna) (in prep). New biological traits and ecological preferences of European freshwater organisms for freshwaterecology.info.
- Young PS, Cech JJ, & Thompson LC. 2011. Hydropower-related pulsed-flow impacts on stream fishes: A brief review, conceptual model, knowledge gaps, and research needs. *Reviews in Fish Biology and Fisheries*, 21, 713–731. https://doi.org/10.1007/s11160-011-9211-0

8 Annex

8.1 Macroinvertebrate data ZHAW and Aquabug

Macroinvertebrate taxa identified by the ZHAW and Aquabug were summarized in the Excel file "MZB_Feldscreening_Laboratory". There, the Excel sheet "Feldscreening_Raw" compiles the macroinvertebrates data from the field-screening protocols. This Excel sheet reports the counted abundances by study site and kick-sample at various taxonomic levels (column A): $P \rightarrow Phylum$, $C \rightarrow Class$, $O \rightarrow Order$, $SupF \rightarrow Superfamily$, $F \rightarrow Family$, $SF \rightarrow Subfamily$, $TR \rightarrow Tribe$, $G \rightarrow Genus$, $S \rightarrow Species$, $UR \rightarrow Unranked$. The Excel sheet "Feldscreening_Family" compiles the data from the sheet "Feldscreening_Raw" at the family level or higher, following the taxonomic resolution of the "IBCH-Laborprotokoll".

The EPT data obtained by Aquabug were summarized and recorded together with the non-EPT laboratory data of the ZHAW in the Excel sheet "Labor_Raw". It reports the counted abundances by study site and kick-sample with the lowest possible taxonomic level (column A). The Excel sheet "Labor_Family" compiles the data from the sheet "Labor_Raw" at the family level or higher, following the taxonomic resolution of the "IBCH-Laborprotokoll".

The Excel sheet "IBCH_Overview" provides an overview of the calculated IBCH values (incl. DK and IG values) by study site for both the field-screening and laboratory datasets.

8.2 Environmental variables

Environmental variables, either collected in the field or computed, are summarized for each study site in the Excel file "Environmental_Variables." This file also includes details on the flow modeling approach, the reliability of the reconstructed flow data, and the presence/absence of tributaries, as described in Chapter 3.3.1.

8.3 Macroinvertebrate data BOKU

Table 15 provides for field-screening taxa the metric values concerning hp_sen, interstitial-surface dwelling, lentic-lotic preference, flow optimum and tolerance (basis for CEFI) calculated using an Austrian dataset (adapted) and the Canadian dataset (Arm). The hydropeaking sensitivity index (hp_sen) for a site (consisting of 12 individual samples) was calculated using the following equation:

$$hp_sen = \sum_{i=1}^{n} hp_sen_i$$

where *hp_sen_i* is the hydropeaking sensitivity index of the *i-th* taxon.

Table 15. Metric values for field-screening taxa concerning hp_sen, interstitial-surface dwelling, lentic-lotic preference, flow optimum and tolerance (basis for CEFI) calculated based on an Austrian dataset (adapted) and for the Canadian dataset (Arm).

Group	Family	Taxon name	hp_sen	Inter_Surf	Lentic_Lotic	Flow_opt (adapted)	Flow_tol (adapted)	Flow_opt (Arm)	Flow_tol (Arm)
AMPHIPODA	GAMMARIDAE	Gammarus fossarum	-5	surface	lentic	0.4	4		
ARHYNCHOBDELLIDA	HIRUDIDAE	Hirudinea Gen. sp.	0	interstitial	not classified	0.69	4		
COLEOPTERA	ELMIDAE	Elmidae Gen. sp.	5	not classified	indifferent	0.55	2	0.29	4
COLEOPTERA	GYRINIDAE	Gyrinidae Gen. sp.	-2	interstitial	lentic				
COLEOPTERA	HYDRAENIDAE	Hydraena sp.	5	not classified	lotic	0.42	4		
COLEOPTERA	SCIRTIDAE	Scirtidae Gen. sp.	-2	not classified	not classified				_
DIPTERA	LIMONIIDAE/PEDICIIDAE	Antocha sp.	0			0.36	4		
DIPTERA	ATHERICIDAE	Athericidae Gen. sp. Blep	4	interstitial	lotic	0.41	4	0.35	2
DIPTERA	BLEPHARICERIDAE	hariceridae Gen. sp.	5	surface	lotic				
DIPTERA	CERATOPOGONIDAE	Ceratopogonidae Gen. sp.	-3	not classified	lentic	0.2	4	0.21	4
DIPTERA	CHIRONOMIDAE	Chironomidae Gen. sp.	-2	not classified	indifferent	0.41	2	0.31	4
DIPTERA	EMPIDIDAE	Empididae Gen. sp.	-4	interstitial	lentic	0.34	4	0.4	2
DIPTERA	LIMONIIDAE/PEDICIIDAE	Limoniidae/Pediciidae Gen. sp.	2	interstitial	indifferent	0.4	4		
DIPTERA	PSYCHODIDAE	Psychodidae Gen. sp.	5	not classified	indifferent	0.49	2	0.37	4
DIPTERA	SIMULIIDAE	Simuliidae Gen. sp.	2	surface	lotic	1.14	2	0.42	2
DIPTERA	STRATIOMYIDAE	Stratiomyidae Gen. sp.	0	not classified					
DIPTERA	TABANIDAE	Tabanidae Gen. sp.	1	interstitial	not classified	0.16	4		
DIPTERA	TIPULIDAE	Tipulidae Gen. sp.	3	interstitial	lentic	0.68	2	0.39	4
EPHEMEROPTERA	BAETIDAE	Baetis alpinus	0	surface	lotic	0.68	2	0.43	2
EPHEMEROPTERA	BAETIDAE	Baetis sp.	1	surface	lotic	0.55	4	0.43	2
EPHEMEROPTERA	HEPTAGENIIDAE	Ecdyonurus sp.	2	surface	lentic	0.38	2	0.48	2
EPHEMEROPTERA	HEPTAGENIIDAE	Epeorus sp.	3	surface	lotic	0.86	2	0.48	2
EPHEMEROPTERA	EPHEMERIDAE	Ephemera danica	0	interstitial	lentic	0.14	8		
EPHEMEROPTERA	EPHEMERELLIDAE	Ephemerellidae Gen. sp.	3	surface	indifferent	0.67	4	0.43	4
EPHEMEROPTERA	HEPTAGENIIDAE	Heptageniidae Gen. sp.	0	surface	indifferent	0.3	4	0.48	2
EPHEMEROPTERA	LEPTOPHLEBIIDAE	Leptophlebiidae Gen. sp.	2	interstitial	lentic	0.4	2	0.26	4
EPHEMEROPTERA	HEPTAGENIIDAE	Rhithrogena sp.	2	surface	lotic	0.86	2	0.48	2
EPHEMEROPTERA	EPHEMERELLIDAE	Torleya major	0		indifferent			0.43	4
HETEROPTERA	CORIXIDAE	Micronecta sp.	0	surface	not classified	0.13	4		
ISOPODA	ASELLIDAE	Asellus aquaticus							
MYIDA	DREISSENIDAE	Dreissena sp.	0					_	
PLECOPTERA	NEMOURIDAE	Amphinemura sp.	5	surface	indifferent	0.26	4	0.44	2
PLECOPTERA	TAENIOPTERYGIDAE	Brachyptera/Rhabdiopteryx sp.	1	surface	lotic	0.32	8	0.5	4
PLECOPTERA	LEUCTRIDAE	Capniidae/Leuctridae Gen. sp.	1	interstitial	indifferent	0.23	4	0.38	2
PLECOPTERA	CHLOROPERLIDAE	Chloroperlidae Gen. sp.	2	interstitial	lentic	0.48	4	0.49	2
PLECOPTERA	PERLIDAE	Dinocras sp.	3	interstitial	lotic	0.63	2	0.54	2
PLECOPTERA	PERLODIDAE	Isoperla sp.	3	interstitial	indifferent	0.71	2	0.47	4
PLECOPTERA	NEMOURIDAE	Nemoura/Nemurella sp.	5	surface	lentic	0.25	2	0.44	2
PLECOPTERA	NEMOURIDAE	Nemouridae Gen. sp.	5	surface	indifferent	0.6	2	0.44	2
PLECOPTERA	PERLIDAE	Perla sp.	1	interstitial	lotic	0.56	2	0.54	2
PLECOPTERA	PERLIDAE	Perlidae Gen. sp.	-3	interstitial	lotic	0.56	4	0.54	2
PLECOPTERA	PERLODIDAE	Perlidae/Perlodidae Gen. sp.	-5	interstitial	indifferent			0.47	4
PLECOPTERA	PERLODIDAE	Perlodes/Dictyogenus sp.	3	interstitial	lotic	0.41	5	0.47	4
PLECOPTERA	PERLOIDEA	Perloidea sp.	5						
PLECOPTERA	NEMOURIDAE	Protonemura sp.	5	surface	lotic	0.56	2	0.44	2
SERIATA	PLANARIIDAE	Planariidae Gen. sp.	5					0.33	4
TRICHOPTERA	LIMNEPHILIDAE	Allogamus auricollis	2	surface	lentic	0.19	4	0.33	4
TRICHOPTERA	GLOSSOSOMATIDAE	Glossosomatidae Gen. sp.	4	surface	lotic	0.33	4	0.41	4
TRICHOPTERA	GOERIDAE	Goeridae Gen. sp.	5	surface	indifferent	0.27	4		
TRICHOPTERA	HYDROPSYCHIDAE	Hydropsyche sp.	3	interstitial	lotic	0.4	2	0.43	2
TRICHOPTERA	RHYACOPHILIDAE	Hyporhyacophila torrentium-Gr.	3	interstitial	lotic	0.54	4	0.44	2
TRICHOPTERA	LEPIDOSTOMATIDAE	Lepidostoma sp.	3			0.28	4	0.39	2
TRICHOPTERA	LIMNEPHILIDAE	Limnephilidae Gen. sp.	2	surface	lentic	0.65	2	0.33	4
TRICHOPTERA	PHILOPOTAMIDAE	Philopotamidae Gen. sp.	0	interstitial	not classified		0.49	2	
TRICHOPTERA	POLYCENTROPODIDAE	Polycentropodidae Gen. sp.	0	interstitial	lentic	0.24	8	0.22	4
	PSYCHOMYIIDAE	Psychomyia pusilla	3	surface	indifferent	0.33	8	0.22	
TRICHOPTERA		, monty or protette	5						_
TRICHOPTERA TRICHOPTERA	RHYACOPHILIDAE	Rhvacophila s. str. sp.	-1	interstitial	lotic	0.39	4	().44	2
TRICHOPTERA TRICHOPTERA TRICHOPTERA	RHYACOPHILIDAE RHYACOPHILIDAE	Rhyacophila s. str. sp. Rhyacophilidae Gen. sp.	-1 0	interstitial interstitial	lotic lotic	0.39 0.46	4	0.44 0.44	

8.4 Potential influence of silicate bedrock

The greatest deviation between hydropeaking sites and hydrologically unaffected reference sites was observed in the Southern Alps biogeographical region (Figure 11). However, in this region, the reference sites on the Verzasca River are distinguished by silicate bedrock, in contrast to the other rivers, which are situated on carbonate bedrock. This geological difference may therefore serve as a covariate, which was further investigated through an indicator species analysis (according to Dufrene & Legendre, 1997) and a non-metric multidimensional scaling (NMDS) analysis.

The macroinvertebrate community in the Verzasca is primarily characterized by higher abundances of

the taxa Polycentropodidae Gen.sp., Antocha sp., Philopotamidae, Planariidae, Protonemura sp., Epeorus sp., Rhyacophilidae, Athericidae, Hyporhyacophila torrentium Gr., and Perlidae, compared to the other study sites in the hydropeaked rivers Ticino and Moesa (Figure 16). Of these 10 indicative field-screening taxa (30 in total at the Verzasca river), only four taxa (Protonemura sp., Philopotamidae, Rhycophilidae and Polycentropodidae) were found exclusively in the Verzasca, making them probably indicative of the geological differences. The remaining taxa are more likely to be indicative of a reference status. Thus, including the Verzasca in the analysis is justified.

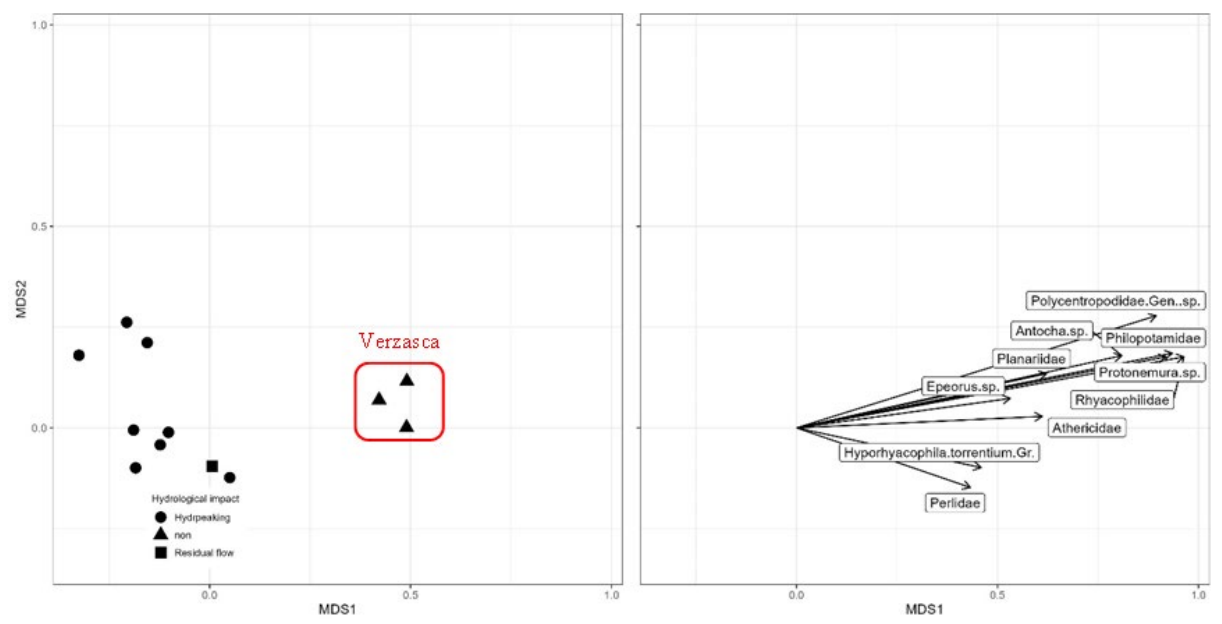


Figure 16. NMDS for the Southern Alps, representing the separation of the Verzasca River from the rest based on the field-screening dataset (left) and the taxa indicating these differences (right). Only indicator taxa identified through indicator species analysis (according to Dufrene & Legendre, 1997) are visualized.

8.5 Reference values for metric calculation

To standardize the metrics for integration into the multimetric indices, reference values were applied. These reference values correspond to the 75th percentile of each metric within reference sites with a (near-) natural flow regime (Table 16).

Table 16. Values for standardization of the individual metrics for the integration into the MMI_HP_X equation. They represent the 75th percentile of the metric within the sites with a (near-) natural flow regime.

Metric	Reference v	alue
Metric	Fieldscreening	Laboratory
CEFI	0.52	0.54
nr_ple_taxa	9.00	9.00
DI	78.00	94.00
dom_inter	20.89	14.79
mar div	3.52	4.00
dom_lotic	75.65	75.91
DK_IBCH	0.77	0.94
sha div	4.19	3.92

8.6 Validation of the multimetric indices

8.6.1 Scatterplots

The MMI_HP_FIE yielded results similar to the MMI_HP_ALL (Figure 17 vs Figure 9). The strongest correlation between the MMI_HP_FIE calculated with the field-screening dataset and the multimetric hydrological index (CNT_MAFR_RATIO; Chapter 3.3) was found in the Southern Alps (R² = 0.19), while the weakest correlation was found in the Eastern Central Alps (R² = 0.022) (Figure 17, top panels). When calculated with the laboratory dataset, the strongest correlation was observed in the Eastern Central Alps and the Southern Alps (R² = 0.13), though the correlation for the Central Plateau/Northern Alps was weaker (R² = 0.014) (Figure 17, bottom panels). However, all relationship were non-significant (p > 0.05).

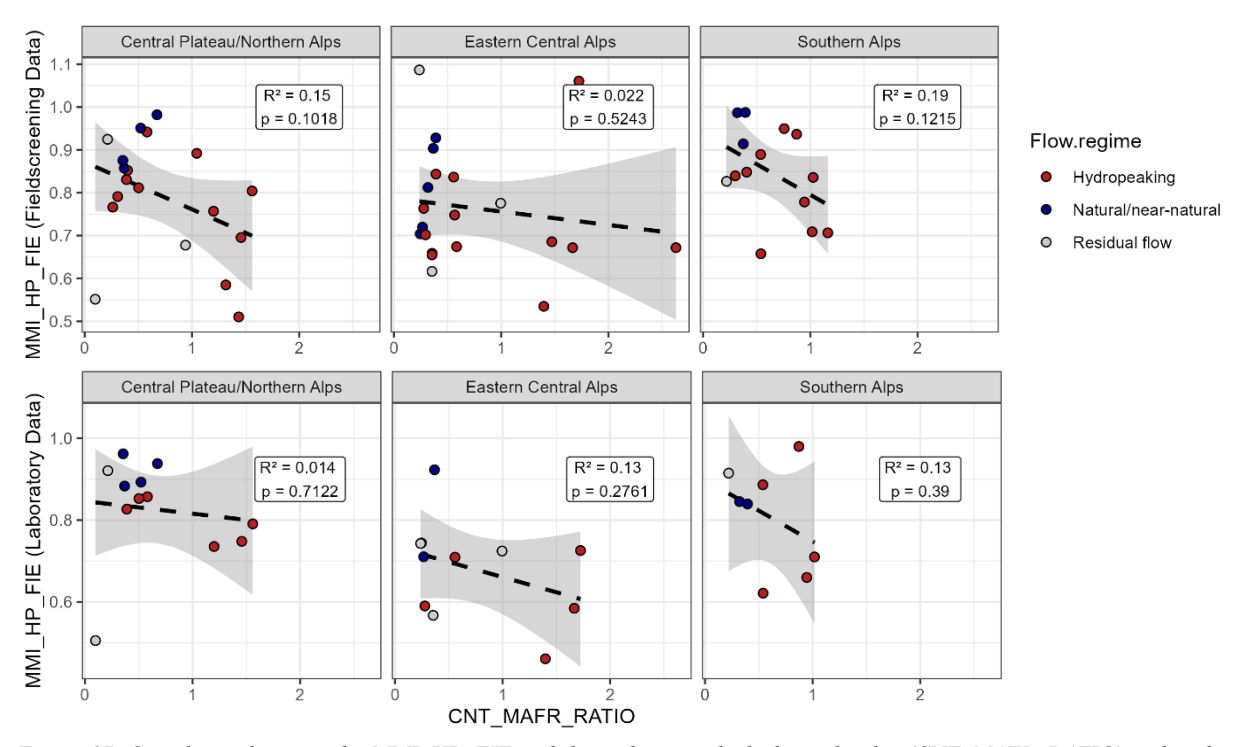


Figure 17. Correlation between the MMI_HP_FIE and the multimetric hydrological index (CNT_MAFR_RATIO) within the different biogeographical regions Central Plateau/Northern Alps, Eastern Central Alps, and Southern Alps. The correlation is depicted for the field-screening dataset (top panels) and the laboratory dataset (bottom panels).

The MMI_HP_LAB calculated using the field-screening dataset showed the strongest correlations for the Central Plateau/Northern Alps ($R^2 = 0.24$) (Figure 18, top panels). In contrast, the Southern Alps exhibited a weak, opposite correlation ($R^2 = 0.031$). When calculated with the laboratory dataset, similar trends were observed in the Eastern Central Alps ($R^2 = 0.21$) and Southern Alps ($R^2 = 0.28$), while the correlation for the Central Plateau/Northern Alps was weaker ($R^2 = 0.11$) (Figure 18, bottom panels). The correlation for the Central Plateau/Northern Alps using the field screening dataset was significant (p < 0.05), whereas all other correlations were non-significant.

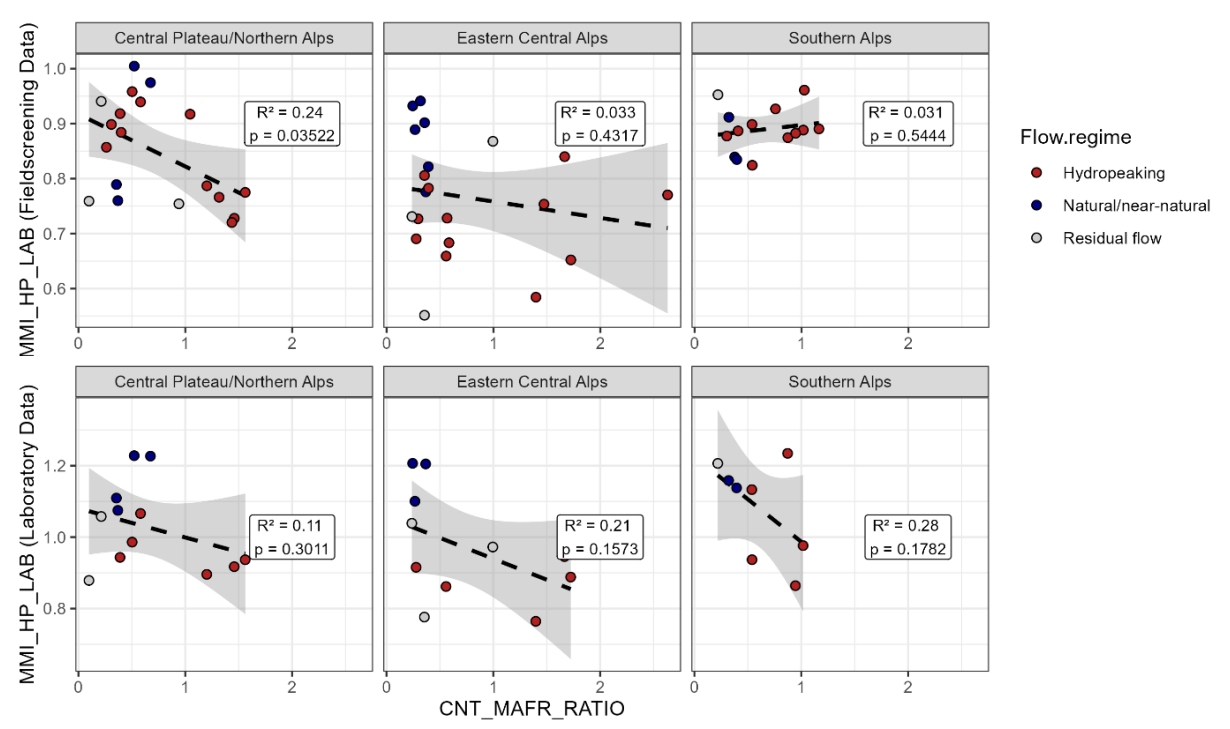


Figure 18. Correlation between the MMI_HP_LAB and the multimetric hydrological index (CNT_MAFR_RATIO) within the different biogeographical regions Central Plateau/Northern Alps, Eastern Central Alps, and Southern Alps. The correlation is depicted for the field-screening dataset (top panels) and the laboratory dataset (bottom panels).

The hydrological variability in the rivers shown in the figures 17, 18 and 9 was represented using the multimetric hydrological index CNT_MAFR_RATIO (Chapter 3.3). However, there are other ways to combine hydrological variables to emphasize different aspects of hydrology. One alternative option is to multiply the variables CNT, MAFR, and AMP (CNT*MAFR*AMP). This metric may show slightly better relationships with biological factors, has shown by Auhser et al. (in prep). The significance levels of the correlations are also slightly better in the case of our study (Central Plateau/Northern Alps: p < 0.05, and Southern Alps: p < 0.05). However, since the difference to the index CNT_MAFR_RATIO very little and the distribution of data points along the variable CNT*MAFR*AMP is less suitable for a linear model compared to that of the variable CNT_MAFR_RATIO, the latter was chosen for the main part of the analyses.

The hydrological variability in the rivers shown in Figures 17, 18, and 9 was represented using the multimetric hydrological index CNT_MAFR_RATIO (Chapter 3.3). However, alternative combinations of hydrological variables can be used to emphasize different aspects of flow variability. One option is to multiply the variables CNT, MAFR, and AMP (CNT*MAFR*AMP).

$$CNT * MAFR * AMP = CNT_{DC_tot} * MAFR_{DC_median} * AMP_{DC_median}$$

This index may exhibit slightly stronger relationships with biological factors, as reported by Auhser et al. (in prep.), and in our study it also yielded marginally higher correlation significance (Figure 19; Central Plateau/Northern Alps: p < 0.05; Southern Alps: p < 0.05). Nevertheless, because the difference from CNT_MAFR_RATIO was minimal and the distribution of data points along CNT \times MAFR \times AMP was less suitable for linear modeling, we selected CNT MAFR RATIO for the main analyses.

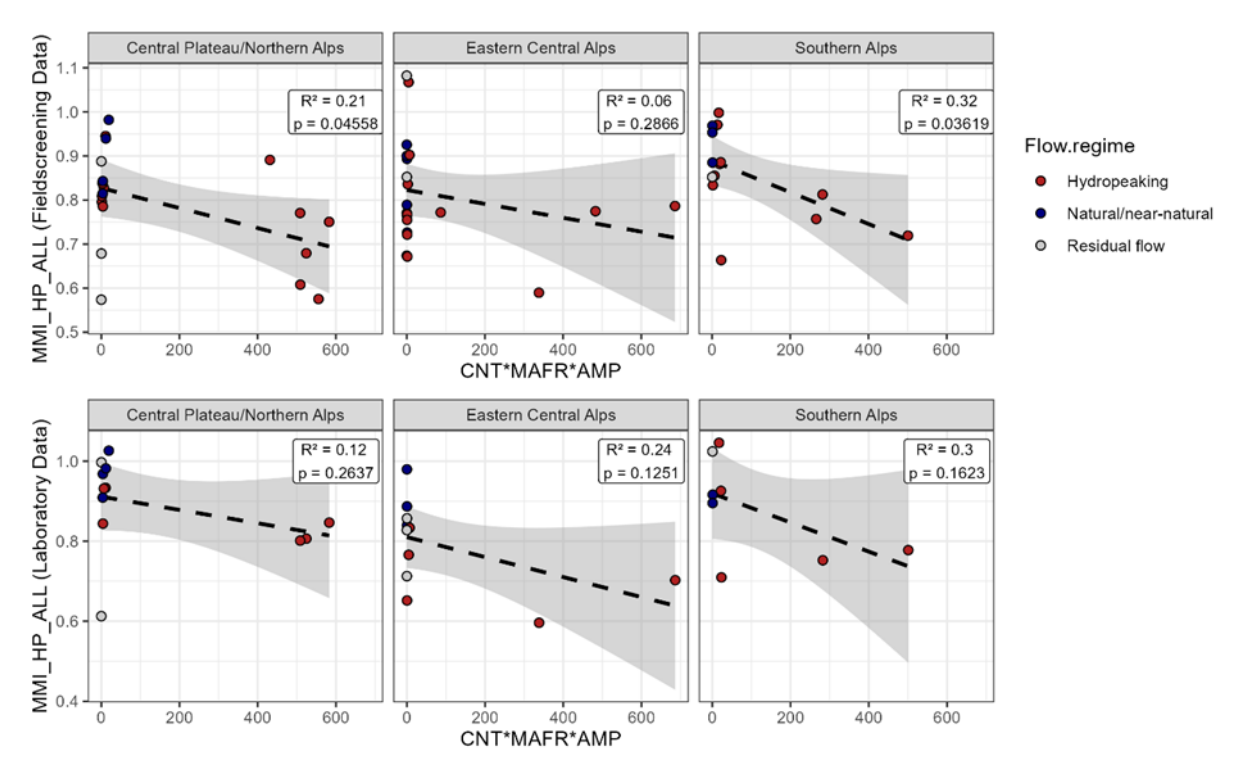


Figure 19. Correlation between the MMI_HP_ALL and an alternative multimetric hydrological index (CNT*MAFR*AMP) within the different biogeographical regions Central Plateau/Northern Alps, Eastern Central Alps, and Southern Alps. The correlation is depicted for the field-screening dataset (top panels) and the laboratory dataset (bottom panels)

8.6.2 Correlation between single biological and single hydrological metrics

The individual metrics used to calculate the multimetric indices (Chapter 4.3.4) were correlated with the individual hydrological metrics composing the multimetric hydrological index (CNT_MAFR_RATIO; Chapter 3.3). As also depicted in the scatterplots in Annex 8.6.1, the strongest correlations, aligned with the expected negative trends, were observed in the Southern Alps (Figure 20). There, the Shannon-Wiener diversity (sha_div) and the degradation index (DI) showed the strongest negative correlation with the frequency of decreasing events (CNT_DC_tot) ($r = -0.56 \triangleq R^2 = 0.31$). The DI exhibited also the strongest negative correlation with the flow ratio of decreasing events (RATIO_DC_median) ($r = -0.65 \triangleq R^2 = 0.42$). Interestingly, the dominance of lotic taxa (dom_lotic) was positively correlated with all three hydrological metrics. In the Eastern Central Alps, the strongest negative correlation was found between the DI and the maximum flow rate of decreasing events (MAFR_DC_median) ($r = -0.47 \triangleq R^2 = 0.22$). Furthermore, the weighted average of Diversity Class of the Swiss water quality index (DK_IBCH) was positively correlated with all three hydrological metrics in this biogeographical region. In the Central Plateau/Northern Alps, the strongest negative correlation was observed between dom_lotic and MAFR_DC_median ($r = -0.58 \triangleq R^2 = 0.34$) (Figure 20).

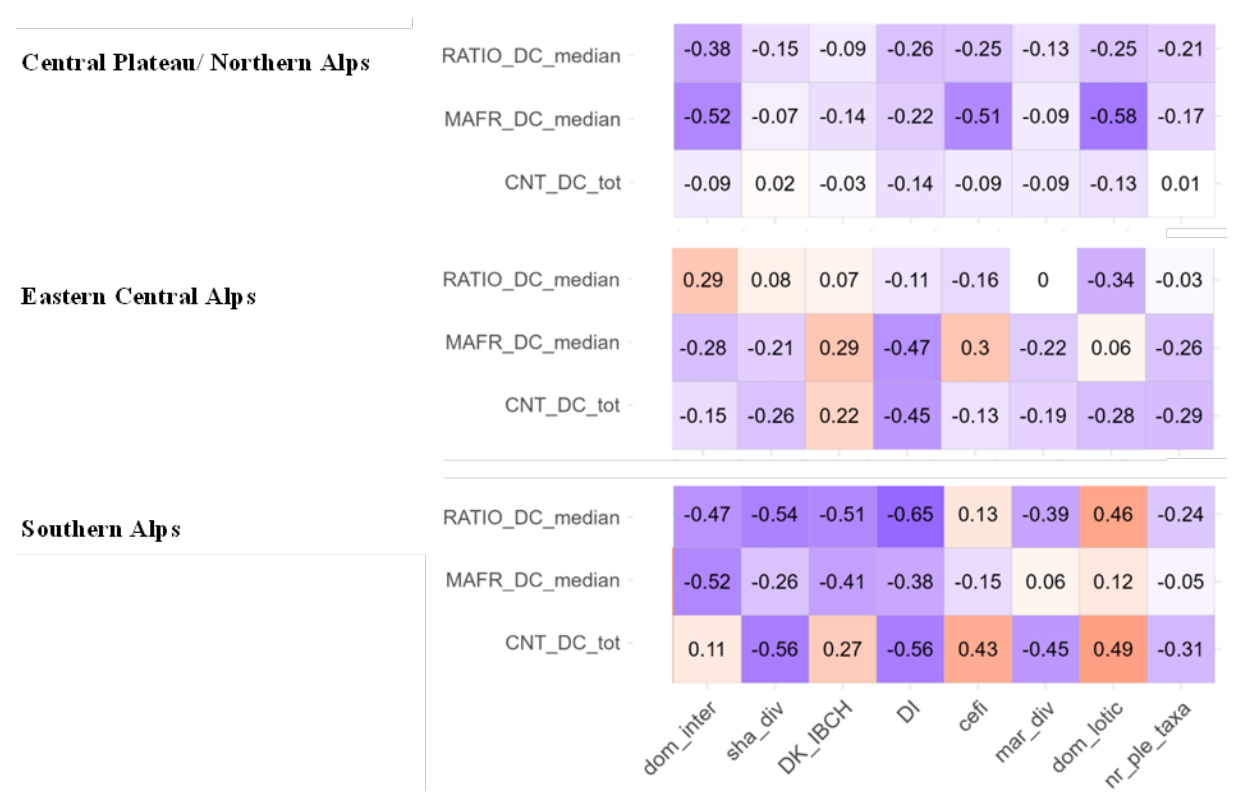


Figure 20. Correlation between the individual metrics used to calculate the multimetric indices (Chapter 4.3.4) and the individual hydrological metrics composing the multimetric hydrological index (CNT_MAFR_RATIO; Chapter 3.3). Negative correlations are highlighted in blue, while positive correlations are highlighted in red.

8.6.3 Hydrological variables across biogeographical regions and rivers

The highest hydropeaking intensities occurred in the biogeographical region "Eastern Central Alps", specifically in the river Vorderrhein (VR) (Figure 21). Here, hydropeaking intensity is characterized by a high frequency of events, steep ramping rates, and large flow ratios. In contrast, the river with the highest intensity in the biogeographical region "Central Plateau/Northern Alps" exhibited lower event frequency but particularly high ramping rates. While its flow ratios did not reach the extreme maxima observed in the Vorderrhein, the median values were comparable. In the "Southern Alps", the highest intensities were recorded in the river Ticino, where hydropeaking was driven by frequent events and steep ramping rates, although flow ratios were comparatively lower. Interestingly, the Thur River (TH) exhibited a high frequency of events despite its (near-) natural flow regime – an occurrence even more pronounced than in the hydropeaked rivers of the same biogeographical region (Figure 21). This was probably an effect of the run-off the river hydropower plants along the Thur River.

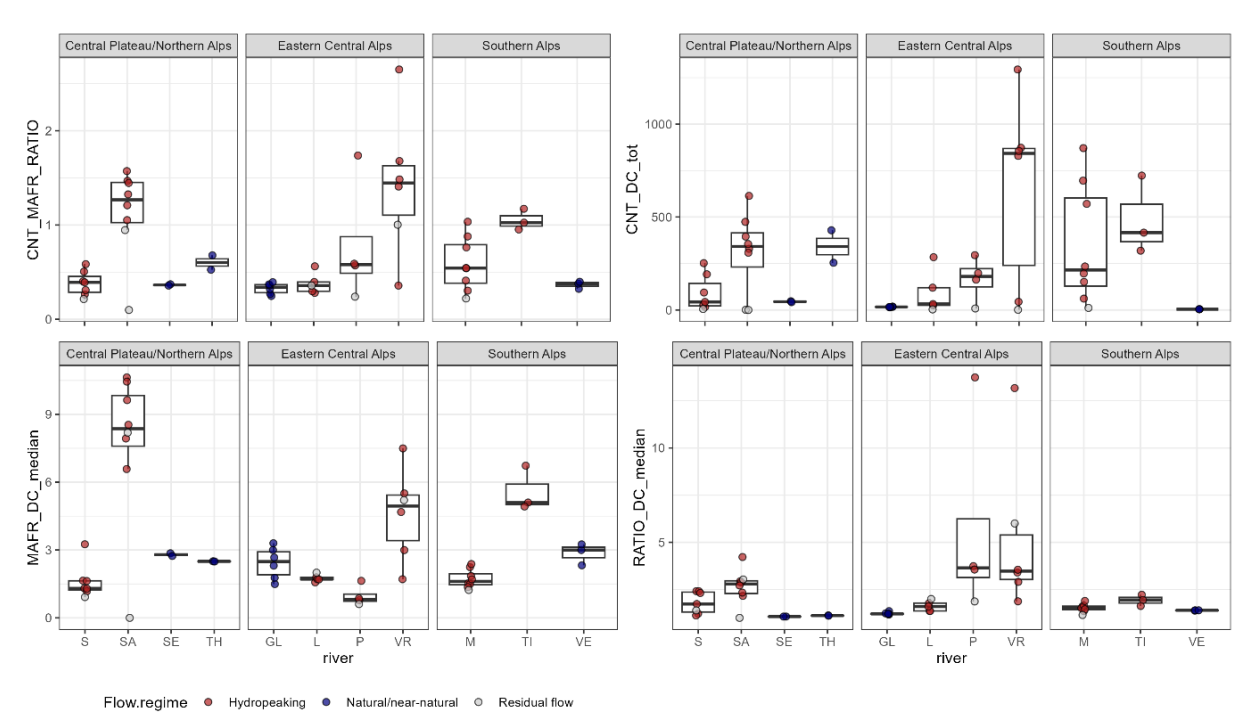


Figure 21. Characterization of hydrological variables across the investigated rivers and biogeographical regions. For hydrological variable abbreviation see Table 8.

8.6.4 Influence of flow-data reliability

A validation was also conducted to assess the reliability of the reconstructed flow data (Table 9, Chapter 3.3.1) on the MMI_HP_ALL. Figure 22 shows that, despite variations in flow data reliability, overall trends remain largely unaffected. Specifically, in the biogeographical regions Central Plateau/Northern Alps and Southern Alps, the trends would not differ substantially even if the reliability classes "Poor" and "Moderate" were excluded. However, in the Eastern Central Alps, the trend would become positive. Notably, the availability of flow data with "High" or "Good" reliability is generally limited. Only in the biogeographical region Central Plateau/Northern Alps more than half of the study sites (52.6%) had flow data classified with "Good" or "High" reliability. In contrast, in the Eastern Central Alps and Southern Alps, only 28.6% and 21.4% of sites, respectively, fell into these categories.

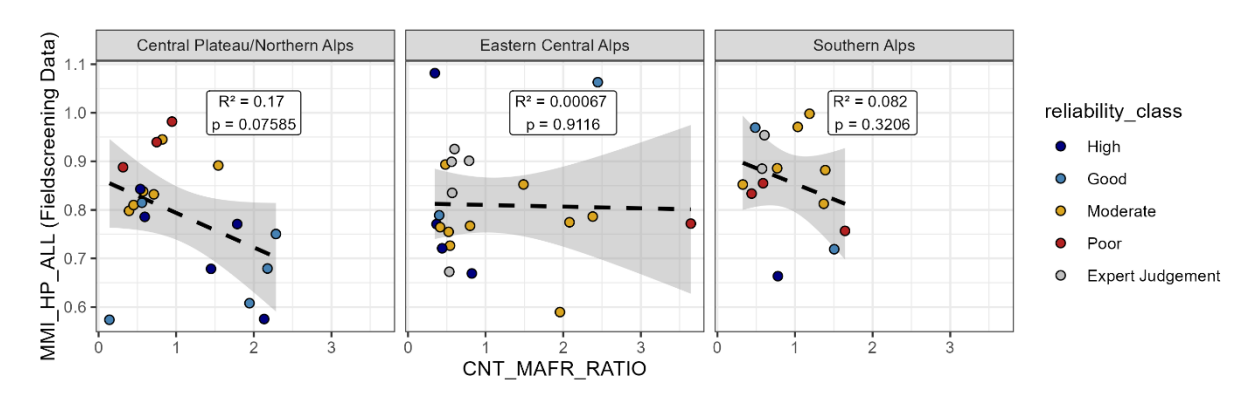


Figure 22. Correlation between the MMI_HP_ALL, calculated with the field-screening dataset, and the multimetric hydrological index (CNT_MAFR_RATIO) within the different biogeographical regions Central Plateau/Northern Alps, Eastern Central Alps, and Southern Alps. Study sites are color-coded according to the reliability of the reconstructed flow data, as defined in Table 9 (Chapter 3.3.1).

8.7 Spatial distribution of flow velocity classes

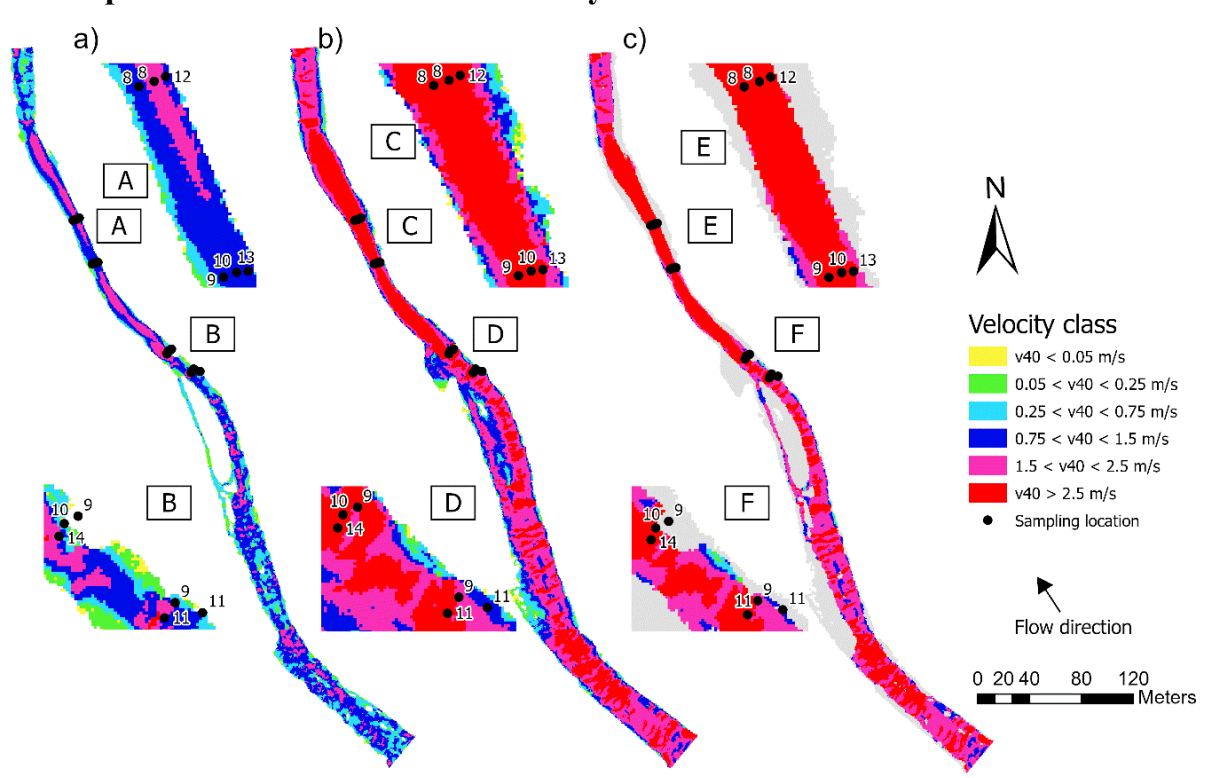


Figure 23. Spatial distribution of flow velocity classes in the GL1 study site. a) Q_{min} scenario (3.3 m^3/s); b) Q_{max} scenario (31.8 m^3/s); c) Q_{max} scenario considering only the permanently wetted zone. The dewatering area is shaded grey. A-F represent an enlarged view of the locations (black dots), where macroinvertebrates were sampled, whereas the numbers indicate the different macroinvertebrate taxa found with the laboratory identification. For study site abbreviation and location see Figure 2 and Table 5.

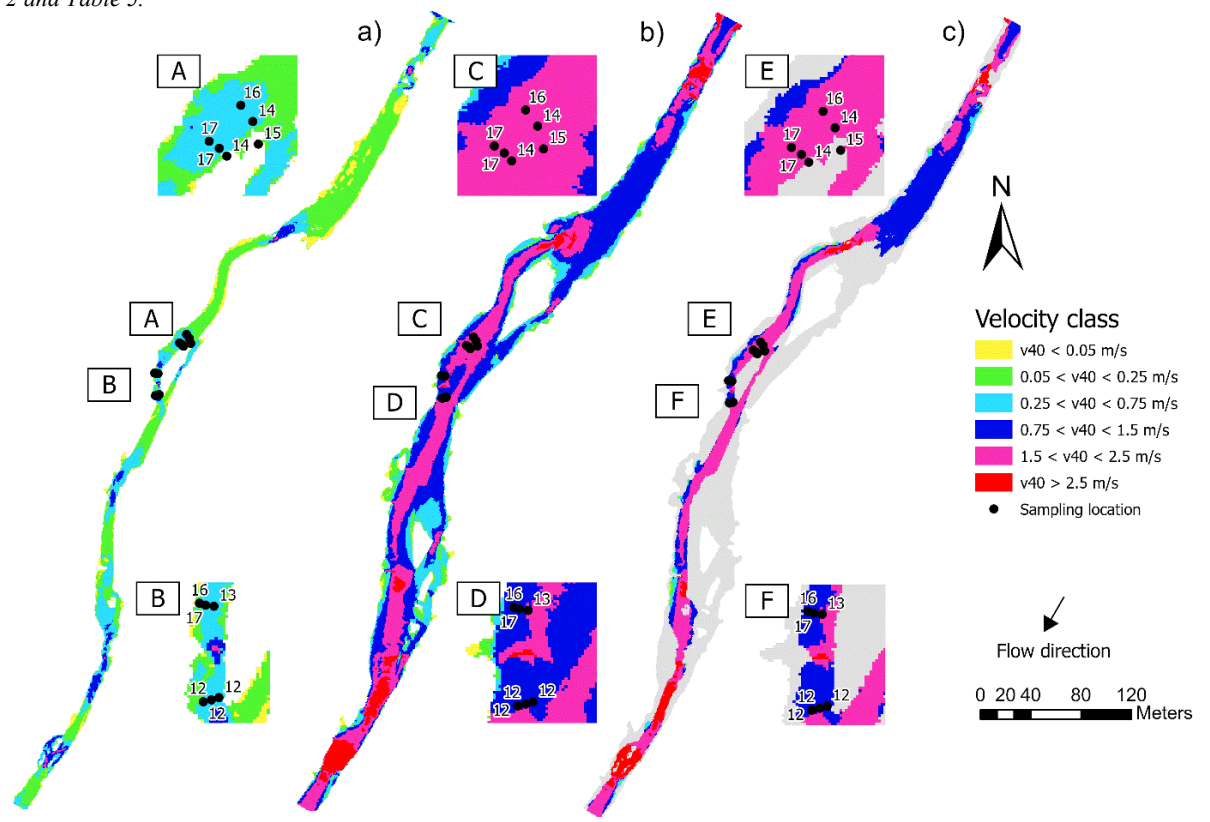


Figure 24. Spatial distribution of flow velocity classes in the M1 study site. a) Q_{min} scenario (0.5 m^3/s); b) Q_{max} scenario (22.8 m^3/s); c) Q_{max} scenario considering only the permanently wetted zone. The dewatering area is shaded grey. A-F represent an enlarged view of the locations (black dots), where macroinvertebrates were sampled, whereas the numbers indicate the different macroinvertebrate taxa found with the laboratory identification. For study site abbreviation and location see Figure 2 and Table 5.

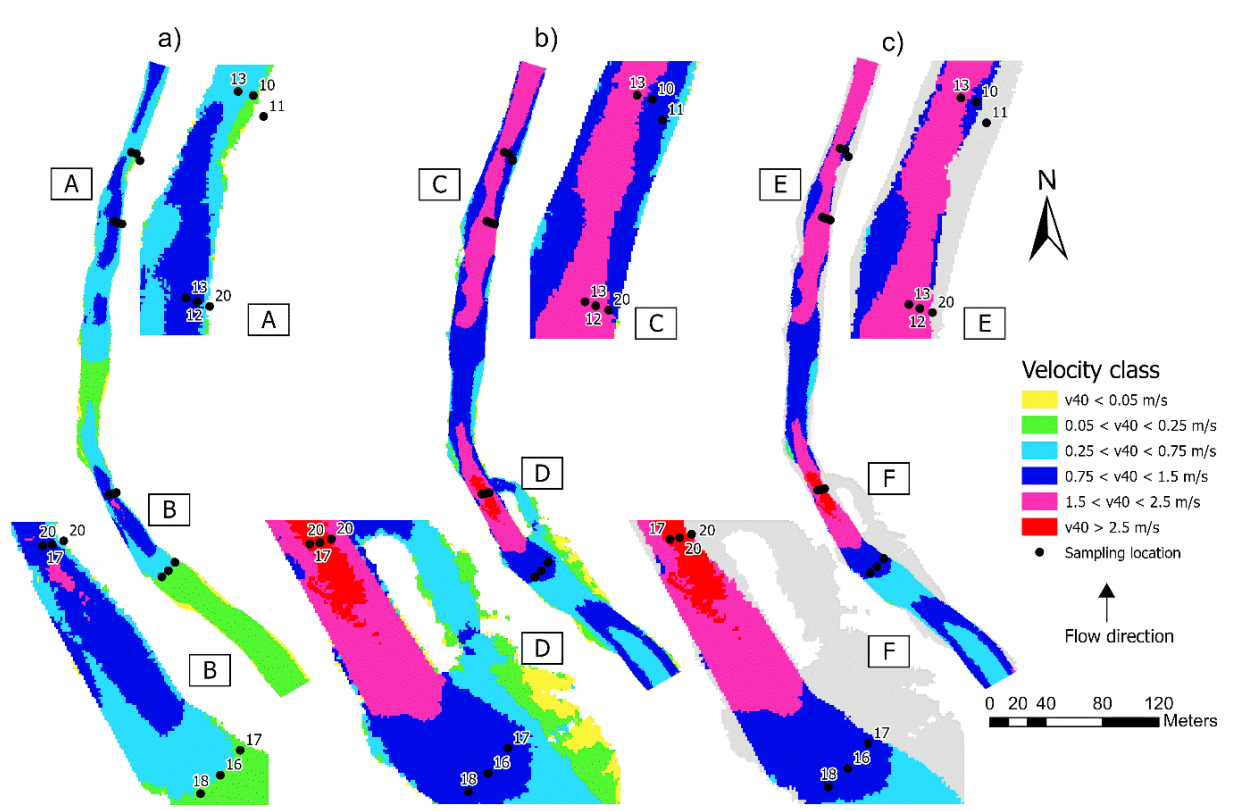


Figure 25. Spatial distribution of flow velocity classes in the S1 study site. a) Q_{min} scenario (2.0 m^3/s); b) Q_{max} scenario (20.0 m^3/s); c) Q_{max} scenario considering only the permanently wetted zone. The dewatering area is shaded grey. A-F represent an enlarged view of the locations (black dots), where macroinvertebrates were sampled, whereas the numbers indicate the different macroinvertebrate taxa found with the laboratory identification. For study site abbreviation and location see Figure 2 and Table 5.

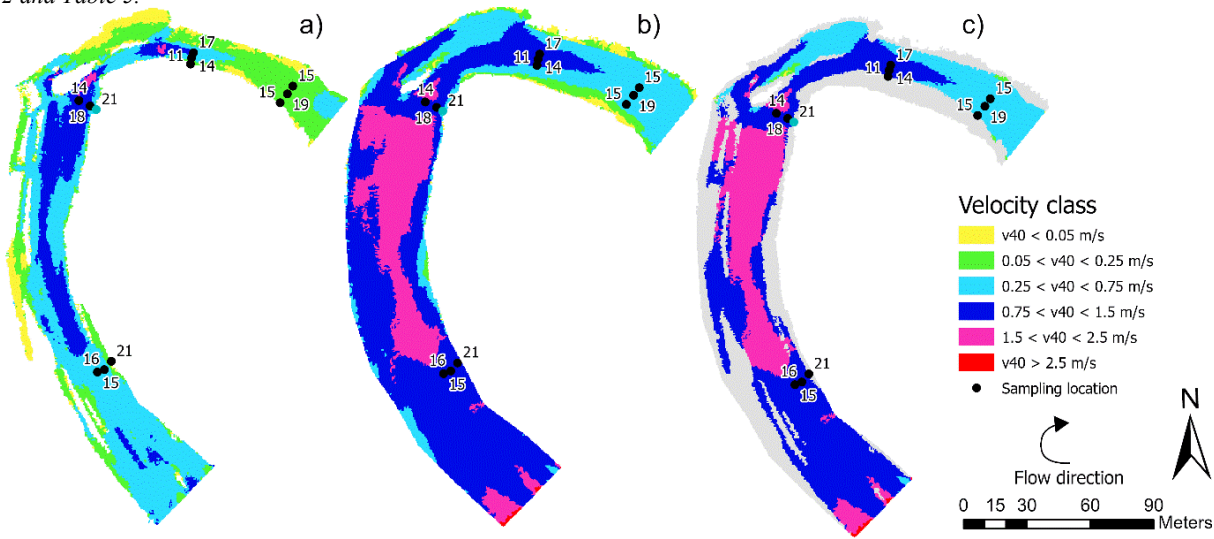


Figure 26. Spatial distribution of flow velocity classes in the S2 study site. a) Q_{min} scenario (2.0 m^3/s); b) Q_{max} scenario (20.0 m^3/s); c) Q_{max} scenario considering only the permanently wetted zone. The dewatering area is shaded grey. Black dots represent locations where macroinvertebrates were sampled, whereas the numbers indicate the different macroinvertebrate taxa found with the laboratory identification. For study site abbreviation and location see Figure 2 and Table 5.

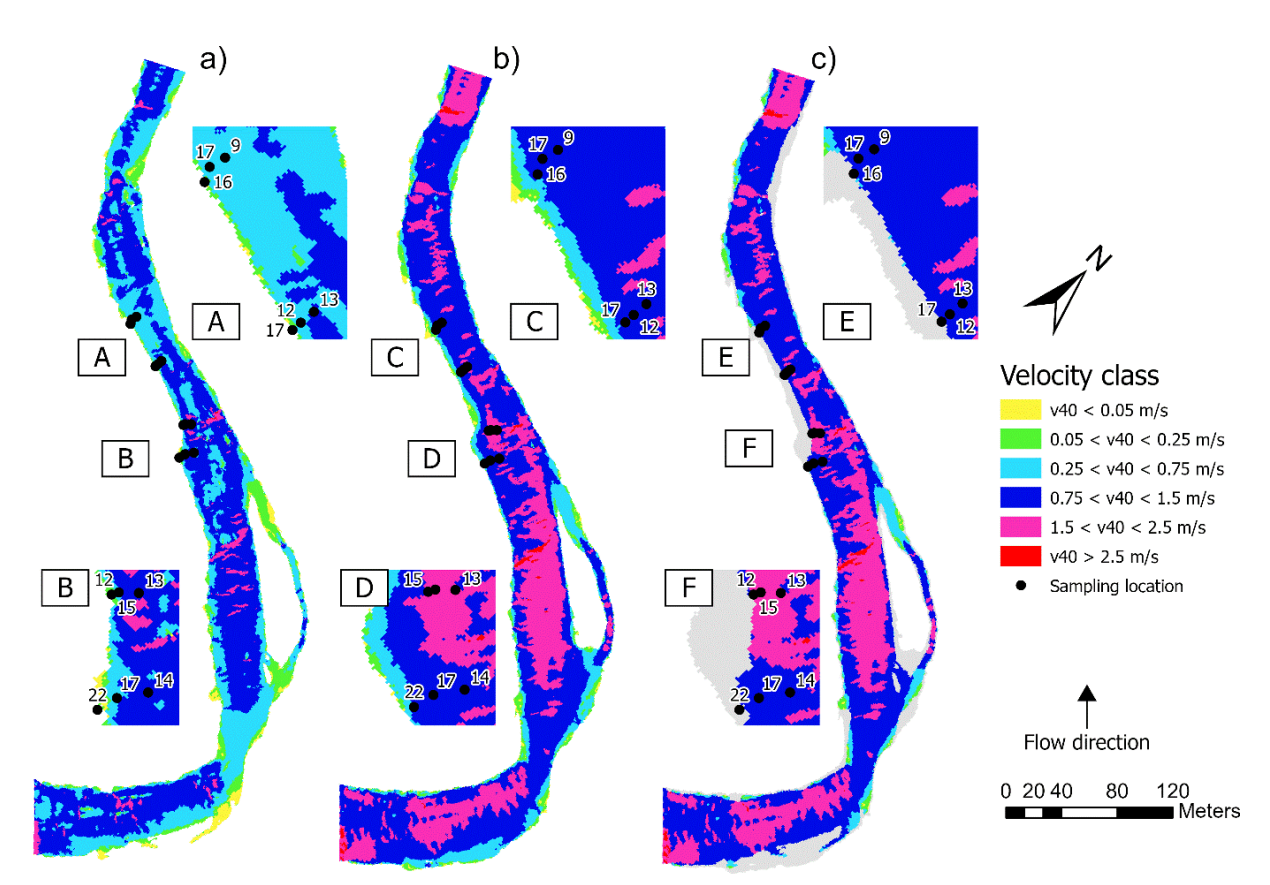


Figure 27. Spatial distribution of flow velocity classes in the TH4 study site. a) Q_{min} scenario (11.5 m^3/s); b) Q_{max} scenario (36.3 m^3/s); c) Q_{max} scenario but considering only the permanently wetted zone. The dewatering area is shaded grey. A-F represent an enlarged view of the locations (black dots), where macroinvertebrates were sampled, whereas the numbers indicate the different macroinvertebrate taxa found with the laboratory identification. For study site abbreviation and location see Figure 2 and Table 5.

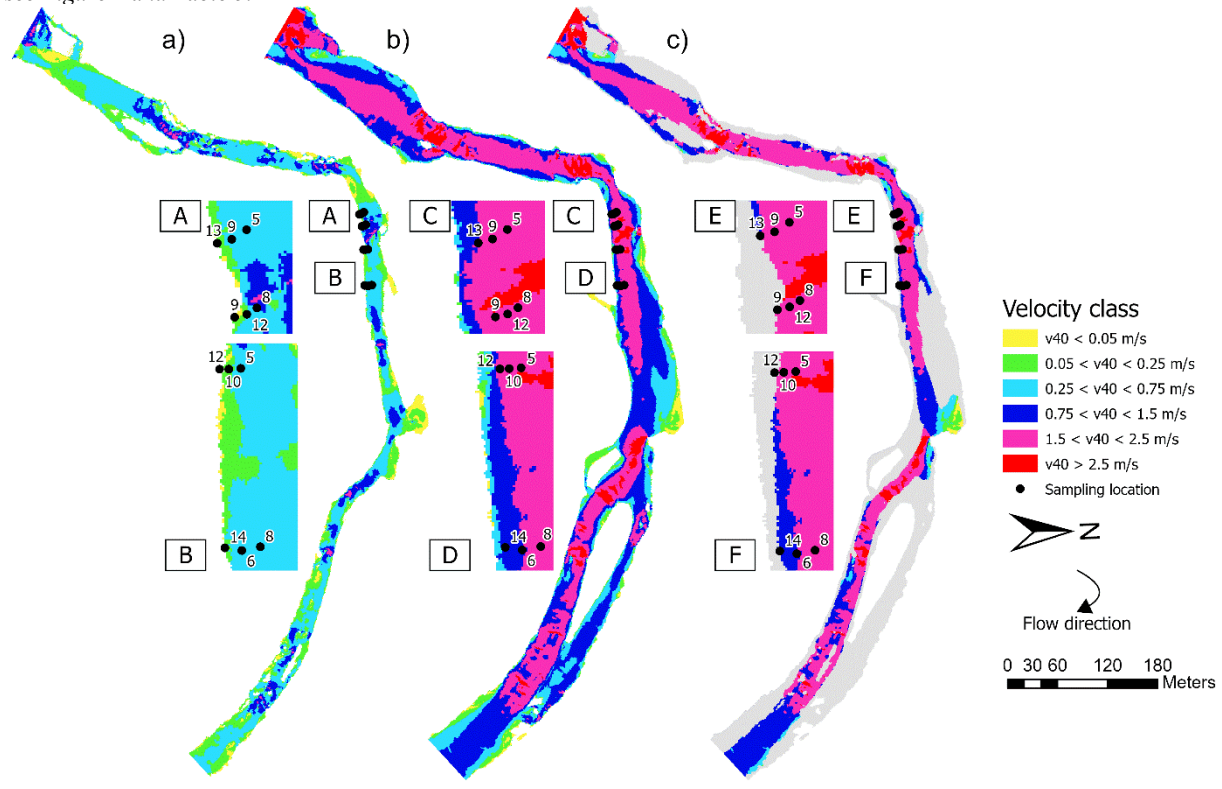


Figure 28. Spatial distribution of flow velocity classes in the VR3 study site. a) Q_{min} scenario (2.9 m^3/s); b) Q_{max} scenario (52.9 m^3/s); c) Q_{max} scenario but considering only the permanently wetted zone. The dewatering area is shaded grey. A-F represent an enlarged view of the locations (black dots), where macroinvertebrates were sampled, whereas the numbers indicate the different macroinvertebrate taxa found with the laboratory identification. For study site abbreviation and location see Figure 2 and Table 5.

8.8 Data delivery

The files listed in Table 17 were supplied with this report.

Table 17. File name, format and content of the supplied data.

Folder name / File name	Format	Content
File: MZB_Feldscreening_Laboratory	XLSX	Macroinvertebrate taxa identified by the ZHAW and Aquabug. More information in Chapter 8.1 and 3.2.
File: Metrics_fie_lab	CSV	 25 candidate metrics used to characterize the macroinvertebrate communities as outlined in Table 10. More information in Chapter 4.2.1. K-Index and MMI_HP_AT: Multimetric macroinvertebrate indices from Greece (Theodoropolus et al., 2018) respectively Austria ((Leitner et al., 2025). More information in Chapter 4.2.3. MMI_Field_3 and MMI_Field_5: Swiss multimetric macroinvertebrate indices based on field-screening data computed with the best three respectively five candidate metrics. More information in Chapter 4.3.4. MMI_Labor_3 and MMI_Labor_5: Swiss multimetric macroinvertebrate indices based on laboratory data computed with the best three respectively five candidate metrics. More information in Chapter 4.3.4. MMI_Combi_3 and MMI_Combi_5: Swiss multimetric macroinvertebrate indices based on both datasets computed with the best three respectively five candidate metrics. More information in Chapter 4.3.4. All candidate metrics as well as all multimetric indices were calculated with the field-screening respectively the laboratory data for each study site.
File: Environmental_Variables	XLSX	Environmental variables either collected in the field or computed. More information in Chapters 8.2 and 3.3.
Folder: R_scripts Sub-Folder: 01_taxalist_compilation Sub-Sub-Folder: 03_compiled_taxalist File: 20250909_taxalist_ges	CSV	Taxa identified by the fieldscreening method and the laboratory method
Folder: R_scripts Sub-Folder: 02_metric_calculation Sub-Sub-Folder: 01_raw_data_metrics Sub-Sub-Sub-Folder: Metric Listen	CSV/ XLSX	All trait lists used for the metric calculation
Folder: R_scripts Sub-Folder: 04_outputs	PNG	All graphical outputs used within the report
Folder: Q_Metrics Sub-Folder: Hydrographs	CSV	Reconstructed flow data for 47 study sites. These data were used for computing the hydrological variables. More information in Chapter 3.3.1
Folder: Q_Metrics File: Q_metrics	CSV	Eight hydrological variables as outlined in Table 8. Calculated using the "hydropeak" package (Greimel et al., 2016; Grün et al., 2022). More information in Chapter 3.3.
Folder: Habitat_Modeling Sub-Folder: Basement Sub-Sub-Folder: Computational Mesh	2DM	2D mesh computed using BASEMesh (version 2.0.0; VAW-ETHZ, 2022) for the eight study sites used for hydrodynamic modeling. More information in Chapter 5.2.2.
Folder: Habitat_Modeling Sub-Folder: Basement Sub-Sub-Folder: Results_Raster	TIF	Results of the univariate habitat modeling for the seven suitable study sites. More information in Chapters 5.2.3 and 5.3. File name structure: SS_HV_Q.tif; with - SS: Study site - HV: Hydraulic variable, either water depth (wd) or velocity (v) - Q: Simulated discharge
Folder: Habitat_Modeling Sub-Folder: T Univariate_Habitat_Modeling		Results of the univariate habitat modeling for the seven suitable study sites. More information in Chapters 5.2.3 and 5.3. File name structure: SS_Modtyp_Q.tif; with - SS: Study site - Modtyp: o foen_class: modeling results for the whole wetted zone o foen_class_perm: modeling results for the permanently wetted zone - Q: simulated discharge